# *In vivo* characterization of candidate genes for heart rate variability identifies culprits for sinoatrial pauses and arrests

Benedikt von der Heyde[1,2], Anastasia Emmanouilidou[1,2], Tiffany Klingström[1,2], Eugenia Mazzaferro[1,2], Silvia Vicenzi[1,2], Sitaf Jumaa[1,2], Olga Dethlefsen[3,4], Harold Snieder[5], Eco de Geus[6], Erik Ingelsson[2,7,8,9], Amin Allalou[2,10], Hannah L. Brooke[11], Marcel den Hoed[#1,2]

[1]Department of Immunology, Genetics and Pathology, Uppsala University, Uppsala, Sweden.
[2]Science for Life Laboratory, Uppsala University, Uppsala, Sweden.
[3]Science for Life Laboratory, Stockholm University, Stockholm, Sweden.
[4]National Bioinformatics Infrastructure Sweden, Stockholm University, Stockholm, Sweden.
[5]Department of Epidemiology, University of Groningen, University Medical Center Groningen, Groningen, the Netherlands.
[6]Department of Biological Psychology, Vrije Universiteit Amsterdam, Amsterdam, the Netherlands.
[7]Department of Medical Sciences, Molecular Epidemiology, Uppsala University, Uppsala, Sweden.
[8]Department of Medicine, Division of Cardiovascular Medicine, Stanford University School of Medicine, Stanford, CA, USA.
[9]Stanford Cardiovascular Institute, Stanford University, Stanford, CA 94305.
[10]Department of Information Technology, Visual Information and Interaction, Uppsala University, Uppsala, Sweden.
[11]Department of Public Health and Caring Sciences, Uppsala University, Uppsala, Sweden.

[#]Corresponding author: marcel.den_hoed@igp.uu.se

Running title: Causal genes for sinoatrial arrest in HRV loci

Keywords: heart rate variability, CRISPR-Cas9, zebrafish, sinoatrial arrest, GWAS

**ABSTRACT**

A meta-analysis of genome-wide association studies (GWAS) recently identified eight loci that are associated with heart rate variability (HRV) in data from 53,174 individuals. However, functional follow-up experiments - aiming to identify and characterize causal genes in these loci - have not yet been performed. We developed an image- and CRISPR-Cas9-based pipeline to systematically characterize candidate genes for HRV in live zebrafish embryos and larvae. Nine zebrafish orthologues of six human candidate genes were targeted simultaneously in fertilized eggs from fish that transgenically express GFP on smooth muscle cells (Tg(*acta2:GFP*)), to visualize the beating heart. An automated analysis of 30s recordings of 384 live zebrafish atria at 2 and 5 days post-fertilization helped identify genes that influence HRV (*kiaa1755* and *gngt1*); heart rate (*kiaa1755*); sinoatrial pauses and arrests (*syt10*, *hcn4* and *kiaa1755*); and early cardiac development (*gngt1, neo1a*). Hence, comprehensively characterizing candidate genes in GWAS-identified loci for HRV *in vivo* helped us identify previously unanticipated culprits for life-threatening cardiac arrhythmias.

51 **INTRODUCTION**

52 Heart rate variability (HRV) reflects the inter-beat variation of heart rate. HRV is
53 controlled by the sinoatrial node, which receives input from the autonomic nervous
54 system. Autonomic imbalance, which has been associated with work stress and other
55 modifiable or non-modifiable risk factors (Thayer et al. 2010), is reflected in lower
56 HRV. Lower HRV has been associated with higher cardiac morbidity and mortality
57 (de Bruyne et al. 1999), and with a higher risk of all-cause mortality (Dekker et al.
58 1997). HRV can be quantified non-invasively using the RR interval of a 12-lead ECG,
59 making HRV a useful clinical marker for perturbations of the autonomic nervous
60 system. However, the genetic basis of HRV remains largely elusive.

61 Recently, we and others identified the first loci that are robustly associated with
62 HRV, using a meta-analysis of genome-wide association studies (GWAS) with data
63 from 53,174 participants (Nolte et al. 2017). Eleven of the 17 associated single
64 nucleotide polymorphisms (SNPs) overlapped with loci that we previously identified
65 as being associated with resting heart rate (den Hoed et al. 2013). The heart rate
66 associated loci in turn had on aggregate been associated with altered cardiac
67 conduction and risk of sick sinus syndrome (den Hoed et al. 2013). *In silico*
68 functional annotation of the five loci that are associated with both HRV (Nolte et al.
69 2017) and heart rate (den Hoed et al. 2013) previously resulted in the prioritization of
70 six candidate genes that are anticipated to be causal (Nolte et al. 2017). Functional
71 follow-up experiments - ideally *in vivo* - are required to conclude if these genes are
72 indeed causal, and examine if they influence HRV, heart rate, and/or cardiac
73 conduction.

74 Mouse models are commonly used in cardiac research, but mice show substantial
75 differences in cardiac rate and electrophysiology compared with humans (Poon and

76 Brand 2013). Inherently, these differences complicate extrapolation of results from
77 mouse models to humans (Poon and Brand 2013). Additionally, rodents are not
78 suitable for high-throughput, *in vivo* screens of cardiac rhythm and rate. Such screens
79 are essential to systematically characterize positional candidate genes in the large
80 number of loci that have now been identified by GWAS for cardiac rhythm, rate
81 (Eppinga et al. 2016) and conduction (Arking et al. 2014). Hence, novel model
82 systems that facilitate systematic, *in vivo* characterization of a large number of
83 candidate genes are desirable.

84 In recent years, the zebrafish has become an important model system for genetic
85 and drug screens for human disease (Lieschke and Currie 2007; MacRae and Peterson
86 2015). Amongst the many advantages of zebrafish larvae as a model system are their
87 short generation time, large number of offspring produced regularly, relatively low
88 maintenance costs, rapid early development, and optical transparency. Zebrafish have
89 a fully functional, beating heart at ~24 hours post-fertilization, and the ECG of the
90 two-chambered zebrafish heart is comparable to that of humans (Liu et al. 2016).
91 Fluorescently labeled transgenes facilitate visualization of cell types and tissues of
92 interest, which can now be accomplished in high-throughput thanks to advances in
93 automated positioning of non-embedded, live zebrafish embryos (Pardo-Martin et al.
94 2013). In addition, the zebrafish has a well-annotated genome, with orthologues of at
95 least 71.4% of human genes (Howe et al. 2013). These genes can be targeted
96 efficiently and in a multiplexed manner (i.e. in multiple genes simultaneously) thanks
97 to recent advances in Clustered, Regulatory Interspaced, Short Palindromic Repeats
98 (CRISPR) and CRISPR-associated systems (Cas) (Varshney et al. 2016). All
99 characteristics combined make zebrafish embryos an attractive model system to
100 systematically characterize candidate genes for cardiac rhythm, rate and conduction.

101 The aim of this study was to objectively characterize the most promising candidate
102 genes in GWAS-identified loci for HRV and heart rate for a role in cardiac rhythm,
103 rate and function using a large-scale, image-based screen in zebrafish embryos and
104 larvae.
105

106 **RESULTS**

107 *Experimental pipeline*

108 Our experimental pipeline is outlined in Figure 1. Founder mutants ($F_0$ generation)
109 were generated in which all nine zebrafish orthologues of six human candidate genes
110 were targeted using a multiplexed CRISPR-Cas9 approach (Table 1, Supplemental
111 Table S1) (Varshney et al. 2016). Generating mutants in a background with a
112 transgenically expressed fluorescent label on smooth muscle cells (Tg(*acta2*:*gfp*))
113 allowed us to visualize the beating atrium with minimal background noise. $F_0$ mutants
114 were in-crossed, and the atria of 384 $F_1$ embryos were recorded for 30s at 2 days post
115 fertilization (dpf). In addition, we captured bright field images of the embryos to
116 quantify body length, surface area and volume. Of the 384 imaged embryos, 326 were
117 imaged again at 5dpf (Supplemental Fig. S1), to capture genetic effects on cardiac
118 outcomes and body size at two key stages of early cardiac development (Hou et al.
119 2014).

120

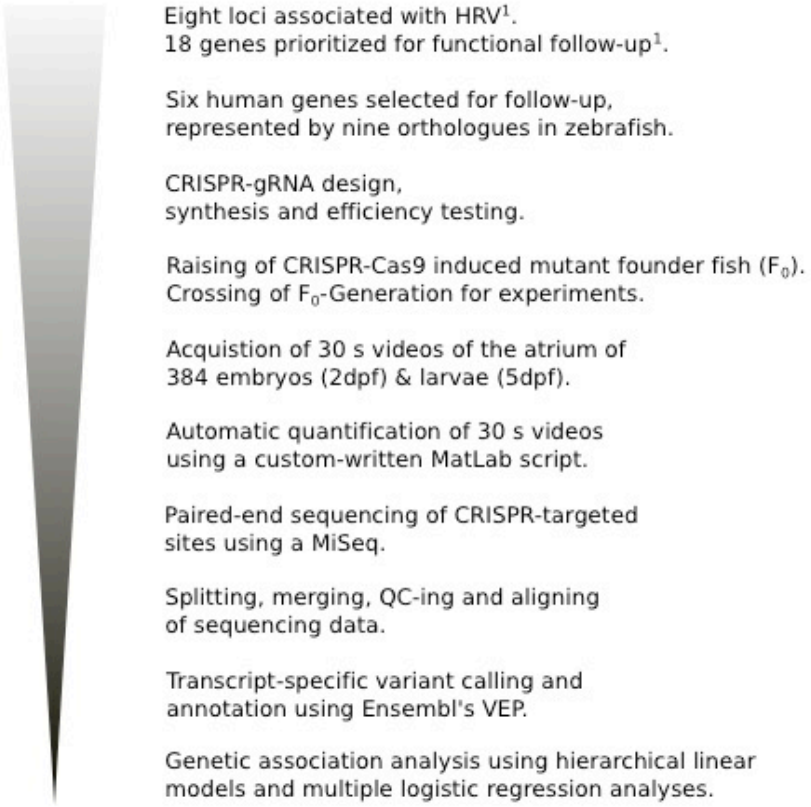


**Fig. 1**: Experimental pipeline describing the workflow from candidate gene selection to trait association. dpf = days post fertilization. VEP = Variant Effect Predictor.
1: Nolte et al. 2017

**Table 1: Selected candidate genes and their zebrafish orthologues in GWAS-identified heart rate variability associated loci**

| rsID | Chr | Human gene | ENSG | Zebrafish orthologue | ENSDARG |
|---|---|---|---|---|---|
| rs4262, rs180238 | 7 | *GNG11* | ENSG00000127920 | *gngt1* | ENSDARG00000035798 |
| rs7980799, rs1351682, rs1384598 | 12 | *SYT10* | ENSG00000110975 | *syt10* | ENSDARG00000045750 |
| rs4899412, rs2052015, rs2529471, rs36423 | 14 | *RGS6* | ENSG00000182732 | *rgs6* | ENSDARG00000015627 |
| rs2680344 | 15 | *HCN4* | ENSG00000138622 | *hcn4* | ENSDARG00000061685 |
| | | | | *hcn4l* | ENSDARG00000074419 |
| rs1812835 | 15 | *NEO1* | ENSG00000067141 | *neo1a* | ENSDARG00000102855 |
| | | | | *neo1b* | ENSDARG00000075100 |
| rs6123471 | 20 | *KIAA1755* | ENSG00000149633 | *quo (kiaa1755_1)* | ENSDARG00000073684 |
| | | | | *si:dkey-65j6.2 (kiaa1755_2)* | ENSDARG00000103586 |

rsID refers to the lead SNP(s) of the GWAS-identified loci (Nolte et. al, 2017). Multiple independent SNPs per locus can be present. For simplicity, *quo* is referred to as *kiaa1755_1*, and *si:dkey-65j6.2* as *kiaa1755_2*.

*Descriptive information*

At 2dpf, some embryos showed sinoatrial pauses (n=39, 10.3%**,** Supplemental Movie S1) and arrests (n=36, 9.5%, Supplemental Movie S2); cardiac edema (n=15, 4.0%); or uncontrolled atrial contractions (n=1, 0.2%, Supplemental Movie S3). At 5dpf, a subset of larvae displayed sinoatrial pauses (n=9, 2.7%); sinoatrial arrests (n=3,

128 0.9%); cardiac edema (n=14, 4.2%); uncontrolled atrial contractions (n=9, 2.7%); or
129 an abnormal cardiac morphology and impaired cardiac contractility (n=6, 1.8%,
130 Supplemental Movie S4). In the 279 embryos without cardiac abnormalities that
131 survived quality control at 2dpf (Supplemental Fig. S1), HRV was 15.5±10 ms
132 (mean±SD) and heart rate 208±24 bpm. In the 291 larvae included in the analysis at
133 5dpf, HRV was 13.18±17.06 ms and heart rate 265±35 bpm (Table 2).

**Table 2: Descriptive information on HRV and heart rate at 2 and 5dpf**

| Age | Trait | Mean | SD | 1st | Median | 3rd |
|---|---|---|---|---|---|---|
| 2 | SDNN | 19.52 | 12.60 | 9.84 | 17.39 | 26.55 |
| | RMSSD | 11.60 | 8.93 | 6.43 | 8.73 | 13.12 |
| | HRV | 15.56 | 10.04 | 8.74 | 12.96 | 19.65 |
| | HR | 208 | 24 | 192 | 207 | 225 |
| 5 | SDNN | 13.30 | 17.18 | 5.18 | 7.60 | 11.72 |
| | RMSSD | 13.05 | 18.26 | 5.93 | 7.48 | 12.01 |
| | HRV | 13.18 | 17.06 | 5.65 | 7.72 | 12.06 |
| | HR | 265 | 35 | 244 | 261 | 286 |

Information based on data from 279 embryos at 2 days post-fertilization (dpf) and 291 larvae at 5 dpf. HRV was calculated by averaging SDNN and RMSSD. HRV, SDNN and RMSSD are shown in ms, whereas HR is shown in beats per min. 1st and 3rd refers to the respective quartile. HRV: heart rate variability; SDNN: standard deviation of the normal-to-normal interval; RMSSD: root mean square of successive heart beat interval differences; HR: heart rate.

134

135 After imaging at 5dpf, all larvae were sequenced at the nine CRISPR-Cas9
136 targeted and three putative off-target sites (2x250 bp paired end), and transcript-
137 specific dosages were calculated by weighting the number of mutated alleles by their
138 predicted impact on protein function based on Ensembl's variant effect predictor
139 (VEP). At the three putative off-target sites, no CRISPR-Cas9 induced mutations
140 were identified (Supplemental Table S2). A total of 164 unique mutations were
141 identified across the nine CRISPR-targeted sites, ranging from three unique mutations
142 in *hcn4l* to 37 in *kiaa1755_2* (Supplemental Table S3). Frameshift mutations were
143 most common (48.5%), followed by missense variants (24.5%), in-frame deletions
144 (14.7%), and synonymous variants (5.5%). Eighty-five, sixty-nine and nine variants
145 were predicted to have a high, moderate, and low impact on protein function,

146 respectively (Supplemental Table S3). Mutant allele frequencies ranged from 4.1%
147 for *hcn4l* to 92.0% for *neo1b* (Supplemental Table S4).

148

149 *Genetic effects on cardiac rhythm, rate and function*

150 We examined the effect of the induced mutations on HRV and heart rate after
151 excluding cases with cardiac abnormalities that would drive effects on HRV and heart
152 rate, i.e. sinoatrial pauses or arrests, uncontrolled atrial contractions, cardiac edema,
153 and abnormal cardiac morphology or contractility (primary analyses, Supplemental
154 Fig. S1). We also examined the impact of mutations on cardiac abnormalities for
155 events that affected at least five embryos (2dpf) or larvae (5dpf), and we examined the
156 effect of mutations on body size (secondary analyses, Supplemental Fig. S1).

157 Each additional mutated allele in *gngt1* was associated with higher odds of
158 abnormal cardiac morphology and impaired cardiac contractility at 2dpf
159 (Supplemental Table S5), as well as with higher odds of cardiac edema and a higher
160 HRV at 5dpf (Figure 2, Supplemental Table S6-S7). *Gngt1* mutants also had a smaller
161 dorsal body surface area at 5dpf.

162 Each additional mutated allele in the main transcript of *kiaa1755_1* was associated
163 with a higher HRV and a trend for a higher heart rate at 2dpf (Figure 2, Supplemental
164 Tables S6-S7). Mutations in *kiaa1755_1* were also associated with a larger body
165 volume at 5dpf (Supplemental Table S8). Embryos with mutations in *kiaa1755_2*
166 tended to be shorter and smaller at 2dpf (Supplemental Table S8), and had higher
167 odds of sinoatrial pauses and a higher heart rate at 5dpf (Figure 2, Supplemental
168 Tables S5-S7).

169 Each additional mutated allele in *hcn4* was associated with higher odds of
170 sinoatrial pauses and arrests at 2dpf (Supplemental Table S5). In larvae free from
171 severe cardiac abnormalities, each additional mutated allele in *hcn4* was associated
172 with a trend for higher heart rate at 5dpf (Figure 2, Supplemental Tables S6-S7),
173 without affecting body size (Supplemental Table S8). Mutations in *hcn4l* were
174 positively associated with lateral body surface area at 5dpf (Supplemental Table S8),
175 but not with cardiac rhythm, rate, or abnormalities at 2dpf or 5dpf.

176 Mutations in *neo1a* and *neo1b* did not affect cardiac rhythm, rate, or abnormalities
177 at 2dpf. However, embryos with mutations in *neo1a* tended to be shorter and had a
178 larger dorsal body surface area normalized for length. Embryos with mutations in
179 *neo1b* had a larger lateral body surface area at 2dpf. At 5dpf, mutations in *neo1a* were
180 associated with lower odds of abnormal cardiac morphology and impaired cardiac
181 contractility, uncontrolled atrial contractions (trend), and edema (Supplemental Table
182 S5), but not with body size.

183 Each additional mutated allele in *syt10* was associated with higher odds of a
184 sinoatrial pause at 2dpf (Supplemental Table S5), but did not affect HRV, heart rate
185 or body size (Supplemental Tables S6-S8).

186

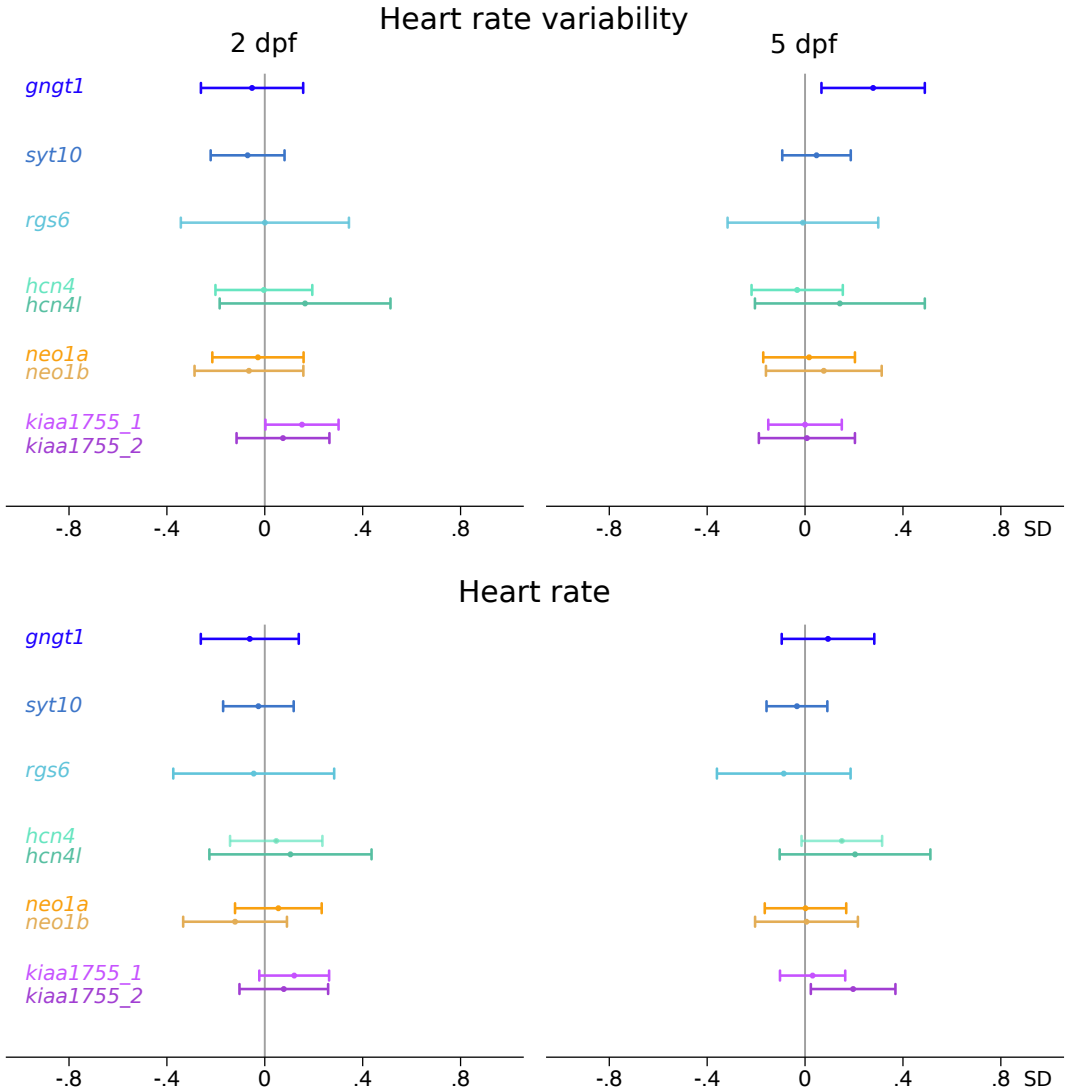


**Fig. 2**: Effect of mutations in candidate genes on heart rhythm and rate at 2 (n=279) and 5dpf (n=291). Dots and whiskers show the effect size and its 95% confidence interval for each additional mutated allele, weighted by its predicted effect on protein function. Effects were adjusted for the number of mutated alleles in the other genes, as well as for heart rate or heart rate variability and time of day (fixed factor), with larvae nested in batches (random factor). Genes are ordered by chromosomal position in humans.

Five of the six human candidate genes taken forward for experimental follow-up showed at least one relevant cardiac phenotype in zebrafish embryos or larvae (i.e. *GNGT1*, *SYT10*, *HCN4*, *NEO1*, *KIAA1755*). Only a trend towards an effect - on sinoatrial pauses at 2dpf - was observed for the *RGS6* orthologue, for which the mutant allele frequency was only 4%. We next examined the druggability of the five genes for which we showed most evidence of a causal role using the drug-gene interaction (DGI) database. This only highlighted *HCN4* as being druggable (Cotto et

195 al. 2018). Indeed, ivabradine is already being used as an open channel blocker of
196 *HCN4* (Böhm et al. 2010). We next identified interaction partners of the proteins
197 encoded by the five genes using GeneMania (Warde-Farley et al. 2010) and STRING
198 (Szklarczyk et al. 2017). A total of 49 interacting partners were identified, 31 of
199 which were considered to be druggable or belong to a "favorable" protein family.
200 Seven of these are targeted by FDA-approved medication (Supplemental Table S9),
201 amongst which are several anti-hypertensive agents (e.g. Telmisartan, Iloprost and
202 Diazoxide), as well as a neuromuscular blocking agent (i.e. Botulinum toxin type A).
203 It would be worthwhile to examine if these agents can be repurposed to prevent
204 cardiac arrhythmias in individuals at risk, or whether cardiac arrhythmias represent
205 on-target, adverse side effects of these drugs.
206

207 **DISCUSSION**

208 Large-scale, *in vivo* follow-up studies of candidate genes in GWAS-identified loci
209 remain sparse. Here we present an objective, image-based pipeline to systematically
210 characterize candidate genes for cardiac rhythm, rate, and conduction-related
211 disorders. Using a zebrafish model system, we identified orthologues of genes in
212 HRV and heart rate associated loci that influence not only the complex traits for
213 which they were identified (i.e. *kiaa1755*, *gngt1*), but also body size (*kiaa1755, hcn4,*
214 *gngt1, neo1a*, *neo1b*), early cardiac development (*gngt1, neo1a*, *neo1b*), and/or the
215 odds of sinoatrial pauses and arrests (*hcn4, syt10, kiaa1755*). These results add weight
216 to the notion that GWAS-identified common variants for complex traits can flag
217 genes for which rare, detrimental mutations cause severe, early-onset disorders
218 (Arking et al. 2014; Flannick et al. 2016; Ganna et al. 2018). We show here that
219 systematic characterization of candidate genes in GWAS-identified loci for complex
220 traits using an image- and CRISPR-Cas9-based zebrafish model system can help
221 identify clinically relevant causal genes, and aid confirmation of the role of such
222 genes in whole-exome sequencing efforts in humans by reducing the multiple testing
223 burden (Flannick et al. 2018).

224 The HRV increasing T-allele of rs4262 in the 5' untranslated region of *GNG11* is
225 associated with a lower expression of *GNG11* in the tibial artery, atrial appendage and
226 aorta (GTEx (Battle et al. 2017)). This is directionally consistent with 5dpf *gngt1*
227 mutant zebrafish larvae - i.e. mutants for the zebrafish orthologue of the human
228 paralogues *GNGT1* and *GNG11* (Lagman et al. 2012) - having a higher HRV. *GNG11*
229 encodes the γ-subunit of a G-protein complex, which interacts with G-protein-coupled
230 inwardly rectifying potassium channels (GIRKs) that transduce signals rapidly
231 enough to induce changes in HRV (Mark and Herlitze 2000). The zebrafish heart

232 normally has a tube-like appearance at 28 hours post fertilization (hpf) (Bakkers
233 2011). Higher odds of abnormal cardiac morphology, contractility and edema with
234 each additional mutated *gngt1* allele at 5 but not 2dpf suggests that this gene affects
235 cardiac development between 2 and 5dpf.

236 Non-synonymous SNPs in *KIAA1755* have been identified in GWAS for HRV
237 (Nolte et al. 2017) and heart rate (den Hoed et al. 2013). In humans, the C-allele of
238 the HRV-associated rs6123471 in the 3' UTR of *KIAA1755* is associated with a lower
239 expression of *KIAA1755* in brain and aorta (GTEx (Battle et al. 2017)), a higher HRV
240 (Nolte et al. 2017), and a lower heart rate (den Hoed et al. 2013). Our results show
241 that mutations in *kiaa1755_1* predispose to a higher HRV and, in a sensitivity
242 analysis, a higher heart rate at 2dpf. Mutations in *kiaa1755_2* on the other hand result
243 in a higher heart rate and higher odds of sinoatrial pauses at 5dpf. Hence, a higher
244 HRV at 2dpf for each additional mutated allele in *kiaa1755_1* is directionally
245 consistent with results in humans, while the effects of mutations in *kiaa1755_1* and
246 *kiaa1755_2* on heart rate are not. Genetic effects on HRV and heart rate were
247 mutually adjusted in our study, which may have revealed the unbiased direction of
248 effect for mutations in *KIAA1755* on heart rate. In other words: the GWAS-identified
249 association of the *KIAA1755* locus - and possibly other loci - with heart rate may have
250 been driven by HRV. This would explain why the eleven HRV-associated loci that
251 showed evidence of an association with heart rate all did so in the expected (i.e.
252 opposite) direction from a phenotypic point of view (Nolte et al. 2017). *KIAA1755* is
253 a previously uncharacterized gene that shows a broad expression pattern, including
254 different brain regions and the left atrial appendage (GTEx (Battle et al. 2017)).
255 Future mechanistic studies are required to distill how *KIAA1755* influences heart
256 rhythm and rate.

257 The locus harboring *HCN4* has been flagged in GWAS for HRV (Nolte et al.
258 2017), heart rate (den Hoed et al. 2013) and atrial fibrillation (Ellinor et al. 2012).
259 *HCN4* is arguably the most well-characterized gene in the context of cardiac rhythm.
260 It belongs to the family of "funny" channels, aptly named for being activated upon
261 hyperpolarization. It is expressed in the sinoatrial node (Ludwig et al. 1999; Shi et al.
262 1999) and plays an important role in cardiac pace making (Stieber et al. 2003). The
263 heart-rate lowering agent ivabradine (Bucchi et al. 2013) is an open channel blocker
264 of *HCN4*, and reduces cardiovascular and all-cause mortality in heart failure patients
265 (Swedberg et al. 2010). Hcn4$^{-/-}$ mice die prenatally, and analyses of their hearts show
266 no arrhythmias and a lower heart rate compared with wildtype and heterozygotes
267 (Stieber et al. 2003). In line with this, humans that are heterozygous for an *HCN4* loss
268 of function mutation are typically characterized by bradycardia. We identified nine
269 zebrafish embryos that were compound heterozygous for mutations in *hcn4*, and one
270 embryo that was compound heterozygous for *hcn4l*, without a deviation from HWE
271 for either gene (Supplemental Table S4). Four of the nine compound heterozygous
272 larvae for *hcn4*, and six of the eight larvae that were heterozygous for mutations in
273 *hcn4* as well as *hcn4l* showed a sinoatrial arrest before or during the atrial recording at
274 2dpf. Zebrafish embryos can survive without a functional heart at this stage, thanks to
275 tissue oxygenation by diffusion (Burggren and Pinder 1991). This allowed us to
276 witness genetically driven cardiac arrests that would have been lethal in embryos of
277 other species. At 5dpf, larvae carrying mutations in *hcn4* that were free from severe
278 cardiac abnormalities tended to have a higher heart rate than larvae without CRISPR-
279 induced mutations. This unexpected result may reflect overcompensation by *hcn4l* or
280 cardiac compensation in response to unobserved sinoatrial arrests outside the 30s
281 recording.

282 In addition to the locus in *HCN4*, the GWAS for HRV identified an independent
283 locus in the adjacent *NEO1* (Nolte et al. 2017). Neogenin-1 is a transmembrane
284 receptor that is involved in cell migration, angiogenesis and neuronal survival
285 (reviewed by Wilson et al. (Wilson and Key 2007)). In line with our results,
286 morpholino-mediated knockdown of *neo1a* expression in zebrafish larvae was
287 previously shown to result in shorter, thicker larvae due to defects in somitogenesis,
288 with loss of neuronal differentiation due to malformation of the neural tube
289 (Mawdsley et al. 2004). *NEO1* has a pro-apoptotic function in humans (Wilson and
290 Key 2007), so the cardioprotective effect we observed in 5dpf mutants may result
291 from inefficient propagation of apoptotic signals by specific effectors. Inhibiting
292 NEO1 in early development may thus help protect cardiac integrity - perhaps
293 temporarily - but will likely have adverse effects due to inadequate apoptosis at later
294 stages of development.

295 *SYT10* belongs to the family of synaptogamins: transmembrane proteins that are
296 involved in regulation of membrane trafficking in neurons (Sudhof 2002), which is
297 important for neurotransmitter release (Chapman 2008). Variants in/near *SYT10* have
298 previously been associated with HRV (Nolte et al. 2017) as well as with heart rate
299 (den Hoed et al. 2013) and heart rate recovery (Verweij et al. 2018). We observed an
300 effect of mutations in *syt10* on the odds of sinoatrial pauses at 2dpf. Since *SYT10* is
301 mainly expressed in brain, tibial nerve and pituitary (GTEx (Battle et al. 2017)),
302 mutations in *syt10* may affect the odds of sinoatrial pauses through altered
303 neurotransmitter release.

304 Of the five genes for which we show causal effects, only *HCN4* is highlighted as
305 being druggable by DGIdb. The protein encoded by *HCN4* has already been targeted
306 using several compounds (Stieber et al. 2006). Although four of the five causal genes

307 are not highlighted as being druggable by current pharmaceutical standards, targeting
308 via antisense oligonucleotides or antibodies can still be explored. Expanding our
309 search revealed several druggable interaction partners of causal genes that are already
310 targeted by FDA-approved anti-hypertensive and neuromuscular blocking agents,
311 amongst others. For existing drugs that target interaction partners of the five causal
312 genes, it is worthwhile examining their effect on cardiac rhythm, rate and
313 development, since repurposing FDA-approved drugs would imply the quickest and
314 safest route to the clinic, while quantifying possibly unknown adverse side effects
315 would also be informative.

316 A few limitations of our study should be discussed. Firstly, acquiring 30s
317 recordings implies that false negatives for sinoatrial pauses or arrests are inevitable. In
318 fact, we observed 54 pauses or arrests at 2dpf (14.3%) and eight at 5dpf (2.5%) while
319 positioning the larva for imaging, without observing abnormalities during the
320 subsequent 30s recording. This suggests that at least 15.9% of all embryos without a
321 sinoatrial pause at 2dpf are false negatives, which negatively affects the statistical
322 power to find genetic effects. This limitation will have resulted in conservative effect
323 estimates. Secondly, CRISPR guide-RNAs with predicted off-targets free from
324 mismatches were avoided. However, two of the selected targets - i.e. for *hcn4* and
325 *kiaa1755_2* - have exonic off-targets with three mismatches (Supplemental Table S1).
326 Human orthologues of potential off-targets *dclk1* and *galnt10* have previously been
327 associated with heart-rate variability-related traits (Newton-Cheh et al. 2007) (*dclk1*),
328 as well as with carotid intima-media thickness (Dong et al. 2015) and body mass
329 index (Locke et al. 2015; Justice et al. 2017; Ng et al. 2017) (*galnt10*). Sequencing
330 larvae at the three predicted off-target regions did not show any CRISPR-Cas9
331 induced mutations (Supplemental Table S2). In line with predictions by Varshney *et*

332 *al*., off-target effects are thus unlikely to have influenced our results (Varshney et al.
333 2015). Thirdly, we in-crossed mosaic founder mutants ($F_0$) and phenotypically
334 screened and sequenced the $F_1$ generation. For some genes, this yielded a small
335 number of larvae with 0 or 2 mutated alleles (i.e. *rgs6*, *hcn4*, and *hcn4l*), resulting in
336 a lower power to find true genetic effects for these genes. In spite of this limitation,
337 we were able to detect significant effects of mutations in all genes except *rgs6*, for
338 which we observed a trend for an effect on the odds of sinoatrial pauses at 2dpf.
339 Furthermore, screening the $F_0$ or $F_2$ generation instead has its own advantages and
340 disadvantages, and we argue that non-conclusive results for a small subset of
341 candidate genes in the primary screen is not problematic when aiming to
342 systematically characterize a large number of candidate genes. Finally, we recorded
343 the atrium only, to enable a higher frame rate, a higher resolution in time for HRV,
344 and a higher statistical power to detect small genetic effects on HRV. As a result, any
345 ventricular abnormalities were not registered, and uncontrolled atrial contractions
346 may thus reflect atrial fibrillation, premature atrial contractions, high atrial rate, or
347 atrial tachycardia. Additional studies with a larger frame and longer acquisition time
348 are required to replicate and clarify the effect of mutations in *neo1a* on uncontrolled
349 atrial contractions.

350 Our study benefits from a repeated measures design, which enabled us to capture
351 genetic effects at different stages of early development in zebrafish. Furthermore, the
352 throughput of the setup allowed us to examine the effect of multiple genes
353 simultaneously, in an unprecedented sample size for *in vivo* genetic screens. Our
354 results demonstrate that a large sample size is paramount to robustly detect genetic
355 effects on complex traits in zebrafish embryos and larvae, even for functional
356 knockout mutations. Identifying CRISPR-Cas9-induced mutations allele-specifically

357 helped us classify larvae as heterozygous and compound heterozygous, which in turn
358 helped pinpoint the true effect of mutations in these genes.

359 Our study is based on an objective, high-throughput imaging approach and aimed
360 to identify and characterize causal genes in GWAS-identified loci for HRV. In all
361 genes that show an effect on HRV (*kiaa1755* and *gngt1*), directions of effect were
362 directionally consistent with eQTL associations in humans (based on GTEx (Battle et
363 al. 2017)). This emphasizes the merit of our model system and the robustness of our
364 findings. Furthermore, our results extend beyond the complex outcomes for which
365 these genes were prioritized, and helped identify *KIAA1755*, *HCN4* and *SYT10* as
366 likely effectors of detrimental mutations that predispose to sinoatrial pauses and
367 arrests.

368

369 **METHODS**

370 *Candidate gene selection*

371 Candidate genes in GWAS-identified loci for HRV were identified as described in
372 detail in Nolte et al. (2017). Of the 18 identified candidate genes, six were selected for
373 experimental follow-up. This selection was based on overlap with findings from
374 GWAS for heart rate (*KIAA1755*, *SYT10*, *HCN4*, *GNG11*) (den Hoed et al. 2013), as
375 well as with results from eQTL analyses in sinoatrial node and brain (*RGS6*).
376 Additional candidate genes from the same or nearby loci were also selected for
377 experimental follow-up, i.e. *NEO1*, which resides next to *HCN4*. Zebrafish
378 orthologues of the human genes were identified using Ensembl, as well as using a
379 comprehensive synteny search using Genomicus (Louis et al. 2015) (Supplemental
380 Table S1). Of the selected genes, *GNG11*, *SYT10* and *RGS6* have one orthologue in
381 zebrafish, and *KIAA1755*, *HCN4* and *NEO1* each have two orthologues, resulting in a
382 total of nine zebrafish orthologues for six human candidate genes (Table 1). For
383 simplicity, the *KIAA1755* orthologues *quo* and *si:dkey-65j6.2* have been referred to as
384 *kiaa1755_1* and *kiaa1755_2*.

385

386 *Mutagenesis*

387 All nine zebrafish genes were targeted together using a multiplexed CRISPR-Cas9
388 approach described recently (Varshney et al. 2016). Briefly, guide-RNAs (gRNAs)
389 were selected using ChopChop (Labun et al. 2016) and CRISPRscan (Moreno-Mateos
390 et al. 2015) (Supplemental Table S1), based on their predicted efficiency, a moderate
391 to high GC-content, location in an early exon, and absence of predicted off-target
392 effects without mismatches. Oligonucleotides were designed as described (Varshney

393 et al. 2016), consisting of a T7 or SP6 promotor sequence (for gRNAs starting with
394 'GG' or 'GA', respectively), a gene-specific gRNA-target sequence, and an overlap
395 sequence to a generic gRNA. The gene-specific oligonucleotides were annealed to a
396 generic 80 bp long oligonucleotide at 98°C for 2 mins, 50°C for 10 mins, and 72°C
397 for 10 mins. The products were checked for correct length on a 2% agarose gel. The
398 oligonucleotides were subsequently transcribed *in vitro* using the manufacturer's
399 instructions (TranscriptAid T7 high yield transcription kit / MEGAscript SP6
400 transcription kit, both ThermoFisher Scientific, Waltham, USA). The gRNAs were
401 purified, after which the integrity of the purified gRNAs was examined on a 2%
402 agarose gel. The zebrafish codon-optimized plasmid pT3TS-nls-zCas9-nls was used
403 as a template to produce Cas9 mRNA (Jao et al. 2013). The plasmid was linearized
404 with Xba1, and then purified using the Qiaprep Spin Miniprep kit (Qiagen, Hilden,
405 Germany). The DNA was transcribed using the mMESSAGE mMACHINE T3
406 Transcription Kit (ThermoFisher Scientific, Waltham, USA), followed by LiCl
407 precipitation. The quality of the RNA was confirmed on a 1% agarose gel.

408

409 *Husbandry & microinjections*

410 A zebrafish line with GFP-labelled α-smooth muscle cells Tg(*acta2*:GFP) (Whitesell
411 et al. 2014) was used to visualize the beating heart. To this end, eggs from an in-cross
412 of Tg(*acta2*:GFP) fish were co-injected with a mix of Cas9 mRNA (final
413 concentration 150 ng/µl) and all nine gRNAs (final concentration 25 ng/µl each) in a
414 total volume of 2nL at the single-cell stage. CRISPR-Cas9 injected embryos were
415 optically screened for the presence of Tg(*acta2*:GFP) at 2 days post fertilization (dpf),
416 using an automated fluorescence microscope (EVOS FL Cell imaging system,
417 ThermoFisher Scientific, Waltham, USA). Tg(*acta2*:GFP) carriers were retained and

418 raised to adulthood in systems with circulating, filtered and temperature controlled
419 water (Aquaneering, Inc, San Diego, CA). All procedures and husbandry were
420 conducted in accordance with Swedish and European regulations, and have been
421 approved by the Uppsala University Ethical Committee for Animal Research
422 (C142/13 and C14/16).

423

424 *Experimental procedure imaging*

425 The founder mutants ($F_0$ generation) were only used for reproduction. After crossing
426 the founder mutants, $F_1$ embryos were used for experiments. Eggs were collected after
427 $F_0$ fish were allowed to reproduce for 45 mins to minimize variation in developmental
428 stage. Fertilized eggs were placed in an incubator at 28.5°C. At 1dpf, embryos were
429 dechorionated using pronase (Roche Diagnostics, Mannheim, Germany).

430 At 2dpf, embryos were removed from the incubator and allowed to adapt to controlled
431 room temperature (21.5 °C) for 20 mins. Individual embryos were exposed to 100
432 µg/ml Tricaine (MS-222, Sigma-Aldrich, Darmstadt, Germany) for 1 min before
433 being aspirated, positioned in the field of view of a fluorescence microscope, and
434 oriented dorsally using a Vertebrate Automated Screening Technology (VAST)
435 BioImager (Union Biometrica Inc., Geel, Belgium). We subsequently acquired twelve
436 whole-body images, one image every 30 degrees of rotation, using the camera of the
437 VAST BioImager to quantify body length, dorsal and lateral surface area and volume,
438 as well as the presence or absence of cardiac edema. The VAST BioImager then
439 positioned and oriented the larva to visualize the beating atrium and triggered the
440 upright Leica DM6000B fluorescence microscope to start imaging using a HCX APO
441 L 40X/0.80 W objective and L5 ET, k filter system (Micromedic AB, Stockholm,

442 Sweden). Images of the beating atrium were acquired for 30s at a frame rate of 152
443 frames/s using a DFC365 FX high-speed CCD camera (Micromedic AB, Stockholm,
444 Sweden). After acquisition, the larvae were dispensed into a 96-well plate, rinsed
445 from tricaine, and placed back into the incubator. The procedure was repeated at 5dpf
446 (i.e. the larval stage), to allow genetic effects that influence HRV and heart rate
447 differently at different stages of development to be captured (Hou et al. 2014). After
448 imaging at 5dpf, the larvae were once again dispensed into 96-well plates, sacrificed,
449 and stored at -80°C for further processing.

450

451 *Quantification of cardiac traits and body size*

452 A custom-written MATLAB script was used to convert the images acquired by the
453 CCD camera into quantitative traits. To acquire the heart rate, each frame of the
454 sequence was correlated with a template frame. The repeating pattern yields a
455 periodic graph from the correlation values and by detecting the peaks in the graph we
456 can assess the heart rate. The template frame should represent one of the extreme
457 states in the cardiac cycle, i.e. end-systole or end-diastole. To detect these frames, we
458 examined the correlation between the first 100 frames. The combination of frames
459 that showed the lowest correlation corresponded to the heart being in opposite states.
460 One of these frames was chosen as the template (Niazi et al. 2009).

461 This numeric information was subsequently used to quantify: 1) heart rate as the
462 inverse of RR-interval; 2) the standard deviation of the normal-to-normal RR interval
463 (SDNN); and 3) the root mean square of successive heart beat interval differences
464 (RMSSD). Finally, a graph of pixel changes over time was generated across the 30s
465 recording to help annotate the script's performance. The files containing the inter-

466 beat-intervals were used to objectively quantify sinoatrial pauses (i.e. the atrium stops
467 beating for longer than 3x the median inter-beat-interval of the larva, Supplemental
468 Movie S1) and sinoatrial arrests (i.e. the atrium stops beating for longer than 2s,
469 Supplemental Movie S2) using a custom-written Stata script. The graphs of pixel
470 changes over time were also used to identify larvae with other abnormalities in
471 cardiac rhythm. Such abnormalities were annotated as: uncontrolled atrial
472 contractions (Supplemental Movie S3); abnormal cardiac morphology (i.e. a tube-like
473 atrium, Supplemental Movie S4); or impaired cardiac contractility (i.e. a vibrating
474 rather than a contracting atrium, Supplemental Movie S4). These phenotypes were
475 annotated independently by two investigators (B.v.d.H. and M.d.H.), resulting in an
476 initial concordance rate >90%. Discrepancies in annotation were discussed and re-
477 evaluated to reach consensus.

478 Bright-field images of the larvae were used to assess body length, dorsal and lateral
479 surface area, and volume. Images were automatically segmented and quantified using
480 a custom-written CellProfiler (Lamprecht et al. 2007) pipeline, followed by manual
481 annotation for segmentation quality. Larvae with suboptimal segmentation quality due
482 to the presence of an air-bubble, a bent body, an incomplete rotation within the
483 capillary, partial capturing of the larva, or an over-estimation of size were replaced by
484 images with a 180° difference in rotation, or excluded if that image was also sub-
485 optimally segmented. The larva was excluded from the analysis for body volume if
486 more than four of the 12 images had a bad segmentation. Imaging, image
487 quantification and image quality control were all performed blinded to the sequencing
488 results.

489

490

491 *Quality control of phenotype data*

492 A series of quality control steps was performed to ensure only high-quality data was
493 included in the genetic association analysis (Supplemental Fig. S1). First, graphs
494 indicating that one or more true beats were missed by the script were removed from
495 the analysis *a priori* (Supplemental Fig. S1). Second, larvae with any secondary
496 phenotype (i.e. uncontrolled atrial contractions, sinoatrial pause or arrest, edema,
497 abnormal morphology and/or reduced contractility) were excluded from the analyses
498 for HRV and heart rate (primary analysis) (Supplemental Fig. S1). Third, genetic
499 effects on these secondary traits were examined at 2dpf and 5dpf for traits with at
500 least five cases (secondary analysis). Furthermore, embryos and larvae that showed a
501 sinoatrial pause or arrest in between positioning and video acquisition, but not during
502 the recording, were excluded from the analysis for sinoatrial pauses and arrests, since
503 we cannot ascertain case status in the same rigorous manner for such samples, but
504 they are not appropriate controls either.

505

506 *Sample preparation for sequencing*

507 After imaging at 5dpf, larvae were sacrificed by prolonged exposure to tricaine, and
508 DNA was extracted by exposure to lysis buffer (10mM Tris-HCl pH8, 50mM KCl,
509 1mM EDTA, 0.3% Tween 20, 0.3% Igepal) and proteinase K (Roche Diagnostics,
510 Mannheim, Germany) for 2 h at 55°C, followed by 10 min at 95°C to deactivate the
511 proteinase K. Gene-specific primers (150bp-300bp) amplifying gRNA-targeted and
512 putative off-target regions in *dclk1b* and both *galnt10* orthologues (Supplemental
513 Table S1) were distilled from ChopChop (Labun et al. 2016) and Primer3 (Koressaar
514 and Remm 2007), and Illumina adaptor-sequences were added. The first PCR was

515 conducted by denaturation at 98°C for 30s; amplification for 35 cycles at 98°C for
516 10s, 62°C for 30s and 72°C for 30s; followed by a final extension at 72°C for 2 mins.
517 Amplified PCR products were cleaned using magnetic beads (Mag-Bind PCR Clean-
518 up Kit, Omega Bio-tek Inc. Norcross, GA). The purified products were used as a
519 template for the second PCR, in which Illumina Nextera DNA library sequences were
520 attached to allow multiplexed sequencing of all CRISPR-targeted sites across 384
521 larvae in a single lane. The second PCR amplification was performed by denaturation
522 at 98°C for 30s; amplification for 25 cycles at 98°C for 10s, 66°C for 30s and 72°C
523 for 30s; followed by a final extension at 72°C for 2 mins. Products were then purified
524 using magnetic beads. All liquid handling was performed using a Hamilton Nimbus
525 robot equipped with a 96-head (Hamilton robotics, Kista, Sweden). Samples were
526 pooled and sequenced in a single lane on a MiSeq (300 bp paired-end, Illumina Inc.,
527 San Diego, CA) at the National Genomics Infrastructure, Sweden.

528

529 *Processing of sequencing data*

530 A custom-written bioinformatics pipeline was developed in collaboration with the
531 National Bioinformatics Infrastructure Sweden to prepare .fastq files for analysis.
532 First, a custom-written script was used to de-multiplex the .fastq files by gene and
533 well. PEAR (Zhang et al. 2014) was then used to merge paired-end reads, followed by
534 removal of low-quality reads using FastX (Pearson et al. 1997). The reads were then
535 mapped to the wildtype zebrafish genome (Zv11) using STAR (Dobin et al. 2013).
536 Next, we converted files from .sam to .bam format using samtools (Li et al. 2009),
537 after which variants - mostly indels and SNVs - were called allele specifically using a
538 custom-written variant calling algorithm in R (Danio rerio Identification of Variants
539 by Haplotype - DIVaH). A summary of all unique sequences identified for the

540 orthologues and their respective alignment report string (Concise Idiosyncratic
541 Gapped Alignment Report (CIGAR)) is shown in Supplemental Table S2. All unique
542 variants (Supplemental Table S3) located within ±30bps of the CRISPR-targeted sites
543 that were identified across the two alleles were subsequently pooled, and used for
544 functional annotation using Ensembl's VEP (McLaren et al. 2016). Transcript-
545 specific dosage scores were then calculated by retaining the variant with the highest
546 predicted impact on protein function, and assigning it a score of 0 (no effect), 0.2
547 (modifier variant), 0.33 (low), 0.66 (moderate) or 1 (high). Transcript-specific dosage
548 scores were subsequently calculated by summing the allele-specific scores at each
549 embryo and target site. Since all transcripts within a target site were affected virtually
550 identically, we only used the main transcript of each target site for the genetic
551 association analysis.

552 Most larvae had successfully called sequences in all nine CRISPR-targeted sites
553 (n=288, 75%). Of the 96 remaining embryos, 83 larvae (22%) had a missing sequence
554 at one target site, and 11 larvae (3%) had two missing sequences. The remaining two
555 larvae (0.5%) had three and four missing sequences, respectively. These two larvae
556 have been excluded from the genetic association analysis. For the remaining larvae,
557 the mean dosage of the transcript was imputed for missing calls. At a gene-level, a
558 median of 380 larvae were successfully sequenced and called across all nine main
559 transcripts, and all but one gene had successfully called mutations in ≥375 larvae. For
560 *neo1b*, calling failed in 77 larvae (Supplemental Table S4). The imputed mean dosage
561 for the main transcript of *neo1b* was still included in the genetic association analysis,
562 since the mutant allele frequency in successfully called larvae was high (i.e. 0.798),
563 and using an imputed dosage was anticipated to influence the results less than to
564 discard the gene while it had been targeted. However, the results for *neo1b* should be

565 interpreted in light of its call rate. The mutant allele frequency was low for *hcn4*,
566 *hcn4l* and *rgs6*. For the remaining orthologues we had at least 10 wildtype and 10
567 compound heterozygous mutants. All three putative off-targets regions (*dclk1b*, both
568 *galnt10* orthologues, Supplemental Table S1) were classified as wildtype across all
569 larvae and had no CRISPR-Cas9 induced mutations within ±30bps of the cut-site
570 (Supplemental Table S2).

571

572 *Interrogating the druggability of the candidate genes*

573 All human orthologues of the zebrafish genes that we found an effect for were
574 interrogated in the drug-gene interaction database (DGIdb) v3.0.2 (Cotto et al. 2018).
575 The human interaction partners of the candidates (Supplemental Table S9) were
576 distilled from STRING v10.5 (Szklarczyk et al. 2017) and GeneMania (Warde-Farley
577 et al. 2010). The GeneMania search was limited to physical interactions and pathway
578 data.

579

580 *Statistical analysis*

581 The standard deviation of NN-intervals (SDNN) and the root mean square of
582 successive differences (RMSSD) were strongly correlated at 2dpf ($r^2$=0.77) and 5dpf
583 ($r^2$=0.85), so a composite endpoint 'HRV' was calculated as the average of SDNN
584 and RMSSD. In larvae free from sinoatrial pauses and arrests, abnormal cardiac
585 morphology, impaired cardiac contractility, and edema HRV and heart rate at 2dpf
586 (n=279) or 5dpf (n=291) were inverse-normally transformed to ensure a normal
587 distribution, and to allow comparison of effect sizes across traits. Please see the
588 Supplemental methods for a detailed description of the cardiac phenotypes that were

589 used as exclusion criteria for the analysis for HRV and heart rate. Genetic effects on
590 HRV and heart rate were subsequently examined using hierarchical linear models at
591 2dpf and 5dpf separately (Stata's xtmixed), mutually adjusted for the other outcome
592 (i.e. heart rate and HRV) and time of imaging (fixed factors), and with larvae nested
593 in six batches (random factor with fixed slope). Embryos and larvae in which a
594 sinoatrial pause and/or arrest was observed in between positioning and recording were
595 excluded from the analysis (see Supplemental Table S7 for a sensitivity analysis). In
596 secondary analyses, genetic effects were examined for cardiac abnormalities that were
597 observed in ≥5 larvae at 2dpf and/or 5dpf, using a logistic regression analysis. Genetic
598 effects on body size were also examined, using hierarchical linear models on inverse-
599 normally transformed outcomes.

600 For dichotomous as well as continuous outcomes, genetic effects were examined
601 using an additive model, with dosage scores for all target sites as independent
602 exposures in the same model, i.e. mutually adjusted for effects of mutations in the
603 other orthologues. Missing genotypes were imputed at the mean in this analysis. For
604 each outcome, association analyses were examined for the main transcript of the
605 orthologue. We performed two independent primary and six independent secondary
606 tests at 2 and 5dpf – on different data – and considered *P*-values <0.05 to reflect
607 statistically significant effects. All statistical analyses were performed using Stata MP
608 14.2.
609

610 **DATA ACCESS**

611 Raw data and scripts will be made publicly available after publication if desirable.
612 Supplemental videos have been deposited at
613 https://www.dropbox.com/s/3dboz7nq3emkz6z/Supp_videos.zip?dl=0.

614

615 **ACKNOWLEDGMENTS**

616 The computations were performed on resources provided by SNIC through Uppsala
617 Multidisciplinary Center for Advanced Computational Science (UPPMAX) under
618 Project SNIC b2015283. The authors would like to acknowledge support from
619 Science for Life Laboratory, the National Genomics Infrastructure (NGI) and
620 UPPMAX for providing assistance in massive parallel sequencing and computational
621 infrastructure. Support from the National Bioinformatics Infrastructure Sweden
622 (NBIS) is also gratefully acknowledged. MdH is a fellow of the Swedish Heart-Lung
623 Foundation (20170872) and is supported by project grants from the Swedish Heart-
624 Lung Foundation (20140543, 20170678), the Swedish Research Council (2015-
625 03657), and NIH/NIDDK (R01DK106236, R01DK107786, U01DK105554).

626

627 **AUTHOR CONTRIBUTIONS**: B.v.d.H. and M.d.H. conceived the study design.
628 B.v.d.H., A.E., T.K., S.V. and S.J. performed the experiments. B.v.d.H., A.E., E.M.,
629 O.D. and M.d.H. conceived the sequencing quality control and variant calling
630 pipeline. B.v.d.H., A.A., H.L.B. and M.d.H. performed the image quantification and
631 statistical analysis. B.v.d.H. and M.d.H. wrote the manuscript. All authors provided
632 critical feedback to the manuscript.

633

## DISCLOSURE DECLARATION

There are no competing interests.

636 **REFERENCES**


637 Arking DE Pulit SL Crotti L van der Harst P Munroe PB Koopmann TT
638 Sotoodehnia N Rossin EJ Morley M Wang X et al. 2014. Genetic association
639 study of QT interval highlights role for calcium signaling pathways in
640 myocardial repolarization. *Nat Genet* **46**: 826-836.
641 Bakkers J. 2011. Zebrafish as a model to study cardiac development and human
642 cardiac disease. *Cardiovasc Res* **91**: 279-288.
643 Battle A, Brown CD, Engelhardt BE, Montgomery SB. 2017. Genetic effects on
644 gene expression across human tissues. *Nature* **550**: 204-213.
645 Böhm M, Swedberg K, Komajda M, Borer JS, Ford I, Dubost-Brama A, Lerebours
646 G, Tavazzi L. 2010. Heart rate as a risk factor in chronic heart failure
647 (SHIFT): the association between heart rate and outcomes in a
648 randomised placebo-controlled trial. *The Lancet* **376**: 886-894.
649 Bucchi A, Baruscotti M, Nardini M, Barbuti A, Micheloni S, Bolognesi M,
650 DiFrancesco D. 2013. Identification of the molecular site of ivabradine
651 binding to HCN4 channels. *PLoS One* **8**: e53132.
652 Burggren WW, Pinder AW. 1991. Ontogeny of cardiovascular and respiratory
653 physiology in lower vertebrates. *Annu Rev Physiol* **53**: 107-135.
654 Chapman ER. 2008. How does synaptotagmin trigger neurotransmitter release?
655 *Annu Rev Biochem* **77**: 615-641.
656 Cotto KC, Wagner AH, Feng YY, Kiwala S, Coffman AC, Spies G, Wollam A, Spies
657 NC, Griffith OL, Griffith M. 2018. DGIdb 3.0: a redesign and expansion of
658 the drug-gene interaction database. *Nucleic Acids Res* **46**: D1068-D1073.
659 de Bruyne MC, Kors JA, Hoes AW, Klootwijk P, Dekker JM, Hofman A, van Bemmel
660 JH, Grobbee DE. 1999. Both decreased and increased heart rate variability
661 on the standard 10-second electrocardiogram predict cardiac mortality in
662 the elderly: the Rotterdam Study. *Am J Epidemiol* **150**: 1282-1288.
663 Dekker JM, Schouten EG, Klootwijk P, Pool J, Swenne CA, Kromhout D. 1997.
664 Heart rate variability from short electrocardiographic recordings predicts
665 mortality from all causes in middle-aged and elderly men - The zutphen
666 study. *Am J Epidemiol* **145**: 899-908.
667 den Hoed M Eijgelsheim M Esko T Brundel BJ Peal DS Evans DM Nolte IM Segre
668 AV Holm H Handsaker RE et al. 2013. Identification of heart rate-
669 associated loci and their effects on cardiac conduction and rhythm
670 disorders. *Nat Genet* **45**: 621-631.
671 Dobin A, Davis CA, Schlesinger F, Drenkow J, Zaleski C, Jha S, Batut P, Chaisson M,
672 Gingeras TR. 2013. STAR: ultrafast universal RNA-seq aligner.
673 *Bioinformatics* **29**: 15-21.
674 Dong C, Della-Morte D, Beecham A, Wang L, Cabral D, Blanton SH, Sacco RL,
675 Rundek T. 2015. Genetic variants in LEKR1 and GALNT10 modulate sex-
676 difference in carotid intima-media thickness: a genome-wide interaction
677 study. *Atherosclerosis* **240**: 462-467.
678 Ellinor PT, Lunetta KL, Albert CM, Glazer NL, Ritchie MD, Smith AV, Arking DE,
679 Muller-Nurasyid M, Krijthe BP, Lubitz SA et al. 2012. Meta-analysis
680 identifies six new susceptibility loci for atrial fibrillation. *Nat Genet* **44**:
681 670-675.
682 Eppinga RN, Hagemeijer Y, Burgess S, Hinds DA, Stefansson K, Gudbjartsson DF,
683 van Veldhuisen DJ, Munroe PB, Verweij N, van der Harst P. 2016.
684 Identification of genomic loci associated with resting heart rate and

685 shared genetic predictors with all-cause mortality. *Nat Genet* **48**: 1557-
686 1563.
687 Flannick J, Johansson S, Njolstad PR. 2016. Common and rare forms of diabetes
688 mellitus: towards a continuum of diabetes subtypes. *Nat Rev Endocrinol*
689 **12**: 394-406.
690 Flannick JA, Mercader JMM, Fuchsberger C, Udler MS, Mahajan A, Wessel J,
691 Altshuler D, Burtt NP, Scott L, Morris A et al. 2018. Genetic discovery and
692 translational decision support from exome sequencing of 20,791 type 2
693 diabetes cases and 24,440 controls from five ancestries. *bioRxiv*
694 doi:10.1101/371450.
695 Ganna A, Satterstrom FK, Zekavat SM, Das I, Kurki MI, Churchhouse C, Alfoldi J,
696 Martin AR, Havulinna AS, Byrnes A et al. 2018. Quantifying the Impact of
697 Rare and Ultra-rare Coding Variation across the Phenotypic Spectrum. *Am*
698 *J Hum Genet* **102**: 1204-1211.
699 Hou JH, Kralj JM, Douglass AD, Engert F, Cohen AE. 2014. Simultaneous mapping
700 of membrane voltage and calcium in zebrafish heart in vivo reveals
701 chamber-specific developmental transitions in ionic currents. *Front*
702 *Physiol* **5**: 344.
703 Howe K Clark MD Torroja CF Torrance J Berthelot C Muffato M Collins JE
704 Humphray S McLaren K Matthews L et al. 2013. The zebrafish reference
705 genome sequence and its relationship to the human genome. *Nature* **496**:
706 498-503.
707 Jao LE, Wente SR, Chen W. 2013. Efficient multiplex biallelic zebrafish genome
708 editing using a CRISPR nuclease system. *Proc Natl Acad Sci U S A* **110**:
709 13904-13909.
710 Justice AE Winkler TW Feitosa MF Graff M Fisher VA Young K Barata L Deng X
711 Czajkowski J Hadley D et al. 2017. Genome-wide meta-analysis of 241,258
712 adults accounting for smoking behaviour identifies novel loci for obesity
713 traits. *Nature communications* **8**: 14977.
714 Koressaar T, Remm M. 2007. Enhancements and modifications of primer design
715 program Primer3. *Bioinformatics* **23**: 1289-1291.
716 Labun K, Montague TG, Gagnon JA, Thyme SB, Valen E. 2016. CHOPCHOP v2: a
717 web tool for the next generation of CRISPR genome engineering. *Nucleic*
718 *Acids Res* **44**: W272-276.
719 Lagman D, Sundstrom G, Ocampo Daza D, Abalo XM, Larhammar D. 2012.
720 Expansion of transducin subunit gene families in early vertebrate
721 tetraploidizations. *Genomics* **100**: 203-211.
722 Lamprecht MR, Sabatini DM, Carpenter AE. 2007. CellProfiler: free, versatile
723 software for automated biological image analysis. *Biotechniques* **42**: 71-
724 75.
725 Li H, Handsaker B, Wysoker A, Fennell T, Ruan J, Homer N, Marth G, Abecasis G,
726 Durbin R. 2009. The Sequence Alignment/Map format and SAMtools.
727 *Bioinformatics* **25**: 2078-2079.
728 Lieschke GJ, Currie PD. 2007. Animal models of human disease: zebrafish swim
729 into view. *Nat Rev Genet* **8**: 353-367.
730 Liu CC, Li L, Lam YW, Siu CW, Cheng SH. 2016. Improvement of surface ECG
731 recording in adult zebrafish reveals that the value of this model exceeds
732 our expectation. *Sci Rep* **6**: 25073.

733 Locke AE Kahali B Berndt SI Justice AE Pers TH Day FR Powell C Vedantam S
734 Buchkovich ML Yang J et al. 2015. Genetic studies of body mass index
735 yield new insights for obesity biology. *Nature* **518**: 197-206.
736 Louis A, Nguyen NT, Muffato M, Roest Crollius H. 2015. Genomicus update 2015:
737 KaryoView and MatrixView provide a genome-wide perspective to
738 multispecies comparative genomics. *Nucleic Acids Res* **43**: D682-689.
739 Ludwig A, Zong X, Stieber J, Hullin R, Hofmann F, Biel M. 1999. Two pacemaker
740 channels from human heart with profoundly different activation kinetics.
741 *EMBO J* **18**: 2323-2329.
742 MacRae CA, Peterson RT. 2015. Zebrafish as tools for drug discovery. *Nat Rev*
743 *Drug Discov* **14**: 721-731.
744 Mark MD, Herlitze S. 2000. G-protein mediated gating of inward-rectifier K+
745 channels. *Eur J Biochem* **267**: 5830-5836.
746 Mawdsley DJ, Cooper HM, Hogan BM, Cody SH, Lieschke GJ, Heath JK. 2004. The
747 Netrin receptor Neogenin is required for neural tube formation and
748 somitogenesis in zebrafish. *Dev Biol* **269**: 302-315.
749 McLaren W, Gil L, Hunt SE, Riat HS, Ritchie GR, Thormann A, Flicek P,
750 Cunningham F. 2016. The Ensembl Variant Effect Predictor. *Genome Biol*
751 **17**: 122.
752 Moreno-Mateos MA, Vejnar CE, Beaudoin JD, Fernandez JP, Mis EK, Khokha MK,
753 Giraldez AJ. 2015. CRISPRscan: designing highly efficient sgRNAs for
754 CRISPR-Cas9 targeting in vivo. *Nat Methods* **12**: 982-988.
755 Newton-Cheh C, Guo CY, Wang TJ, O'Donnell C J, Levy D, Larson MG. 2007.
756 Genome-wide association study of electrocardiographic and heart rate
757 variability traits: the Framingham Heart Study. *BMC Med Genet* **8 Suppl 1**:
758 S7.
759 Ng MCY Graff M Lu Y Justice AE Mudgal P Liu CT Young K Yanek LR Feitosa MF
760 Wojczynski MK et al. 2017. Discovery and fine-mapping of adiposity loci
761 using high density imputation of genome-wide association studies in
762 individuals of African ancestry: African Ancestry Anthropometry Genetics
763 Consortium. *PLoS Genet* **13**: e1006719.
764 Niazi MKK, Nilsson MF, Danielsson BR, Bengtsson E. 2009. Fully Automatic Heart
765 Beat Rate Determination in Digital Video Recordings of Rat Embryos.
766 doi:http://urn.kb.se/resolve?urn=urn:nbn:se:uu:diva-88052.
767 Nolte IM Munoz ML Tragante V Amare AT Jansen R Vaez A von der Heyde B
768 Avery CL Bis JC Dierckx B et al. 2017. Genetic loci associated with heart
769 rate variability and their effects on cardiac disease risk. *Nature*
770 *communications* **8**: 15805.
771 Pardo-Martin C, Allalou A, Medina J, Eimon PM, Wahlby C, Fatih Yanik M. 2013.
772 High-throughput hyperdimensional vertebrate phenotyping. *Nature*
773 *communications* **4**: 1467.
774 Pearson WR, Wood T, Zhang Z, Miller W. 1997. Comparison of DNA sequences
775 with protein sequences. *Genomics* **46**: 24-36.
776 Poon KL, Brand T. 2013. The zebrafish model system in cardiovascular research:
777 A tiny fish with mighty prospects. *Glob Cardiol Sci Pract* **2013**: 9-28.
778 Shi W, Wymore R, Yu H, Wu J, Wymore RT, Pan Z, Robinson RB, Dixon JE,
779 McKinnon D, Cohen IS. 1999. Distribution and prevalence of
780 hyperpolarization-activated cation channel (HCN) mRNA expression in
781 cardiac tissues. *Circ Res* **85**: e1-6.

782 Stieber J, Herrmann S, Feil S, Loster J, Feil R, Biel M, Hofmann F, Ludwig A. 2003.
783 The hyperpolarization-activated channel HCN4 is required for the
784 generation of pacemaker action potentials in the embryonic heart. *Proc*
785 *Natl Acad Sci U S A* **100**: 15235-15240.
786 Stieber J, Wieland K, Stockl G, Ludwig A, Hofmann F. 2006. Bradycardic and
787 proarrhythmic properties of sinus node inhibitors. *Mol Pharmacol* **69**:
788 1328-1337.
789 Sudhof TC. 2002. Synaptotagmins: why so many? *J Biol Chem* **277**: 7629-7632.
790 Swedberg K, Komajda M, Bohm M, Borer JS, Ford I, Dubost-Brama A, Lerebours
791 G, Tavazzi L. 2010. Ivabradine and outcomes in chronic heart failure
792 (SHIFT): a randomised placebo-controlled study. *Lancet* **376**: 875-885.
793 Szklarczyk D, Morris JH, Cook H, Kuhn M, Wyder S, Simonovic M, Santos A,
794 Doncheva NT, Roth A, Bork P et al. 2017. The STRING database in 2017:
795 quality-controlled protein-protein association networks, made broadly
796 accessible. *Nucleic Acids Res* **45**: D362-d368.
797 Thayer JF, Yamamoto SS, Brosschot JF. 2010. The relationship of autonomic
798 imbalance, heart rate variability and cardiovascular disease risk factors.
799 *Int J Cardiol* **141**: 122-131.
800 Varshney GK, Carrington B, Pei W, Bishop K, Chen Z, Fan C, Xu L, Jones M, LaFave
801 MC, Ledin J et al. 2016. A high-throughput functional genomics workflow
802 based on CRISPR/Cas9-mediated targeted mutagenesis in zebrafish. *Nat*
803 *Protoc* **11**: 2357-2375.
804 Varshney GK, Pei W, LaFave MC, Idol J, Xu L, Gallardo V, Carrington B, Bishop K,
805 Jones M, Li M et al. 2015. High-throughput gene targeting and
806 phenotyping in zebrafish using CRISPR/Cas9. *Genome Res* **25**: 1030-1042.
807 Verweij N, van de Vegte YJ, van der Harst P. 2018. Genetic study links
808 components of the autonomous nervous system to heart-rate profile
809 during exercise. *Nature communications* **9**: 898.
810 Warde-Farley D, Donaldson SL, Comes O, Zuberi K, Badrawi R, Chao P, Franz M,
811 Grouios C, Kazi F, Lopes CT et al. 2010. The GeneMANIA prediction server:
812 biological network integration for gene prioritization and predicting gene
813 function. *Nucleic Acids Res* **38**: W214-220.
814 Whitesell TR, Kennedy RM, Carter AD, Rollins EL, Georgijevic S, Santoro MM,
815 Childs SJ. 2014. An alpha-smooth muscle actin (acta2/alphasma)
816 zebrafish transgenic line marking vascular mural cells and visceral
817 smooth muscle cells. *PLoS One* **9**: e90590.
818 Wilson NH, Key B. 2007. Neogenin: one receptor, many functions. *Int J Biochem*
819 *Cell Biol* **39**: 874-878.
820 Zhang J, Kobert K, Flouri T, Stamatakis A. 2014. PEAR: a fast and accurate
821 Illumina Paired-End reAd mergeR. *Bioinformatics* **30**: 614-620.

822

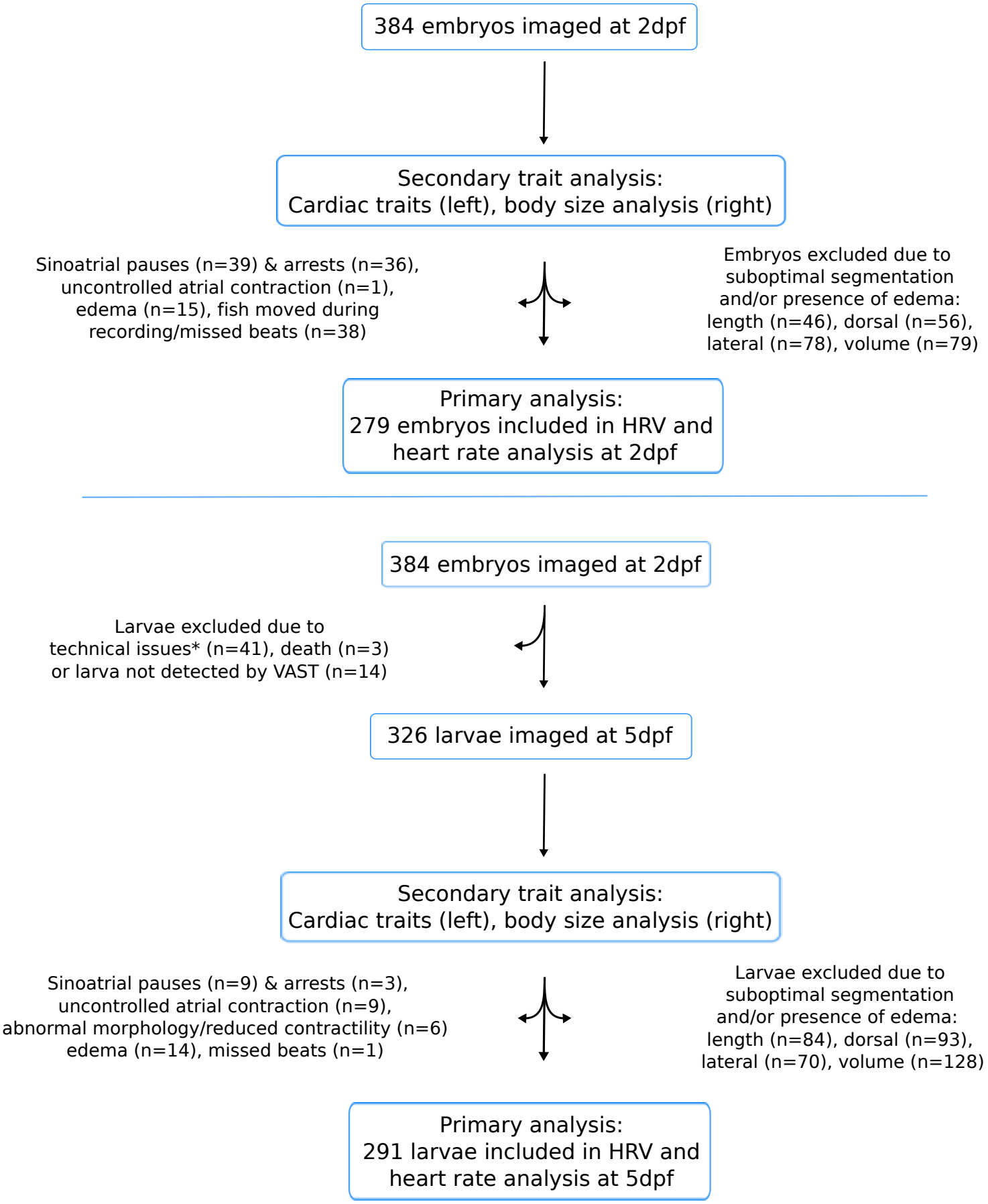


**Supplementary Figure S1**: Flow chart showing the number of included larvae in the analysis and reasons for exclusions. Embryos/larvae can show more than one phenotype. *Technical issues refers to not being able to image due to microscope complications. VAST: Vertebrate automated screening technology.

**Supplemental Table 1: Overview of zebrafish orthologues and designed gRNAs**

| Zebrafish orthologue | ENSDARG | Conservation Zebrafish - Human | Conservation Zebrafish - Spotted gar | Main transcript | Target sequence gRNA | Exon target (transcript name) | CRISPRscan rank | ChopChop rank | Activity test rank | Predicted off-targets | Nr of mismatches | Genomic location of potential off-target 1 | ENSDARG (gene-ID) of potential off-target 1, Feature | ENSG (gene-ID) of potential off-target 1 | Genomic location of potential off-target 2 | ENSDARG (gene-ID) of potential off-target 2, Feature | ENSG (gene-ID) of potential off-target 2 | Primer forward | Primer reverse | Amplicon size |
|---|---|---|---|---|---|---|---|---|---|---|---|---|---|---|---|---|---|---|---|---|
| *gngt1* | ENSDARG00000035798 | 17 | 21 | ENSDART00000051950 | gGACCTGGATAAGGCGAAGA | 2/3 (gngt1-001); 1/2 (gngt1-002) | 62 | 4/13 (yellow) | moderate | 1 | 3 | chr25:17488676 | ENSDARG00000051959 (rgc:66449), intron (3/6), intron (4/4) | no human orthologue | | | | GTCCATTTTCCAGAGTGGAGAC | gCCCATAACACAATTGCTTACC | 207 |
| *syt10* | ENSDARG00000045750 | 0 | 1 | ENSDART00000136049 | GGCTGATGCCGTCCTCTGTG | 1/7 (syt10-001); 1/7 (syt10-201) | 36 | 6/129 (green) | low | 0 | | | | | | | | TAGGATATGGACTTGGACGCAT | TTACCTGGTATGTTGCTCTCCA | 227 |
| *rgs6* | ENSDARG00000015627 | 9 | 20 | ENSDART00000135513 | GGCCTCTCAGGACCAAGG | 1/17 (rgs6-201); 2/18 (rgs6-001) | 62 | 1/107 (green) | low | 0 | | | | | | | | AAGGCTAATTCATTGTCTGGGA | GCATGTCAAATGTAAAGGCAAA | 169 |
| *hcn4* | ENSDARG00000061685 | 6 | 3 | ENSDART00000136140 | GGAGAGCCCTCCTGGAGCCG | 1/8 (hcn4-001) | 59 | 11/280 (green) | high | 2 | 3/3 | chr21:45844184 | ENSDARG00000103825 (gaint10), exon (1/3) | ENSG00000164574 (GALNT10) | chr1n_KN150614v1:3424 | ENSDARG00000100453 (gaint10), exon (6/8) | ENSG00000164574 (GALNT10) | CCTTTCGTCCATCACCAGTC | CCGCTTGATAATACCTCTCGTC | 230 |
| *hcn4l* | ENSDARG00000074419 | 3 | 3 | ENSDART00000088249 | gGCCTGGATAGTGTTTAACG | 2/8 (hcn4l-201); 1/7 (hcn4l-001) | / | 2/191 (green) | low | 0 | | | | | | | | TTACTGGGACCTGATCATGCTT | AAGATGTAATCCACAGGGATGG | 235 |
| *neo1a* | ENSDARG00000102855 | 1 | 5 | ENSDART00000158160 | GGAGCCGTCGGATACACTAG | 1/4 (neo1a-001); 2/29 (neo1a-201); 2/30 (neo1a-202) | 48 | 2/55 (green) | very high | 0 | | | | | | | | TTCTGTGTCTCCACAGGATCAG | CCTCATCGGGTTTATTGTGTTT | 215 |
| *neo1b* | ENSDARG00000075100 | 2 | 6 | ENSDART00000115280 | GGACAGAGATGCTCGGCCTG | 3/29 (neo1b-201) | 58 | 18/354 (green) | very high | 0 | | | | | | | | CAGCTCTCTCTCTCATTGGCTT | TATGGTGCAACGGTAGAGTCC | 206 |
| *quo (kiaa1755_1)* | ENSDARG00000073684 | 2 | 5 | ENSDART00000109679 | GGAGATCCGGTTGCCCTGTG | 2/22 (quo-001); 3/23 (quo-201) | 83 | 12/331 (green) | very high | 0 | | | | | | | | ATGACCGTAAGTCAAGGGAAAA | TGAATCTTGTCTAATGGCGTTG | 153 |
| *si:dkey-65j6.2 (kiaa1755_2)* | ENSDARG00000103586 | 3 | 5 | ENSDART00000158832 | GGACGGTTTGGCTCCAGCAG | 1/23 (si:dkey-65j6.2-201); 1/25 (si:dkey-65j6.2-001) | 59 | 14/303 (green) | very high | 2 | 3/3 | chr15:32969618 | ENSDARG00000104664 (dclk1b), exon (3/16), exon (4/17) | ENSG00000133083 (DCLK1) | chr22:28819880 | ENSDARG00000071083 (si:dkeyp-34c12.1), Intron (7/7), Exon (8/9) | no human orthologue | AGCCATTACACCCAAAGAAAAA | GGGAATCATTTCGAAGTAGCTG | 152 |

Table showing zebrafish genes, main transcript used for the analysis and gRNAs; rsID refers to the lead SNP(s) of the GWAS-identified loci (Nolte et. al, 2017), multiple independent SNPs per locus can be present; For simplicity, quo is referred to as *kiaa1755_1*, and *si:dkey-65j6.2* as *kiaa1755_2*; Conservation refers to the number of genes that are preserved in the same locus across species according to Genomicus; A small "g" in the gRNA target sequence indicates a manually introduced nu

**Supplemental Table 2: Unique Cigars**

| Orthologue | Sequence | Cigar | Mean Nr reads | Nr alleles | SD reads |
|---|---|---|---|---|---|
| *gngt1* | CTCATCGTAAGCAGCAGTAAGTTTGCTTATTTCCAGTATATTGAACATCAAATATAATCCATTCATTCAACACAACAT GTAAATGATGTGATTGTTTGATTTCATGCAGAAAATGCCGATCATAGATGTAGAAAATATGACTGACCTGGATAAG GCGAAGATGGAAGTAACCCAGCTCAAAACTGAGGTGAAGCTAGAAAGGGCGAA | 45M1S41M1S119M | 498 | 336 | 381 |
| *gngt1* | CTCATCGTAAGCAGCAGTAAGTTTGCTTATTTCCAGTATATTGAATATCAAATATAATCCATTCATTCAACACAACAT GTAAATGATATGATTGTTTGATTTCATGCAGAAAATGCCGATCATAGATGTAGAAAATATGACTGACCTGGATAAG GCGAAGATGGAAGTAACCCAGCTCAAAACTGAGGTGAAGCTAGAAAGGGCGAA | 207M | 517 | 267 | 372 |
| *gngt1* | CTCATCGTAAGCAGCAGTAAGTTTGCTTATTTCCAGTATATTGAACATCAAATATAATCCATTCATTCAACACAACAT GTAAATGATGTGATTGTTTGATTTCATGCAGAAAATGCCGATCATAGATGTAGAAAATATGACTGACCTGGATAAG GCGTTTTGGAAGTAACCCAGCTCAAAACTGAGGTGAAGCTAGAAAGGGCGAA | 45M1S41M1S69M1D3S46M | 544 | 69 | 405 |
| *gngt1* | CTCATCGTAAGCAGCAGTAAGTTTGCTTATTTCCAGTATATTGAATATCAAATATAATCCATTCATTCAACACAACAT GTAAATGATATGATTGTTTGATTTCATGCAGAAAATGCCGATCATAGATGTAGAAAATATGACTGACCTGGATAAG ATGGAAGTAACCCAGCTCAAAACTGAGGTGAAGCTAGAAAGGGCGAA | 151M6D50M | 500 | 63 | 364 |
| *gngt1* | CTCATCGTAAGCAGCAGTAAGTTTGCTTATTTCCAGTATATTGAACATCAAATATAATCCATTCATTCAACACAACAT GTAAATGATGTGATTGTTTGATTTCATGCAGAAAATGCCGATCATAGATGTAGAAAATATGACTGACCTGGATAAG ATGGAAGTAACCCAGCTCAAAACTGAGGTGAAGCTAGAAAGGGCGAA | 45M1S41M1S63M6D50M | 584 | 13 | 479 |
| *gngt1* | CTCATCGTAAGCAGCAGTAAGTTTGCTTATTTCCAGTATATTGAATATCAAATATAATCCATTCATTCAACACAACAT GTAAATGATATGATTGTTTGATTTCATGCAGAAAATGCCGATCATAGATGTAGAAAATATGACTGACCTGGATAAG GCGATGATGGAAGTAACCCAGCTCAAAACTGAGGTGAAGCTAGAAAGGGCGAA | 158M1S48M | 504 | 4 | 221 |
| *gngt1* | CTCATCGTAAGCAGCAGTAAGTTTGCTTATTTCCAGTATATTGAACATCAAATATAATCCATTCATTCAACACAACAT GTAAATGATGTGATTGTTTGATTTCATGCAGAAAATGCCGATCATAGATGTAGAAAATATGACTGACCTGGATAAG GCGATGGAAGTAACCCAGCTCAAAACTGAGGTGAAGCTAGAAAGGGCGAA | 45M1S41M1S68M3D48M | 606 | 3 | 119 |
| *gngt1* | CTCATCGTAAGCAGCAGTAAGTTTGCTTATTTCCAGTATATTGAACATCAAATATAATCCATTCATTCAACACAACAT GTAAATGATGTGATTGTTTGATTTCATGCAGAAAATGCCGATCATAGATGTAGAAAATATGACTGACCTGGATAAG GCGAAGTAACCCAGAAGTAACCCAGCTCAAAACTGAGGTGAAGCTAGAAAGGGCGAA | 45M1S41M1S72M4I3S44M | 526 | 2 | 143 |
| *gngt1* | CTCATCGTAAGCAGCAGTAAGTTTGCTTATTTCCAGTATATTGAACATCAAATATAATCCATTCATTCAACACAACAT GTAAATGATGTGATTGTTTGATTTCATGCAGAAAATGCCGATAATAGATGTAGAAAATATGACTGACCTGGATAAG GCGTTTTGGAAGTAACCCAGCTCAAAACTGAGGTGAAGCTAGAAAGGGCGAA | 45M1S41M1S32M1S36M1D3S46M | 48 | 1 | - |
| *gngt1* | ATCATCGTAAGCAGCAGTAAGTTTGCTTATTTCCAGTATATTGAACATCAAATATAATCCATTCATTCAACACAACAT GTAAATGATGTGATTGTTTGATTTCATGCAGAAAATGCCGATCATAGATGTAGAAAATATGACTGACCTGGATAAG GCGTTTTGGAAGTAACCCAGCTCAAAACTGAGGTGAAGCTAGAAAGGGCGAA | 1S44M1S41M1S69M1D3S46M | 10 | 1 | - |
| *gngt1* | CTCATCGTAAGCAGCAGTAAGTTTGCTTATTTCCAGTATATTGAATATCAAATATAATCCATTCATTCAACACAACAT GTAAATGATGTGATTGTTTGATTTCATGCAGAAAATGCCGATCATAGATGTAGAAAATATGACTGACCTGGATAAG GCGAAGATGGAAGTAACCCAGCTCAAAACTGAGGTGAAGCTAGAAAGGGCGAA | 87M1S119M | 3 | 1 | - |
| *syt10* | CGGTCTCTCTCCATTCCCGTACGCATCAGCTGCACTCAGCAGCTCACATGGTGCCCCAATGAACTCTCGCCCTCACG CATCGTCCAACATACAATGGATTAACAGGAAAGACATGAATGTCCGCACAGAGGACGGCATCAGCCTGTGCCAAA GGGCTCTCCAAATAGTGACAGAGCTGTGCCTCGCCGGGCACGTCGACCGGGAGAAATGCGCGGATATATTTCCAC | 227M | 1024 | 518 | 644 |
| *syt10* | CGGTCTCTCTCCATTCCCGTACGCATCAGCTGCACTCAGCAGCTCACATGGTGCCCCAATGAACTCTCGCCCTCACG CATCGTCCAACATACAATGGATTAACAGGAAAGACATGAATGTCCGCACAAGAGGACGGCATCAGCCTGTGCCAA AGGGCTCTCCAAATAGTGACAGAGCTGTGCCTCGCCGGGCACGTCGACCGGGAGAAATGCGCGGATATATTTCCA C | 126M1I101M | 735 | 46 | 462 |
| *syt10* | CGGTCTCTCTCCATTCCCGTACGCATCAGCTGCACTCAGCAGCTCACATGGTGCCCCAATGAACTCTCGCCCTCACG CATCGTCCAACATACAATGGATTAACAGGAAAGACATGAATGTCCGACGGCATCAGCCTGTGCCAAAGGGCTCTC CAAATAGTGACAGAGCTGTGCCTCGCCGGGCACGTCGACCGGGAGAAATGCGCGGATATATTTCCAC | 122M8D97M | 606 | 45 | 397 |

*Continued Supplemental Table 2*

| Orthologue | Sequence | Cigar | Mean Nr reads | Nr alleles | SD reads |
|---|---|---|---|---|---|
| *syt10* | CGGTCTCTCTCCATTCCCGTACGCATCAGCTGCACTCAGCAGCTCACATGGTGCCCCAATGAACTCTCGCCCTCACG CATCGTCCAACATACAATGGATTAACAGGAAAGACATGAATGTACAGCTGATGCGTACGGGAATGGAGAGGACG GCATCAGCCTGTGCCAAAGGGCTCTCCAAATAGTGACAGAGCTGTGCCTCGCCGGGCACGTCGACCGGGAGAAAT GCGCGGATATATTTCCAC | 120M1S9I2M1S2M8I101M | 793 | 43 | 405 |
| *syt10* | CGGTCTCTCTCCATTCCCGTACGCATCAGCTGCACTCAGCAGCTCACATGGTGCCCCAATGAACTCTCGCCCTCACG CATCGTCCAACATACAATGGATTAACAGGAAAGACATGAATGTCCGCACATGGACGGCATCAGCCTGTGCCAAAG GGCTCTCCAAATAGTGACAGAGCTGTGCCTCGCCGGGCACGTCGACCGGGAGAAATGCGCGGATATATTTCCAC | 127M1S1D98M | 368 | 42 | 246 |
| *syt10* | CGGTCTCTCTCCATTCCCGTACGCATCAGCTGCACTCAGCAGCTCACATGGTGCCCCAATGAACTCTCGCCCTCACG CATCGTCCAACATACAATGGATTAACAGGAAAGACGGCATCAGCCTGTGCCAAAGGGCTCTCCAAATAGTGACAG AGCTGTGCCTCGCCGGGCACGTCGACCGGGAGAAATGCGCGGATATATTTCCAC | 109M21D97M | 667 | 19 | 267 |
| *syt10* | CGGTCTCTCTCCATTCCCGTACGCATCAGCTGCACTCAGCAGCTCACATGGTGCCCCAATGAACTCTCGCCCTCACG CATCGTCCAACATACAATGGATTAACAGGAAAGACATGAATGTCCGGACGGCATCAGCCTGTGCCAAAGGGCTCT CCAAATAGTGACAGAGCTGTGCCTCGCCGGGCACGTCGACCGGGAGAAATGCGCGGATATATTTCCAC | 122M7D98M | 963 | 16 | 431 |
| *syt10* | CGGTCTCTCTCCATTCCCGTACGCATCAGCTGCACTCAGCAGCTCACATGGTGCCCCAATGAACTCTCGCCCTCACG CATCGTCCAACATACAATGGATTAACAGGAAAGACATGAATGTCCGCACGGCATCAGACGGCATCAGCCTGTGCC AAAGGGCTCTCCAAATAGTGACAGAGCTGTGCCTCGCCGGGCACGTCGACCGGGAGAAATGCGCGGATATATTTC CAC | 126M1S1M3I2S97M | 937 | 11 | 645 |
| *syt10* | CGGTCTCTCTCCATTCCCGTACGCATCAGCTGCACTCAGCAGCTCACATGGTGCCCCAATGAACTCTCGCCCTCACG CATCGTCCAACATACAATGGATTAACAGGAAAGACATGAATGTCCGCACGGCATCAGCCTGTGCCAAAGGGCTCT CCAAATAGTGACAGAGCTGTGCCTCGCCGGGCACGTCGACCGGGAGAAATGCGCGGATATATTTCCAC | 124M7D96M | 502 | 11 | 300 |
| *syt10* | CGGTCTCTCTCCATTCCCGTACGCATCAGCTGCACTCAGCAGCTCACATGGTGCCCCAATGAACTCTCGCCCTCACG CATCGTCCAACATACAATGGATTAACAGGAAAGACATGAATGTCCGCCTGTCAGCCTGTGCCAAAGGGCTCTCCAA ATAGTGACAGAGCTGTGCCTCGCCGGGCACGTCGACCGGGAGAAATGCGCGGATATATTTCCAC | 124M1S10D2S90M | 524 | 4 | 229 |
| *syt10* | CGGTCTCTCTCCATTCCCGTACGCATCAGCTGCACTCAGCAGCTCACATGGTGCCCCAATGAACTCTCGCCCTCACG CATCGTCCAACATACAATGGATTAACAGGAAAGACATGAATGTCCGAGGACGGCATCAGCCTGTGCCAAAGGGCT CTCCAAATAGTGACAGAGCTGTGCCTCGCCGGGCACGTCGACCGGGAGAAATGCGCGGATATATTTCCAC | 122M5D100M | 1247 | 3 | 670 |
| *rgs6* | GTGACAGTACCTTCCTGTATGCAATCATGTTGGGTGAGTCCTCATCTGGGTCGGCTATGCCCACCGCACCTTGGTCC TGAGAGGCCTGAGCCATGCTTGATTGCTGGGTCTCTCTTTCTGTGTCTGTGGGGAACGGGCACAACAGAAAAGGA ATGAGTCCCAGAACAGG | 169M | 1431 | 728 | 813 |
| *rgs6* | GTGACAGTACCTTCCTGTATGCAATCATGTTGGGTGAGTCCTCATCTGGGTCGGCTATGCCCACCGCACTTGGTCCT GAGAGGCCTGAGCCATGCTTGATTGCTGGGTCTCTCTTTCTGTGTCTGTGGGGAACGGGCACAACAGAAAAGGAA TGAGTCCCAGAACAGG | 68M1D100M | 784 | 24 | 453 |
| *rgs6* | GTGACAGTACCTTCCTGTATGCAATCATGTTGGGTGAGTCCTCATCTGGGTCGGCTATGCCCACCGCATTGGTCCT GAGAGGCCTGAGCCATGCTTGATTGCTGGGTCTCTCTTTCTGTGTCTGTGGGGAACGGGCACAACAGAAAAGGAA TGAGTCCCAGAACAGG | 68M2D99M | 540 | 7 | 195 |
| *rgs6* | GTGACAGTACCTTCCTGTATGCAATCATGTTGGGTGAGTCCTCATCTGGGTCGGCTATGCCCACCGCATAGTCCTG AGAGGCCTGAGCCATGCTGAGCCATGCTTGATTGCTGGGTCTCTCTTTCTGTGTCTGTGGGGAACGGGCACAACA GAAAAGGAATGAGTCCCAGAACAGG | 68M3D1M1S12M10I84M | 920 | 4 | 287 |
| *rgs6* | GTGACAGTACCTTCCTGTATGCAATCATGTTGGGTGAGTCCTCATCTGGGTCGGCTATGTGGTCCTGAGAGGCCTG AGCCATGCTTGATTGCTGGGTCTCTCTTTCTGTGTCTGTGGGGAACGGGCACAACAGAAAAGGAATGAGTCCCAG AACAGG | 59M12D98M | 1424 | 1 | - |
| *hcn4* | GTCCGGCAGTATCTGCTCGATGCCTTCCAGCTTAATAAAGCCAGCCTGCTGATCCGGGATGCCCTGATGCTGGCTC GAACCGGCGGCTTCCTCTCCGCCTCCCCCGCCGCTCTGCGCACCGGGCTCCGCGCCGCCACCCGCGGCTCCAGGAG GGCTCTCCTCGCTAGGAGTGACCTCTCCGTCCGTGATCAGACGCCTTTCCTCGGCTACATCCGAGTCGTGGACGTG CC | 230M | 1380 | 638 | 789 |

*Continued Supplemental Table 2*

| Orthologue | Sequence | Cigar | Mean Nr reads | Nr alleles | SD reads |
|---|---|---|---|---|---|
| *hcn4* | GTCCGGCAGTATCTGCTCGATGCCTTCCAGCTTAATAAAGCCAGCCTGCTGATCCGGGATGCCCTGATGCTGGCTCGAACCGGCGGCTTCCTCTCCGCCTCCCCCGCCGCTCTGCGCACCGGGCTCCGCGCCGCCACCCGCGCCGCCACCCAGGAGGGCTCTCCTCGCTAGGAGTGACCTCTCCGTCCGTGATCAGACGCCTTTCCTCGGCTACATCCGAGTCGTGGACGTGCC | 142M1S1M4I1S85M | 725 | 48 | 343 |
| *hcn4* | GTCCGGCAGTATCTGCTCGATGCCTTCCAGCTTAATAAAGCCAGCCTGCTGATCCGGGATGCCCTGATGCTGGCTCGAACCGGCGGCTTCCTCTCCGCCTCCCCCGCCGCTCTGCGCACCGGGCTCCGCGCCGCCATCCGCGCCGCCACCCTCCAGGAGGGCTCTCCTCGCTAGGAGTGACCTCTCCGTCCGTGATCAGACGCCTTTCCTCGGCTACATCCGAGTCGTGGACGTGCC | 136M1S5M7I1S87M | 1314 | 16 | 225 |
| *hcn4* | GTCCGGCAGTATCTGCTCGATGCCTTCCAGCTTAATAAAGCCAGCCTGCTGATCCGGGATGCCCTGATGCTGGCTCGAACCGGCGGCTTCCTCTCCGCCTCCCCCGCCGCTCTGCGCACCGGGCTCCGCGCCGCCACCCGCGGCTCTCCTCCAGGAGCTCCAGGGCTCTCCTCGCTAGGAGTGACCTCTCCGTCCGTGATCAGACGCCTTTCCTCGGCTACATCCGAGTCGTGGACGTGCC | 143M5I7M6I80M | 799 | 15 | 383 |
| *hcn4* | GTCCGGCAGTATCTGCTCGATGCCTTCCAGCTTAATAAAGCCAGCCTGCTGATCCGGGATGCCCTGATGCTGGCTCGAACCGGCGGCTTCCTCTCCGCCTCCCCCGCCGCTCTGCGCACCGGGCTCCGCGCCGCCCTCCAGGAGGGCTCTCCTCGCTAGGAGTGACCTCTCCGTCCGTGATCAGACGCCTTTCCTCGGCTACATCCGAGTCGTGGACGTGCC | 135M8D87M | 917 | 13 | 563 |
| *hcn4* | GTCCGGCAGTATCTGCTCGATGCCTTCCAGCTTAATAAAGCCAGCCTGCTGATCCGGGATGCCCTGATGCTGGCTCGAACCGGCGGCTTCCTCTCCGCCTCCCCCGCCGCTCTGCGCACCGGGCTCCGCGCCGCCACCCGCCCTCCAGGAGGGCTCTCCTCGCTAGGAGTGACCTCTCCGTCCGTGATCAGACGCCTTTCCTCGGCTACATCCGAGTCGTGGACGTGCC | 141M1D1S87M | 987 | 11 | 377 |
| *hcn4* | GTCCGGCAGTATCTGCTCGATGCCTTCCAGCTTAATAAAGCCAGCCTGCTGATCCGGGATGCCCTGATGCTGGCTCGAACCGGCGGCTTCCTCTCCGCCTCCCCCGCCGCTCTGCGCACCGGGCTCCGCGCCGCCACCCACCCAGGAGGGCTCTCCTCGCTAGGAGTGACCTCTCCGTCCGTGATCAGACGCCTTTCCTCGGCTACATCCGAGTCGTGGACGTGCC | 139M1S1M4D85M | 1302 | 10 | 587 |
| *hcn4* | GTCCGGCAGTATCTGCTCGATGCCTTCCAGCTTAATAAAGCCAGCCTGCTGATCCGGGATGCCCTGATGCTGGCTCGAACCGGCGGCTTCCTCTCCGCCTCCCCCGCCGCTCTGCGCACCGGGCTCCGCGCCGCCACCCGCGGGCCCTCCAGGAGGGCTCTCCTCGCTAGGAGTGACCTCTCCGTCCGTGATCAGACGCCTTTCCTCGGCTACATCCGAGTCGTGGACGTGCC | 143M3I87M | 694 | 2 | 49 |
| *hcn4* | GTCCGGCAGTATCTGCTCGATGCCTTCCAGCTTAATAAAGCCAGCCTGCTGATCCGGGATGCCCTGATGCTGGCTCGAACCGGCGGCTTCCTCTCCGCCTCCCCCGCCGCTCTGCGCACCGGGCTCCGCGCCGCCACCCGCCATCCAGGAGGGCTCTCCTCGCTAGGAGTGACCTCTCCGTCCGTGATCAGACGCCTTTCCTCGGCTACATCCGAGTCGTGGACGTGCC | 98M11I43M2S1D86M | 346 | 2 | 36 |
| *hcn4* | GTCCGGCAGTATCTGCTCGATGCCTTCCAGCTTAATAAAGCCAGCCTGCTGATCCGGGATGCCCTGATGCTGGCTCGAACCGGCGGCTTCCTCTCCGCCTCCCCCGCCGCTCTGCGCACCGGGCTCCGCGCCGCCACCCGCGCCAGGAGGGCTCTCCTCGCTAGGAGTGACCTCTCCGTCCGTGATCAGACGCCTTTCCTCGGCTACATCCGAGTCGTGGACGTGCC | 142M3D85M | 222 | 1 | - |
| *hcn4l* | AGGAGAGGAAATCCACGGCAAACCAGCTGCGCAAGTACCTGACCTTGATCTGCTGAGGGTCCAGGATGATTTCTGTACTGTCCTCTTTCACAATCCCCGTGCGGAAGTTCAGCACGAGGTCGACCAGGAAGAAGGTGTCGGAGACCACGTTAAACACTATCCAGGCGGGTGTGTGTTCGTCTTTGAAGAAGGTGATGCCCACGGGGATGATGATCAGGTTGCCCACCATTAGAAG | 115M1S89M1S29M | 1076 | 697 | 671 |
| *hcn4l* | AGGAGAGGAAATCCACGGCAAACCAGCTGCGCAAGTACCTGACCTTGATCTGCTGAGGGTCCAGGATGATTTCTGTACTGTCCTCTTTCACAATCCCCGTGCGGAAGTTCAGCACCAGGTCGACCAGGAAGAAGGTGTCGGAGACCACGTTAAACACTATCCAGGCGGGTGTGTGTTCGTCTTTGAAGAAGGTGATGCCCACGGGAATGATGATCAGGTTGCCCACCATTAGAAG | 235M | 765 | 38 | 389 |
| *hcn4l* | AGGAGAGGAAATCCACGGCAAACCAGCTGCGCAAGTACCTGACCTTGATCTGCTGAGGGTCCAGGATGATTTCTGTACTGTCCTCTTTCACAATCCCCGTGCGGAAGTTCAGCACGAGGTCGACCAGGAAGAAGGTGTCGGAGACCACGTAACACTATCCAGGCGGGTGTGTGTTCGTCTTTGAAGAAGGTGATGCCCACGGGGATGATGATCAGGTTGCCCACCATTAGAAG | 115M1S34M2D53M1S29M | 585 | 18 | 295 |

*Continued Supplemental Table 2*

| Orthologue | Sequence | Cigar | Mean Nr reads | Nr alleles | SD reads |
|---|---|---|---|---|---|
| *hcn4l* | AGGAGAGGAAATCCACGGCAAACCAGCTGCGCAAGTACCTGACCTTGATCTGCTGAGGGTCCAGGATGATTTCTGTACTGTCCTCTTTCACAATCCCCGTGCGGAAGTTCAGCACGAGGTCGACCAGGAAGAAGGTGTCGGAGACCAGGCGGGTGTGTGTTCGTCTTTGAAGAAGGTGATGCCCACGGGGATGATGATCAGGTTGCCCACCATTAGAAG | 115M1S28M16D45M1S29M | 523 | 9 | 176 |
| *hcn4l* | AGGAGAGGAAATCCACGGCAAACCAGCTGCGCAAGTACCTGACCTTGATCTGCTGAGGGTCCAGGATGATTTCTGTACTGTCCTCTTTCACAATCCCCGTGCGGAAGTTCAGCACGAGGTCGACCAGGAAGAAGGTGTCGGAGACCACGTTTAAACACTATCCAGGCGGGTGTGTGTTCGTCTTTGAAGAAGGTGATGCCCACGGGGATGATGATCAGGTTGCCCACCATTAGAAG | 115M1S33M1I56M1S29M | 1218 | 4 | 915 |
| *neo1a* | CAGTGAGGAACTTCAGCCCATTCTGGTTCTCCACGGAGCCGTCGGATACACTAGCGGTGCGAGGAGCGCCAGTTCTCCTCAACTGCTCAGTCCACAGCGAGTCTCCTGCCAAGATCGAGTGGAAAAAAGATGGCTCTTTCCTCAGCCTGGCTTCAGATGAGCGCAGACAGGTCCTGGCCGATGGCTCTCTGCTCATCAGCTCAGTGGTGCACTCC | 157M1S57M | 941 | 151 | 691 |
| *neo1a* | CAGTGAGGAACTTCAGCCCATTCTGGTTCTCCACGGAGCCGTGCGAGGAGCGCCAGTTCTCGCCAGTTCTCCTCAACTGCTCAGTCCACAGCGAGTCTCCTGCCAAGATCGAGTGGAAAAAAGATGGCTCTTTCCTCAGCCTGGCTTCAGATGAGCGCAGACAGGTCCTGGCCGATGGCTCTCTGCTCATCAGCTCAGTGGTGCACTCC | 40M16D10M10I91M1S57M | 957 | 95 | 545 |
| *neo1a* | CAGTGAGGAACTTCAGCCCATTCTGGTTCTCCACGGAGCCGTCGGATACACGGTGCGAGGAGCGCCAGTTCTCCTCAACTGCTCAGTCCACAGCGAGTCTCCTGCCAAGATCGAGTGGAAAAAAGATGGCTCTTTCCTCAGCCTGGCTTCAGATGAGCGCAGACAGGTCCTGGCCGATGGCTCTCTGCTCATCAGCTCAGTGGTGCACTCC | 50M4D103M1S57M | 899 | 82 | 475 |
| *neo1a* | CAGTGAGGAACTTCAGCCCATTCTGGTTCTCCACGGAGCCGTGCGAGGAGCGCCAGTTCTCCTCAACTGCTCAGTCCACAGCGAGTCTCCTGCCAAGATCGAGTGGAAAAAAGATGGCTCTTTCCTCAGCCTGGCTTCAGATGAGCGCAGACAGGTCCTGGCCGATGGCTCTCTGCTCATCAGCTCAGTGGTGCACTCC | 40M16D101M1S57M | 696 | 72 | 413 |
| *neo1a* | CAGTGAGGAACTTCAGCCCATTCTGGTTCTCCACGGAGCCGTCGGATACACGAGGAGCGCCAGTTCTCCTCAACTGCTCAGTCCACAGCGAGTCTCCTGCCAAGATCGAGTGGAAAAAAGATGGCTCTTTCCTCAGCCTGGCTTCAGATGAGCGCAGACAGGTCCTGGCCGATGGCTCTCTGCTCATCAGCTCAGTGGTGCACTCC | 50M9D98M1S57M | 589 | 72 | 305 |
| *neo1a* | CAGTGAGGAACTTCAGCCCATTCTGGTTCTCCACGGAGCCGTCGGTGCGAGGAGCGCCAGTTCTCCTCAACTGCTCAGTCCACAGCGAGTCTCCTGCCAAGATCGAGTGGAAAAAAGATGGCTCTTTCCTCAGCCTGGCTTCAGATGAGCGCAGACAGGTCCTGGCCGATGGCTCTCTGCTCATCAGCTCAGTGGTGCACTCC | 42M12D103M1S57M | 703 | 66 | 359 |
| *neo1a* | CAGTGAGGAACTTCAGCCCATTCTGGTTCTCCACGGAGCAGTTCTCCTCAACTGCTCAGTCCACAGCGAGTCTCCTGCCAAGATCGAGTGGAAAAAAGATGGCTCTTTCCTCAGCCTGGCTTCAGATGAGCGCAGACAGGTCCTGGCCGATGGCTCTCTGCTCATCAGCTCAGTGGTGCACTCC | 38M31D88M1S57M | 985 | 57 | 521 |
| *neo1a* | CAGTGAGGAACTTCAGCCCATTCTGGTTCTCCACGGAGCCGTCGGATACAGCGGTGCGAGGAGCGCCAGTTCTCCTCAACTGCTCAGTCCACAGCGAGTCTCCTGCCAAGATCGAGTGGAAAAAAGATGGCTCTTTCCTCAGCCTGGCTTCAGATGAGCGCAGACAGGTCCTGGCCGATGGCTCTCTGCTCATCAGCTCAGTGGTGCACTCC | 49M3D105M1S57M | 960 | 20 | 653 |
| *neo1a* | CAGTGAGGAACTTCAGCCCATTCTGGTTCTCCACGGAGCCGTCGGATACGAGGAGCGCCAGTTCTCCTCAACTGCTCAGTCCACAGCGAGTCTCCTGCCAAGATCGAGTGGAAAAAAGATGGCTCTTTCCTCAGCCTGGCTTCAGATGAGCGCAGACAGGTCCTGGCCGATGGCTCTCTGCTCATCAGCTCAGTGGTGCACTCC | 48M11D98M1S57M | 633 | 20 | 415 |
| *neo1a* | CAGTGAGGAACTTCAGCCCATTCTGGTTCTCCACGGAGCCGTCGGATAGCGGTGCGAGGAGCGCCAGTTCTCCTCAACTGCTCAGTCCACAGCGAGTCTCCTGCCAAGATCGAGTGGAAAAAAGATGGCTCTTTCCTCAGCCTGGCTTCAGATGAGCGCAGACAGGTCCTGGCCGATGGCTCTCTGCTCATCAGCTCAGTGGTGCACTCC | 46M5D106M1S57M | 1026 | 19 | 474 |
| *neo1a* | CAGTGAGGAACTTCAGCCCATTCTGGTTCTCCACGGAGCCGTCGGATTCTCCTCAACTGCTCAGTCCACAGCGAGTCTCCTGCCAAGATCGAGTGGAAAAAAGATGGCTCTTTCCTCAGCCTGGCTTCAGATGAGCGCAGACAGGTCCTGGCCGATGGCTCTCTGCTCATCAGCTCAGTGGTGCACTCC | 46M26D85M1S57M | 672 | 16 | 404 |
| *neo1a* | CAGTGAGGAACTTCAGCCCATTCAGCCCATTCTGGTTCTCCACGGAGCCGTCGGATACATCCATTCAGCGGTGCGAGGAGCGCCAGTTCTCCTCAACTGCTCAGTCCACAGCGAGTCTCCTGCCAAGATCGAGTGGAAAAAAGATGGCTCTTTCCTCAGCCTGGCTTCAGATGAGCGCAGACAGGTCCTGGCCGATGGCTCTCTGCTCATCAGCTCAGTGGTGCACTCC | 11M9I39M5I2S105M1S57M | 688 | 14 | 336 |
| *neo1a* | CAGTGAGGAACTTCAGCCCATTCTGGTTCTCCACGGAGCGCCAGTTCTCCTCAACTGCTCAGTCCACAGCGAGTCTCCTGCCAAGATCGAGTGGAAAAAAGATGGCTCTTTCCTCAGCCTGGCTTCAGATGAGCGCAGACAGGTCCTGGCCGATGGCTCTCTGCTCATCAGCTCAGTGGTGCACTCC | 34M28D95M1S57M | 807 | 11 | 252 |

*Continued Supplemental Table 2*

| Orthologue | Sequence | Cigar | Mean Nr reads | Nr alleles | SD reads |
|---|---|---|---|---|---|
| *neo1a* | CAGTGAGGAACTTCAGCCCATTCTGGTTCTCCACGGAGCCGTCGGATACAAAGCGAGGAGCGCCAGTTCTCCTCAACTGCTCAGTCCACAGCGAGTCTCCTGCCAAGATCGAGTGGAAAAAAGATGGCTCTTTCCTCAGCCTGGCTTCAGATGAGCGCAGACAGGTCCTGGCCGATGGCTCTCTGCTCATCAGCTCAGTGGTGCACTCC | 50M6D2S99M1S57M | 569 | 10 | 314 |
| *neo1a* | CAGTGAGGAACTTCAGCCCATTCTGGTTCTCCACGGAGCCGTTCTCCTCAACTGCTCAGTCCACAGCGAGTCTCCTGCCAAGATCGAGTGGAAAAAAGATGGCTCTTTCCTCAGCCTGGCTTCAGATGAGCGCAGACAGGTCCTGGCCGATGGCTCTCTGCTCATCAGCTCAGTGGTGCACTCC | 40M31D86M1S57M | 1179 | 9 | 312 |
| *neo1a* | CAGTGAGGAACTTCAGCCCATTCTGGTTCTCCACGGAGCCGTCGGATACACCAGCGGTGCGAGGAGCGCCAGTTCTCCTCAACTGCTCAGTCCACAGCGAGTCTCCTGCCAAGATCGAGTGGAAAAAAGATGGCTCTTTCCTCAGCCTGGCTTCAGATGAGCGCAGACAGGTCCTGGCCGATGGCTCTCTGCTCATCAGCTCAGTGGTGCACTCC | 51M1S105M1S57M | 1569 | 6 | 1406 |
| *neo1a* | CAGTGAGGAACTTCAGCCCATTCTGGTTCTCCACGGAGCCGTCGGATACACCAGCGCCAGTTCTCCTCAACTGCTCAGTCCACAGCGAGTCTCCTGCCAAGATCGAGTGGAAAAAAGATGGCTCTTTCCTCAGCCTGGCTTCAGATGAGCGCAGACAGGTCCTGGCCGATGGCTCTCTGCTCATCAGCTCAGTGGTGCACTCC | 51M1S12D93M1S57M | 1010 | 6 | 552 |
| *neo1a* | CAGTGAGGAACTTCAGCCCATTCTGGTTCTCCACGGAGCCGTCGGATACACGGTGCGGAGCGGTGCGAGGAGCGCCAGTTCTCCTCAACTGCTCAGTCCACAGCGAGTCTCCTGCCAAGATCGAGTGGAAAAAAGATGGCTCTTTCCTCAGCCTGGCTTCAGATGAGCGCAGACAGGTCCTGGCCGATGGCTCTCTGCTCATCAGCTCAGTGGTGCACTCC | 51M6I1S105M1S57M | 760 | 6 | 543 |
| *neo1a* | CAGTGAGGAACTTCAGCCCATTCTGGTTCTCCACGGAGCCGTCGGAGCGGTGCGAGGAGCGCCAGTTCTCCTCAACTGCTCAGTCCACAGCGAGTCTCCTGCCAAGATCGAGTGGAAAAAAGATGGCTCTTTCCTCAGCCTGGCTTCAGATGAGCGCAGACAGGTCCTGGCCGATGGCTCTCTGCTCATCAGCTCAGTGGTGCACTCC | 45M7D105M1S57M | 1451 | 5 | 663 |
| *neo1a* | CAGTGAGGAACTTCAGCCCATTCTGGTTCTCCACGGAGCCGTCGGATAGTCGGATAGTTCTCCTCAACTGCTCAGTCCACAGCGAGTCTCCTGCCAAGATCGAGTGGAAAAAAGATGGCTCTTTCCTCAGCCTGGCTTCAGATGAGCGCAGACAGGTCCTGGCCGATGGCTCTCTGCTCATCAGCTCAGTGGTGCACTCC | 48M2S1M11D3M4D1S87M1S57M | 754 | 5 | 361 |
| *neo1a* | CAGTGAGGAACTTCAGCCCATTCTGGTTCTCCACGGAGCCGTCGGATACACTAGCGGTGCGAGGAGCGCCAGTTCTCCTCAACTGCTCAGTCCACAGCGAGTCTCCTGCCAAGATCGAGTGGAAAAAAGATGGCTCTTTCCTCAGCCTGGCTTCAGACGAACGCAGACAGGTCCTGGCCGATGGCTCTCTGCTCATCAGCTCAGTGGTGCACTCC | 160M1S54M | 734 | 4 | 441 |
| *neo1a* | CAGTGAGGAACTTCAGCCCATTCTGGTTCTCCACGGAGCCGTCCTGGCGAGGAGCGCCAGTTCTCCTCAACTGCTCAGTCCACAGCGAGTCTCCTGCCAAGATCGAGTGGAAAAAAGATGGCTCTTTCCTCAGCCTGGCTTCAGATGAGCGCAGACAGGTCCTGGCCGATGGCTCTCTGCTCATCAGCTCAGTGGTGCACTCC | 43M7D2M1S5D99M1S57M | 376 | 2 | 40 |
| *neo1a* | CAGTGAGGAACTTCAGCCCATTCTGGTTCTCCACGGAGCCGTCGGATGTAGCGGTGCGAGGAGTGTAGCGGTGCGAGGAGCGCCAGTTCTCCTCAACTTCTCAGTCCACAGCGAGTCTCCTGCCAAGATCGAGTGGAAAAAAGATGGCTCTTTCCTCAGCCTGGCTTCAGATGAGCGCAGACAGGTCCTGGCCGATGGCTCTCTGCTCATCAGCTCAGTGGTGCACTCC | 47M2S1M14I1S33M1S72M1S57M | 1242 | 1 | - |
| *neo1a* | CAGTGAGGAACTTCAGCCCATTCTGGTTCTCCACTAGCGGTGCGAGGAGCGCCAGTTCTCCTCAACTGCTCAGTCCACAGCGAGTCTCCTGCCAAGATCGAGTGGAAAAAAGATGGCTCTTTCCTCAGCCTGGCTTCAGATGAGCGCAGACAGGTCCTGGCCGATGGCTCTCTGCTCATCAGCTCAGTGGTGCACTCC | 31M17D109M1S57M | 698 | 1 | - |
| *neo1b* | TGGCAGGTCTTCCGCGGTTCCTCAGTCAGCCGGAGGGTGTTTCTGTTCGCAGCGGTGGGACTGAGATGCTGAGCTGTGAGGTGACGGAGGAGCTGGTCCCGTTCACCCGCTGGGACAGAGATGCTGTGGAGCTGGACAGCAGGGTCATTCAGCTGCCCAGCGGAGCTCTGGTCATCAGCAACGCCTCACAGGCTGACGCC | 123M6D64M1S12M | 733 | 186 | 617 |
| *neo1b* | TGGCAGGTCTTCCGCGGTTCCTCAGTCAGCCGGAGGGTGTTTCTGTTCGCAGCGGTGGGACTGAGATGCTGAGCTGTGAGGTGACGGAGGAGCTGGTCCCGTTCACCCGCTGGGACAGAGATGCTCGGCTGTGGAGCTGGACAGCAGGGTCATTCAGCTGCCCAGCGGAGCTCTGGTCATCAGCAACGCCTCGCAGGCTGACGCC | 128M1D77M | 632 | 84 | 483 |
| *neo1b* | TGGCAGGTCTTCCGCGGTTCCTCAGTCAGCCGGAGGGTGTTTCTGTTCGCAGCGGTGGGACTGAGATGCTGAGCTGTGAGGTGACGGAGGAGCTGGTCCCGTTCACCCGCTGGGACAGAGATGCTCGGCTGTGGAGCTGGACAGCAGGGTCATTCAGCTGCCCAGCGGAGCTCTGGTCATCAGCAACGCCTCGCAGGCTGACGCC | 129M4I77M | 991 | 77 | 818 |
| *neo1b* | TGGCAGGTCTTCCGCGGTTCCTCAGTCAGCCGGAGGGTGTTTCTGTTCGCAGCGGTGGGACTGAGATGCTGAGCTGTGAGGTGACGGAGGAGCTGGTCCCGTTCACCCGCTGGGACAGAGATGCTCGGCAGCTGGACAGCAGGGTCATTCAGCTGCCCAGCGGAGCTCTGGTCATCAGCAACGCCTCGCAGGCTGACGCC | 129M6D71M | 700 | 75 | 505 |

*Continued Supplemental Table 2*

| Orthologue | Sequence | Cigar | Mean Nr reads | Nr alleles | SD reads |
|---|---|---|---|---|---|
| *neo1b* | TGGCAGGTCTTCCGCGGTTCCTCAGTCAGCCGGAGGGTGTTTCTGTTCGCAGCGGTGGGACTGAGATGCTGAGCTGTGAGGTGACGGAGGAGCTGGTCCCGTTCACCCGCTGGGACAGAGATGTGGAGCTGGACAGCAGGGTCATTCAGCTGCCCAGCGGAGCTCTGGTCATCAGCAACGCCTCACAGGCTGACGCC | 121M9D63M1S12M | 739 | 33 | 686 |
| *neo1b* | TGGCAGGTCTTCCGCGGTTCCTCAGTCAGCCGGAGGGTGTTTCTGTTCGCAGCGGTGGGACTGAGATGCTGAGCTGTGAGGTGACGGAGGAGCTGGTCCCGTTCACCCGCTGGGACAGAGATGCTCGGCCTGTGGAGCTGGACAGCAGGGTCATTCAGCTGCCCAGCGGAGCTCTGGTCATCAGCAACGCCTCACAGGCTGACGCC | 193M1S12M | 231 | 28 | 194 |
| *neo1b* | TGGCAGGTCTTCCGCGGTTCCTCAGTCAGCCGGAGGGTGTTTCTGTTCGCAGCGGTGGGACTGAGATGCTGAGCTGTGAGGTGACGGAGGAGCTGGTCCCGTTCACCCGCTGGGACAGAGATGCTGTGGAGCTGGACAGCAGGGTCATTCAGCTGCCCAGCGGAGCTCTGGTCATCAGCAACGCCTCGCAGGCTGACGCC | 123M6D77M | 970 | 27 | 739 |
| *neo1b* | TGGCAGGTCTTCCGCGGTTCCTCAGTCAGCCGGAGGGTGTTTCTGTTCGCAGCGGTGGGACTGAGATGCTGAGCTGTGAGGTGACGGAGGAGCTGGTCCCGTTCACCCGCTGGGACAGAGATGCTCGGCAGCAGGGTCTGGGTCTGGAGCTGGACAGCAGGGTCATTCAGCTGCCCAGCGGAGCTCTGGTCATCAGCAACGCCTCGCAGGCTGACGCC | 129M8I3M4I74M | 915 | 24 | 914 |
| *neo1b* | TGGCAGGTCTTCCGCGGTTCCTCAGTCAGCCGGAGGGTGTTTCTGTTCGCAGCGGTGGGACTGAGATGCTGAGCTGTGAGGTGACGGAGGAGCTGGTCCCGTTCACCCGCTGGGACAGAGATGCTCGGCCTGTGGAGCTGGACAGCAGGGTCATTCAGCTGCCCAGCGGAGCTCTGGTCATCAGCAACGCCTCACAGGCTGACGCC | 206M | 564 | 21 | 525 |
| *neo1b* | TGGCAGGTCTTCCGCGGTTCCTCAGTCAGCCGGAGGGTGTTTCTGTTCGCAGCGGTGGGACTGAGATGCTGAGCTGTGAGGTGACGGAGGAGCTGGTCCCGTTCACCCGCTGGGACAGAGATGCTCTGTGGAGCTGGACAGCAGGGTCATTCAGCTGCCCAGCGGAGCTCTGGTCATCAGCAACGCCTCGCAGGCTGACGCC | 125M4D77M | 689 | 18 | 469 |
| *neo1b* | TGGCAGGTCTTCCGCGGTTCCTCAGTCAGCCGGAGGGTGTTTCTGTTCGCAGCGGTGGGACTGAGATGCTGAGCTGTGAGGTGACGGAGGAGCTGGTCCCGTTCACCCGCTGGGACAGAGATGCTCGGAGCTGGACAGCAGGGTCATTCAGCTGCCCAGCGGAGCTCTGGTCATCAGCAACGCCTCACAGGCTGACGCC | 126M7D60M1S12M | 503 | 11 | 266 |
| *neo1b* | TGGCAGGTCTTCCGCGGTTCCTCAGTCAGCCGGAGGGTGTTTCTGTTCGCAGCGGTGGGACTGAGATGCTGAGCTGTGAGGTGACGGAGGAGCTGGTCCCGTTCACCCGCTGGGACAGAGATGCTCAGCAGGGTCATTCAGCTGCCCAGCGGAGCTCTGGTCATCAGCAACGCCTCACAGGCTGACGCC | 125M17D51M1S12M | 960 | 10 | 710 |
| *neo1b* | TGGCAGGTCTTCCGCGGTTCCTCAGTCAGCCGGAGGGTGTTTCTGTTCGCAGCGGTGGGACTGAGATGCTGAGCTGTGAGGTGACGGAGGAGCTGGTCCCGTTCACCCGCTGGGACAGAGGGACATTCAGGACATTCAGCTGCCCAGCGGAGCTCTGGTCATCAGCAACGCCTCGCAGGCTGACGCC | 120M19D5M4S2M1S55M | 801 | 10 | 567 |
| *neo1b* | TGGCAGGTCTTCCGCGGTTCCTCAGTCAGCCGGAGGGTGTTTCTGTTCGCAGCGGTGGGACTGAGATGCTGAGCTGTGAGGTGACGGAGGAGCTGGTCCCGTTCACCCGCTGGGACAGGACAGCAGGGTCATTCAGCTGCCCAGCGGAGCTCTGGTCATCAGCAACGCCTCACAGGCTGACGCC | 117M22D54M1S12M | 1170 | 3 | 685 |
| *neo1b* | TGGCAGGTCTTCCGCGGTTCCTCAGTCAGCCGGAGGGTGTTTCTGTTCGCAGCGGTGGGACTGAGATGCTGAGCTGTGAGGTGACGGAGGAGCTGGTCCCGTTCACCCACTGGGACAGAGATGCTCGGCCTGTGGAGCTGGACAGCAGGGTCATTCAGCTGCCCAGCGGAGCTCTGGTCATCAGCAACGCCTCACAGGCTGACGCC | 108M1S84M1S12M | 6 | 1 | - |
| *neo1b* | TGGCAGGTCTTCCGCGGTTCCTCAGTCAGCCGGAGGGTGTTTCTGTTCGCAGCGGTGGGACTGAGATGCTGAGCTGTGAGGTGACGGAGGAGCTGGTCCCGTTCACCCGCTGGGACAGAGATGCTCGGCAGCTGTGGAGCTGGACAGCAGGGTCATTCAGCTGCCCAGCGGAGCTCTGGTCATCAGCAACGCCTCGCAGGCTGACGCC | 129M2I77M | 5 | 1 | - |
| *neo1b* | TGGCAGGTCTTCCGCGGTTCCTCAGTCAGCCGGAGGGTGTTTCTGTTCGCAGCGGTGGGACTGAGATGCTGAGCTGTGAGGTGACGGAGGAGCTGGTCCCGTTCACCCACTGGGACAGAGATGCTCGGCCTGTGGAGCTGGACAGCAGGGTCATTCAGCTGCCCAGCGGAGCTCTGGTCATCAGCAACGCCTCGCAGGCTGACGCC | 108M1S97M | 3 | 1 | - |
| *kiaa1755_1* | CGCAGAGTCTCCTGACCAACATATGACCCAACTTATCACCAGCATGGTCCAAGCAAGACAGCCTCACAAGTCATTCCTCACAGGGCAACCGGATCTCCCTCAGACTGTACTGGGAACTAAGGCCTTACCAGATAAAAGACATCCCTGTCTGAA | 6M1S32M1S22M1S90M | 997 | 119 | 507 |
| *kiaa1755_1* | CGCAGAGTCTCCTGACCAACATATGACCCAACTTATCACCAGCATGGTCCAAGCAAGACAGCCTCACAAGTCAACCGGATCTCCCTCAGACTGTACTGGGAACTAAGGCCTTACCAGATAAAAGACATCCCTGTCTGAA | 6M1S32M1S22M1S8M14D68M | 1117 | 99 | 569 |
| *kiaa1755_1* | CGCAGAGTCTCCTGACCAACATATGACCCAACTTATCACCAGCATGGTCCAAGCAAGACAGCCTCACAAGTCATTCCTCAACCGGATCTCCCTCAGACTGTACTGGGAACTAAGGCCTTACCAGATAAAAGACATCCCTGTCTGAA | 6M1S32M1S22M1S15M7D68M | 1175 | 80 | 598 |

*Continued Supplemental Table 2*

| Orthologue | Sequence | Cigar | Mean Nr reads | Nr alleles | SD reads |
|---|---|---|---|---|---|
| *kiaa1755_1* | CGCAGAGTCTCCTGACCAACATATGACCCAACTTATCACCAACTTATCACCAGCATGGTCCAAGCAAGACAGCATCACAAGTCATTCCTCACTTGTAGGCAACCGGATCTCCCTCAGACTGTACTGGGAACTAAGGCCTTACCAGATAAAAGATATCCCTGTCTGAA | 6M1S20M11I12M1S41M3I2S56M1S13M | 882 | 68 | 903 |
| *kiaa1755_1* | CGCAGAGTCTCCTGACCAACATATGACCCAACTTATCACCAGCATGGTCCAAGCAAGACAGCATCACAAGTCATTCCTCCGGATCTCCCTCAGACTGTACTGGGAACTAAGGCCTTACCAGATAAAAGATATCCCTGTCTGAA | 6M1S32M1S38M10D51M1S13M | 541 | 57 | 417 |
| *kiaa1755_1* | CGCAGAGTCTCCTGACCAACATATGACCCAACTTATCACCAGCATGGTCCAAGCAAGACAGCATCACAAGTCATTCCTCACAACCGGGCAACCGGATCTCCCTCAGACTGTACTGGGAACTAAGGCCTTACCAGATAAAAGATATCCCTGTCTGAA | 6M1S32M1S42M3I57M1S13M | 780 | 55 | 596 |
| *kiaa1755_1* | CGCAGAGTCTCCTGACCAACATATGACCCAACTTATCACCAGCATGGTCCAAGCAAGACAGCCTCACAAGTCATTCCTCACCTCAGACTGTACTGGGAACTAAGGCCTTACCAGATAAAAGACATCCCTGTCTGAA | 6M1S32M1S22M1S17M17D56M | 1077 | 38 | 490 |
| *kiaa1755_1* | CGCAGAGTCTCCTGACCAACATATGACCCAACTTATCACCAGCATGGTCCAAGCAAGACAGCCTCACAAGTCATTCCTCACCGGCAACCGGATCTCCCTCAGACTGTACTGGGAACTAAGGCCTTACCAGATAAAAGACATCCCTGTCTGAA | 6M1S32M1S22M1S18M1S1D70M | 876 | 30 | 459 |
| *kiaa1755_1* | CGCAGAGTCTCCTGACCAACATATGACCCAACTTATCACCAGCATGGTCCAAGCAAGACAGCATCACAAGTCATTCCTCACAGGGCAACCGGATCTCCCTCAGACTGTACTGGGAACTAAGGCCTTACCAGATAAAAGATATCCCTGTCTGAA | 6M1S32M1S99M1S13M | 775 | 30 | 588 |
| *kiaa1755_1* | CGCAGAGTCTCCTGACCAACATATGACCCAACTTATCACCAGCATGGTCCAAGCAAGACAGCATCACAAGTCATTCCTCACAACCGCAACCGGATCTCCCTCAGACTGTACTGGGAACTAAGGCCTTACCAGATAAAAGATATCCCTGTCTGAA | 6M1S32M1S42M1S1I1S55M1S13M | 822 | 22 | 547 |
| *kiaa1755_1* | CGCAGAGTCTCCTGACCAACATATGACCCAACTTATCACCAGCATGGTCCAAGCAAGACAGCCTCACAAGTCATTCACAAGTCATTCTCCCTCAGACTGTACTGGGAACTAAGGCCTTACCAGATAAAAGACATCCCTGTCTGAA | 6M1S32M1S22M1S11M3D5M1S1M1S2M5D1S60M | 1190 | 21 | 408 |
| *kiaa1755_1* | CGCAGAGTCTCCTGACCAACATATGACCCAACTTATCACCAGCATGGTCCAAGCAAGACAGCCTCACAAGTCATTCCTCATGACGGCAACCGGATCTCCCTCAGACTGTACTGGGAACTAAGGCCTTACCAGATAAAAGACATCCCTGTCTGAA | 6M1S32M1S22M1S17M1S1I1M1S70M | 1469 | 20 | 683 |
| *kiaa1755_1* | CGCAGAGTCTCCTGACCAACATATGACCCAACTTATCACCAGCATGGTCCAAGCAAGACAGCCTCACAAGTCATTCCTCACAACCGGATCTCCCTCAGACTGTACTGGGAACTAAGGCCTTACCAGATAAAAGACATCCCTGTCTGAA | 6M1S32M1S22M1S17M5D68M | 1365 | 18 | 561 |
| *kiaa1755_1* | CGCAGAGTCTCCTGACCAACATATGACCCAACTTATCACCAGCATGGTCCAAGCAAGACAGCCTCACAAGTCATTCCTCACAAGGGCAACCGGATCTCCCTCAGACTGTACTGGGAACTAAGGCCTTACCAGATAAAAGACATCCCTGTCTGAA | 6M1S32M1S22M1S18M1I72M | 1602 | 14 | 834 |
| *kiaa1755_1* | CGCAGAGTCTCCTGACCAACATAATGTACTGGGAACTAAGGCCTTACCAGATAAAAGATATCCCTGTCTGAA | 6M1S15M81D1M1S34M1S13M | 1070 | 14 | 568 |
| *kiaa1755_1* | CGCAGAGTCTCCTGACCAACATATGACCCAACTTATCACCAGCATGGTCCAAGCAAGACAGCCTCACAAGTCATTCCGCAACCGGATCTCCCTCAGACTGTACTGGGAACTAAGGCCTTACCAGATAAAAGACATCCCTGTCTGAA | 6M1S32M1S22M1S14M7D69M | 1063 | 14 | 794 |
| *kiaa1755_1* | CGCAGAGTCTCCTGACCAACATATGACCCAACTTATCACCAGCATGGTCCAAGCAAGACAGCCTCACTAACAACCGGATCTCCCTCAGACTGTACTGGGAACTAAGGCCTTACCAGATAAAAGACATCCCTGTCTGAA | 6M1S32M1S22M1S4M1S1M15D1S68M | 876 | 12 | 386 |
| *kiaa1755_1* | CGCAGAGTCTCCTGACCAACATATGACCCAACTTATCACCAGCATGGTCCAAGCAAGACAGCCTCACAAGTCATTCCTCAACCGGACTCAGGGCAACCGGATCTCCCTCAGACTGTACTGGGAACTAAGGCCTTACCAGATAAAAGACATCCCTGTCTGAA | 6M1S32M1S22M1S17M8I73M | 950 | 10 | 426 |
| *kiaa1755_1* | CGCAGAGTCTCCTGACCAACATATGACCCAACTTATCACCAGCATGGTCCAAGCAAGACAGCATCACAAGTCATTCCTCAACCGGCAACCGGATCTCCCTCAGACTGTACTGGGAACTAAGGCCTTACCAGATAAAAGATATCCCTGTCTGAA | 6M1S32M1S40M3S56M1S13M | 618 | 9 | 283 |
| *kiaa1755_1* | CGCAGAGTCTCCTGACCAACATATGACCCAACTTATCACCAGCATGGTCCAAGCAAGACAGCATCACAAGTCATTCCTCAAGGGCAACCGGATCTCCCTCAGACTGTACTGGGAACTAAGGCCTTACCAGATAAAAGATATCCCTGTCTGAA | 6M1S32M1S41M1I58M1S13M | 581 | 6 | 250 |
| *kiaa1755_1* | CGCAGAGTCTCCTGACCAACATATGACCCAACTTATCACCAGCATGGTCCAAGCAAGACAGCATCACAAGTCATTCCTCACAACCGCAACCGGATCTCCCTCAGACTGTACTGGGAACTAAGGCCTTACCAGATAAAAGACATCCCTGTCTGAA | 6M1S32M1S42M1S1I1S69M | 145 | 6 | 23 |

*Continued Supplemental Table 2*

| Orthologue | Sequence | Cigar | Mean Nr reads | Nr alleles | SD reads |
|---|---|---|---|---|---|
| *kiaa1755_1* | CGCAGAGTCTCCTGACCAACATATGACCCAACTTATCACCAACTTATCACCAGCATGGTCCAAGCAAGACAGCATCACAAGTCATTCCTCACTTGTAGGCAACCGGATCTCCCTCAGACTGTACTGGGAACTAAGGCCTTACCAGATAAAAGACATCCCTGTCTGAA | 6M1S20M11I12M1S41M3I2S70M | 136 | 6 | 89 |
| *kiaa1755_1* | CGCAGAGTCTCCTGACCAACATATGACCCAACTTATCACCAGCATGGTCCAAGCAAGACAGCATCACAAGTCATTCCTCACCAACCGGATCTCCCTCAGACTGTACTGGGAACTAAGGCCTTACCAGATAAAAGATATCCCTGTCTGAA | 6M1S32M1S41M4D54M1S13M | 1101 | 5 | 323 |
| *kiaa1755_1* | CGCAGAGTCTCCTGACCAACATATGACCCAACTTATCACCAGCATGGTCCAAGCAAGACAGCATCACAAGTCATTCCTCACAGGGCAACCGGATCTCCCTCAGACTGTACTGGGAACTAAGGCCTTACCAGATAAAAGACATCCCTGTCTGAA | 6M1S32M1S113M | 120 | 4 | 48 |
| *kiaa1755_1* | CGCAGAGTCTCCTGACCAACATATGACCCAACTTATCACCAGCATGGTCCAAGCAAGACAGCATCACAAGTCATTCCTCACAACCGGGCAACCGGATCTCCCTCAGACTGTACTGGGAACTAAGGCCTTACCAGATAAAAGACATCCCTGTCTGAA | 6M1S32M1S42M3I71M | 107 | 2 | 65 |
| *kiaa1755_1* | CGCAGAGTCTCCTGACCAACATATGACCCAACTTATCACCAGCATGGTCCAAGCAAGACAGCCTCACAAGTCATTCCTCACCGGCAAGTCATTCGGATCTCCCTCAGACTGTACTGGGAACTAAGGCCTTACCAGATAAAAGACATCCCTGTCTGAA | 6M1S32M1S22M1S17M4I2M1S1M1S2M2S64M | 1184 | 1 | - |
| *kiaa1755_1* | CGCAGAGTCTCCTGACCAACATAATGTACTGGGAACTAAGGCCTTACCAGATAAAAGACATCCCTGTCTGAA | 6M1S15M81D1M1S48M | 233 | 1 | - |
| *kiaa1755_1* | CGCAGACTCTCCTGACCAACATATGACCCAACTTATCACAAGCATGGTCCAAGCAAGACAGCATCACAAGTCATTCCTCACAGGGCAACCGGATCTCCCTCAGACTGTACTGGGAACTAAGGCCTTACCAGATAAAAGACATCCCTGTCTGAA | 153M | 25 | 1 | - |
| *kiaa1755_2* | TCTGATCATCCTAATGAAGCAGAAACTGCTGACCCCTGCGGTGAGGAGAAAATCCAGAGCGCATACCGGGACGGCACATCAGAGAAATGCCACATTGTGATTCAGGGACAGTCAAATCAAGAGGACAGAAG | 48M1S22M21D45M1S2M1S11M | 985 | 120 | 638 |
| *kiaa1755_2* | TCTGATCATCCTAATGAAGCAGAAACTGCTGACCCCTGCGGTGAGGAGAAAATCCAGAGCGCATACCGGGACGGTTTGGCTCCAGCAGTGGTCGGCACATCAGAGAAATGCCACATTGTGATTCAGGGACAGTCAAATCAAGAGGACAGAAG | 48M1S88M1S2M1S11M | 951 | 78 | 613 |
| *kiaa1755_2* | TCTGATCATCCTAATGAAGCAGAAACTGCTGACCCCTGCGGTGAGGAGAAAATCCAGAGCGCATACCGGGTCGGCACATCAGAGAAATGCCACATTGTGATTCAGGGACAGTCAAATCAAGAGGACAGAAG | 48M1S19M21D48M1S2M1S11M | 886 | 63 | 460 |
| *kiaa1755_2* | TCTGATCATCCTAATGAAGCAGAAACTGCTGACCCCTGCGGTGAGGAGAAAATCCAGAGCGCATACCGGGACAGAGAAATGCCACATTGTGATTCAGGGACAGTCAAATCAAGAGGACAGAAG | 48M1S22M29D37M1S2M1S11M | 1070 | 62 | 464 |
| *kiaa1755_2* | TCTGATCATCCTAATGAAGCAGAAACTGCTGACCCCTGCGGTGAGGAGCAAATCCAGAGCGCATACCGGGACGGTTTGGCTCCAGTGGTCGGCACATCAGAGAAATGCCACATTGTGATTCAGGGACAGTCAAACCAGGAGGACAGAAG | 82M3D67M | 772 | 62 | 333 |
| *kiaa1755_2* | TCTGATCATCCTAATGAAGCAGAAACTGCTGACCCCTGCGGTGAGGAGCAAATCCAGAGCGCATACCGGGACGGTTTGGGCACATCAGAGAAATGCCACATTGTGATTCAGGGACAGTCAAACCAGGAGGACAGAAG | 78M15D59M | 856 | 59 | 414 |
| *kiaa1755_2* | TCTGATCATCCTAATGAAGCAGAAACTGCTGACCCCTGCGGTGAGGAGCAAATCCAGAGCGCATACCGGGACGGTTTGGCTCATCAGAGAAACACAGAGAAATGGCACATCAGAGAAATGCCACATTGTGATTCAGGGACAGTCAAACCAGGAGGACAGAAG | 81M1D2M1S3M1S1M11I3S59M | 829 | 55 | 457 |
| *kiaa1755_2* | TCTGATCATCCTAATGAAGCAGAAACTGCTGACCCCTGCGGTGAGGAGCAAATCCAGAGCGCATACCGGGACGGTTTGGCTCATCAGAGAAATGCCACATTGTGATTCAGGGACAGTCAAACCAGGAGGACAGAAG | 81M16D55M | 935 | 35 | 587 |
| *kiaa1755_2* | TCTGATCATCCTAATGAAGCAGAAACTGCTGACCCCTGCGGTGAGGAGCAAATCCAGAGCGCATACCGGGACGGTTTGGTCGGCACATCAGAGAAATGCCACATTGTGATTCAGGGACAGTCAAACCAGGAGGACAGAAG | 76M12D64M | 837 | 33 | 470 |
| *kiaa1755_2* | TCTGATCATCCTAATGAAGCAGAAACTGCTGACCCCTGCGGTGAGGAGCAAATCCAGAGCGCATACCGGGACGGTTTGGCTCCAGCAGTGGTCGGCACATCAGAGAAATGCCACATTGTGATTCAGGGACAGTCAAACCAGGAGGACAGAAG | 152M | 564 | 32 | 351 |
| *kiaa1755_2* | TCTGATCATCCTAATGAAGCAGAAACTGCTGACCCCTGCGGTGAGGAGAAAATCCAGAGCGCATACCGGGACAGTGGTCGGCACATCAGAGAAATGCCACATTGTGATTCAGGGACAGTCAAATCAAGAGGACAGAAG | 48M1S22M14D52M1S2M1S11M | 964 | 26 | 370 |
| *kiaa1755_2* | TCTGATCATCCTAATGAAGCAGAAACTGCTGACCCCTGCGGTGAGGAGAAAATCCAGAGCGCATACCGGGACGGTTTGGCTCCAGTGGTCGGCACATCAGAGAAATGCCACATTGTGATTCAGGGACAGTCAAATCAAGAGGACAGAAG | 48M1S33M3D52M1S2M1S11M | 793 | 20 | 426 |

*Continued Supplemental Table 2*

| Orthologue | Sequence | Cigar | Mean Nr reads | Nr alleles | SD reads |
|---|---|---|---|---|---|
| *kiaa1755_2* | TCTGATCATCCTAATGAAGCAGAAACTGCTGACCCCTGCGGTGAGGAGAAAATCCAGAGCGCATACCGGGACGGG ACCAGTGGTCGGCACATCAGAGAAATGCCACATTGTGATTCAGGGACAGTCAAATCAAGAGGACAGAAG | 48M1S25M1S8D1M1S52M1S2M1S11M | 787 | 19 | 595 |
| *kiaa1755_2* | TCTGATCATCCTAATGAAGCAGAAACTGCTGACCCCTGCGGTGAGGAGAAAATCCAGAGCGCATACCGGGACGGT ACATCAGAGAAATGCCACATTGTGATTCAGGGACAGTCAAATCAAGAGGACAGAAG | 48M1S26M21D41M1S2M1S11M | 1035 | 18 | 370 |
| *kiaa1755_2* | TCTGATCATCCTAATGAAGCAGAAACTGCTGACCCCTGCGGTGAGGAGAAAATCCAGAGCGCATACCGGGACGGT TTGGGTCGGCACATCAGAGAAATGCCACATTGTGATTCAGGGACAGTCAAATCAAGAGGACAGAAG | 48M1S29M11D48M1S2M1S11M | 657 | 17 | 443 |
| *kiaa1755_2* | TCTGATCATCCTAATGAAGCAGAAACTGCTGACCCCTGCGGTGAGGAGAAAATCCAGAGCGCATACCGGGACGGT CGGCACATCAGAGAAATGCCACATTGTGATTCAGGGACAGTCAAATCAAGAGGACAGAAG | 48M1S23M17D48M1S2M1S11M | 1152 | 15 | 331 |
| *kiaa1755_2* | TCTGATCATCCTAATGAAGCAGAAACTGCTGACCCCTGCGGTGAGGAGCAAATCCAGAGCGCATACCGGGACGGT TTAAAAATAAGGCTAGTGGTCGGCACATCAGAGAAATGCCACATTGTGATTCAGGGACAGTCAAACCAGGAGGAC AGAAG | 77M8I4M5D66M | 584 | 11 | 214 |
| *kiaa1755_2* | TCTGATCATCCTAATGAAGCAGAAACTGCTGACCCCTGCGGTGAGGAGCAAATCCAGAGCGCATACCGGGACGGC ACATCAGAGAAATGCCACATTGTGATTCAGGGACAGTCAAACCAGGAGGACAGAAG | 71M21D60M | 1110 | 9 | 532 |
| *kiaa1755_2* | TCTGATCATCCTAATGAAGCAGAAACTGCTGACCCCTGCGGTGAGGAGCAAATCCAGAGCGCATACCGGGACGGC ACATCCAGTGGTCGGCACATCAGAGAAATGCCACATTGTGATTCAGGGACAGTCAAACCAGGAGGACAGAAG | 74M5S1M5D67M | 970 | 9 | 382 |
| *kiaa1755_2* | TCTGATCATCCTAATGAAGCAGAAACTGCTGACCCCTGCGGTGAGGAGCAAATCCAGAGCGCATACCGGGACGGA AATGCCACATTGTGATTCAGGGACAGTCAAACCAGGAGGACAGAAG | 73M31D48M | 976 | 4 | 130 |
| *kiaa1755_2* | TCTGATCATCCTAATGAAGCAGAAACTGCTGACCCCTGCGGTGAGGAGCAAATCCAGAGCGCATACCGGGACGAT GTGGTCGGCACATCAGAGAAATGCCACATTGTGATTCAGGGACAGTCAAACCAGGAGGACAGAAG | 73M1S1M12D65M | 726 | 4 | 358 |
| *kiaa1755_2* | TCTGATCATCCTAATGAAGCAGAAACTGCTGACCCCTGCGGTGAGGAGAAAATCCAGAGCGCATACCGGGACGGT ATGGCACATCAGAGAAATGCCACATTGTGATTCAGGGACAGTCAAATCAAGAGGACAGAAG | 48M1S26M1S1M16D44M1S2M1S11M | 1411 | 3 | 177 |
| *kiaa1755_2* | TCTGATCATCCTAATGAAGCAGAAACTGCTGACCCCTGCGGTGAGGAGCAAATCCAGAGCGCATACCGGGTCGGC ACATCAGAGAAATGCCACATTGTGATTCAGGGACAGTCAAACCAGGAGGACAGAAG | 68M21D63M | 913 | 3 | 550 |
| *kiaa1755_2* | TCTGATCATCCTAATGAAGCAGAAACTGCTGACCCCTGCGGTGAGGAGCAAATCCAGAGCGCATACCGGGACGGT ATGGTCGACATCAGAGAAATGCCACATTGTGATTCAGGGACAGTCAAACCAGGAGGACAGAAG | 75M12D1S6M2D56M | 834 | 3 | 128 |
| *kiaa1755_2* | TCTGATCATCCTAATGAAGCAGAAACTGCTGACCCCTGCGGTGAGGAGAAAATCCAGAGCGCATACCGGGACGGT TTGGTCGAACAGTGGTCGGCACATCAGAGAAATGCCACATTGTGATTCAGGGACAGTCAAATCAAGAGGACAGAA G | 48M1S30M1D2M1S1M1S52M1S2M1S11M | 562 | 1 | - |
| *kiaa1755_2* | TCTGATCATCCTAATGAAGCAGAAACTGCTGACCCCTGCGGTGAGGAGAAAATCCAGAGCGCATACCGGGACATC AGAGAAATGCCACATTGTGATTCAGGGACAGTCAAATCAAGAGGACAGAAG | 48M1S21M26D41M1S2M1S11M | 558 | 1 | - |
| *dclk1b* | ATGTGTGTGGATCAATTGAGCCTTACAAGATGCAGGAATATACTAAAAACGTCAACCCTAACTGGTCGGTCAACAT GAGAACCACTGCCGGAGCAAAACCGCCCACCTCTCTGGCCAGTGCCAAGGGCGGGTCTATAGAAACCAAGGATAA CAGGGATTTCATCCGACCCAAACTGGTGACCATAATCCGTAGCGGGGTAAAGCCTCGGAAAGCCATCCGAATCCTT CTCAACAA | 235M | 1638 | 377 | 1281 |
| *dclk1b* | ATGTGTGTGGATCAATTGAGCCTTACAAGATGCAGGAATATACTAAAAACGTCAACCCTAACTGGTCGGTCAACAT GAGAACCACTGCCGGAGCAAAACCGCCCACCTCTCTGGCCAGTGCCAAGGGCGGGTCTATAGAAACCAAGGATAA CAGGGATTTCATCCGACCCAAACTGGTGACCATAATCCGTAGTGGGGTAAAGCCTCGGAAAGCCATCCGAATCCTT CTCAACAA | 193M1S41M | 1078 | 102 | 877 |
| *galnt10chr21* | GCGTAACGTGGGCACTGGGCTGTGTGTGGAGAGCAAACACTTCTCCTCCGGGTCCCCGATCCGCCTGGAACCATG CCTGAGGAGCCGCGGAGAGCCCAGCTGGAGCCACGGGCAGGTGAGACACGCACCGCTAACAGCGCTAGCACTAG AGACACACACTGCTAACTGCTAATA | 174M | 1246 | 198 | 994 |
| *galnt10chr21* | GCGTAACGTGGGCACTGGGCTGTGTGTGGAGAGCAAACACTTCTCCTCTGGGTCCCCGATCCGCCTGGAACCATG CCTGAGGAGCCGCGGAGAGCCCAGCTGGAGCCACGGGCAGGTGAGACACGCACCGCTAACAGCGCTAGCACTAG AGACACACACTGCTAACTGCTAATA | 48M1S125M | 952 | 364 | 1044 |
| *galnt10scaff* | GTGGGCACTGGGCTGTGTGTGGAGAGCAAACACTTCTCCTCTGGGTCCCCGATCCGCCTGGAACCATGCCTGAGG AGCCGCGGAGAGCCCAGCTGGAGCCACGGGCAGGTGAGACACGCACCGCTAACAGCGCTAGCACTAGAGACACA CACTGCTAACTGCTAATATGGCTAACTCTGTGTGTGTGTGTGTGTGTGTGTGTGT | 41M1S135M12D27M | 272 | 326 | 207 |

*Continued Supplemental Table 2*

| Orthologue | Sequence | Cigar | Mean Nr reads | Nr alleles | SD reads |
|---|---|---|---|---|---|
| *galnt10scaff* | GTGGGCACTGGGCTGTGTGTGGAGAGCAAACACTTCTCCTCCGGGTCCCCGATCCGCCTGGAACCATGCCTGAGG AGCCGCGGAGAGCCCAGCTGGAGCCACGGGCAGGTGAGACACGCACCGCTAACAGCGCTAGCACTAGAGACACA CACTGCTAACTGCTAATATGGCTAACTCTCTGTGTGTGTGTGTGTGTGTGTGTGTGTGTGTGTGTGT | 216M | 148 | 187 | 106 |
| *galnt10scaff* | GTGGGCACTGGGCTGTGTGTGGAGAGCAAACACTTCTCCTCTGGGTCCCCGATCCGCCTGGAACCATGCCTGAGG AGCCGCGGAGAGCCCAGCTGGAGCCACGGGCAGGTGAGACACGCACCGCTAACAGCGCTAGCACTAGAGACACA CACTGCTAACTGCTAATATGGCTAACTCTGTGTGTGTGTGTGTGTGTGTGTGT | 41M1S135M14D25M | 157 | 136 | 94 |
| *galnt10scaff* | GTGGGCACTGGGCTGTGTGTGGAGAGCAAACACTTCTCCTCTGGGTCCCCGATCCGCCTGGAACCATGCCTGAGG AGCCGCGGAGAGCCCAGCTGGAGCCACGGGCAGGTGAGACACGCACCGCTAACAGCGCTAGCACTAGAGACACA CACTGCTAACTGCTAATATGGCTAACTCTGTGTGTGTGTGTGTGTGTGTGTGTGTGTGTGTGTGT | 41M1S135M8D31M | 147 | 82 | 107 |
| *galnt10scaff* | GTGGGCACTGGGCTGTGTGTGGAGAGCAAACACTTCTCCTCCGGGTCCCCGATCCGCCTGGAACCATGCCTGAGG AGCCGCGGAGAGCCCAGCTGGAGCCACGGGCAGGTGAGACACGCACCGCTAACAGCGCTAGCACTAGAGACACA CACTGCTAACTGCTAATATGGCTAACTCTCTGTGTGTGTGTGTGTGTGTGTGTGTGTGTGTGTGTGT | 214M2N | 136 | 13 | 127 |
| *galnt10scaff* | GTGGGCACTGGGCTGTGTGTGGAGAGCAAACACTTCTCCTCTGGGTCCCCGATCCGCCTGGAACCATGCCTGAGG AGCCGCGGAGAGCCCAGCTGGAGCCACGGGCAGGTGAGACACGCACCGCTAACAGCGCTAGCACTAGAGACACA CACTGCTAACTGCTAATATGGCTAACTCTGTGTGTGTGTGTGTGTGTGTGTGTGTGTGTGTGTGT | 41M1S135M10D29M | 4 | 2 | 1 |

All unique sequences identified for targeted orthologues and their respective alignment report string (Cigar). Mean number of reads, the number of alleles the cigar was found in and the standard deviation (SD) are reported. Cigar letters: M=match, D=deletion, I=insertion, S=substitution.

**Supplemental Table 3: Unique variants and affected transcripts**

| Orthologue | Chr | ENSDARG | Affected transcripts | Start (bp) | End (bp) | Mutation | Annotation | Base pair change | VEP impact | Nr affected alleles |
|---|---|---|---|---|---|---|---|---|---|---|
| *gngt1* | 19 | ENSDARG00000035798 | ENSDART00000051950<br>ENSDART00000139083 | 40856888 | 40856893 | AAGGCG/- | inframe_deletion | -6 | MODERATE | 75 |
| | | | | 40856893 | 40856895 | GAA/- | inframe_deletion | -3 | MODERATE | 3 |
| | | | | 40856894 | 40856894 | A/- | frameshift_variant | -1 | HIGH | 69 |
| | | | | 40856895 | 40856895 | A/T | missense_variant | 0 | MODERATE | 3 |
| | | | | 40856895 | 40856897 | AGA/TTT | missense_variant | 0 | MODERATE | 69 |
| | | | | 40856897 | 40856896 | -/TAAC | stop_gained,frameshift_variant | 4 | HIGH | 2 |
| | | | | 40856897 | 40856899 | ATG/CCA | missense_variant | 0 | MODERATE | 2 |
| *syt10* | 4 | ENSDARG00000045750 | ENSDART00000136049 | 10888933 | 10888953 | GACATGAATGTCCGCACAGAG/- | inframe_deletion | -21 | MODERATE | 19 |
| | | | | 10888944 | 10888944 | C/A | synonymous_variant | 0 | LOW | 42 |
| | | | | 10888945 | 10888944 | -/CAGCTGATG | inframe_insertion | 9 | MODERATE | 42 |
| | | | | 10888946 | 10888950 | GCACA/- | frameshift_variant | -5 | HIGH | 3 |
| | | | | 10888946 | 10888952 | GCACAGA/- | frameshift_variant | -7 | HIGH | 15 |
| | | | | 10888946 | 10888953 | GCACAGAG/- | frameshift_variant | -8 | HIGH | 40 |
| | | | | 10888947 | 10888947 | C/T | synonymous_variant | 0 | LOW | 42 |
| | | | | 10888948 | 10888948 | A/C | missense_variant | 0 | MODERATE | 4 |
| | | | | 10888948 | 10888954 | ACAGAGG/- | frameshift_variant | -7 | HIGH | 11 |
| | | | | 10888949 | 10888958 | CAGAGGACGG/- | frameshift_variant | -10 | HIGH | 4 |
| | | | | 10888950 | 10888949 | -/GGGAATGG | frameshift_variant | 8 | HIGH | 42 |
| | | | | 10888950 | 10888949 | -/A | frameshift_variant | 1 | HIGH | 44 |
| | | | | 10888950 | 10888950 | A/G | synonymous_variant | 0 | LOW | 11 |
| | | | | 10888951 | 10888951 | G/T | stop_gained | 0 | HIGH | 42 |
| | | | | 10888952 | 10888951 | -/CAT | stop_gained,protein_altering_variant | 3 | HIGH | 11 |
| | | | | 10888952 | 10888952 | A/- | frameshift_variant | -1 | HIGH | 42 |
| | | | | 10888952 | 10888953 | AG/CA | missense_variant | 0 | MODERATE | 11 |
| | | | | 10888959 | 10888960 | CA/TG | missense_variant | 0 | MODERATE | 4 |
| *rgs6* | 20 | ENSDARG00000015627 | ENSDART00000135513<br>ENSDART00000184779 | 28638811 | 28638822 | CCCACCGCACCT/- | inframe_deletion | -12 | MODERATE | 1 |
| | | | | 28638820 | 28638820 | C/- | frameshift_variant | -1 | HIGH | 24 |
| | | | | 28638820 | 28638821 | CC/- | frameshift_variant | -2 | HIGH | 7 |
| | | | | 28638820 | 28638822 | CCT/- | inframe_deletion | -3 | MODERATE | 4 |
| | | | | 28638824 | 28638824 | G/A | stop_gained | 0 | HIGH | 4 |
| | | | | 28638837 | 28638836 | -/CTGAGCCATG | frameshift_variant | 10 | HIGH | 4 |
| *hcn4* | 18 | ENSDARG00000061685 | ENSDART00000136140<br>ENSDART00000189186 | 1143637 | 1143644 | ACCCGCGG/- | frameshift_variant | -8 | HIGH | 13 |
| | | | | 1143638 | 1143638 | C/T | missense_variant | 0 | MODERATE | 16 |
| | | | | 1143641 | 1143641 | G/A | missense_variant | 0 | MODERATE | 9 |
| | | | | 1143643 | 1143643 | G/- | frameshift_variant | -1 | HIGH | 11 |
| | | | | 1143643 | 1143644 | GG/CA | missense_variant | 0 | MODERATE | 2 |
| | | | | 1143643 | 1143646 | GGCT/- | frameshift_variant | -4 | HIGH | 9 |
| | | | | 1143644 | 1143643 | -/CCGCCAC | frameshift_variant | 7 | HIGH | 16 |
| | | | | 1143644 | 1143644 | G/C | missense_variant | 0 | MODERATE | 75 |
| | | | | 1143644 | 1143646 | GCT/- | inframe_deletion | -3 | MODERATE | 1 |
| | | | | 1143645 | 1143644 | -/CTCTC | frameshift_variant | 5 | HIGH | 15 |
| | | | | 1143645 | 1143644 | -/GCC | protein_altering_variant | 3 | MODERATE | 2 |
| | | | | 1143645 | 1143645 | C/- | frameshift_variant | -1 | HIGH | 2 |
| | | | | 1143646 | 1143645 | -/GCCA | frameshift_variant | 4 | HIGH | 48 |
| | | | | 1143646 | 1143646 | T/C | synonymous_variant | 0 | LOW | 48 |
| | | | | 1143652 | 1143651 | -/AGCTCC | inframe_insertion | 6 | MODERATE | 15 |

*Continued Supplemental Table 3*

| Orthologue | Chr | ENSDARG | Affected transcripts | Start (bp) | End (bp) | Mutation | Annotation | Base pair change | VEP impact | Nr affected alleles |
|---|---|---|---|---|---|---|---|---|---|---|
| *hcn4l* | 25 | ENSDARG00000074419 | ENSDART00000088249<br>ENSDART00000148940 | 29273086 | 29273101 | CCACGTTAAACACTAT/- | frameshift_variant | -16 | HIGH | 9 |
| | | | | 29273091 | 29273090 | -/T | frameshift_variant | 1 | HIGH | 4 |
| | | | | 29273092 | 29273093 | TA/- | frameshift_variant | -2 | HIGH | 18 |
| | | | | 53879228 | 53879244 | CACGGAGCCGTCGGATA/- | frameshift_variant | -17 | HIGH | 1 |
| | | | | 53879231 | 53879258 | GGAGCCGTCGGATACACTAGCGGTGCGA/- | frameshift_variant | -28 | HIGH | 11 |
| | | | | 53879235 | 53879265 | CCGTCGGATACACTAGCGGTGCGAGGAGCGC/- | frameshift_variant | -31 | HIGH | 57 |
| | | | | 53879237 | 53879252 | GTCGGATACACTAGCG/- | frameshift_variant | -16 | HIGH | 157 |
| | | | | 53879237 | 53879267 | GTCGGATACACTAGCGGTGCGAGGAGCGCCA/- | frameshift_variant | -31 | HIGH | 9 |
| | | | | 53879239 | 53879250 | CGGATACACTAG/- | inframe_deletion | -12 | MODERATE | 66 |
| | | | | 53879240 | 53879246 | GGATACA/- | frameshift_variant | -7 | HIGH | 2 |
| | | | | 53879242 | 53879248 | ATACACT/- | frameshift_variant | -7 | HIGH | 5 |
| | | | | 53879243 | 53879247 | TACAC/- | frameshift_variant | -5 | HIGH | 17 |
| | | | | 53879243 | 53879268 | TACACTAGCGGTGCGAGGAGCGCCAG/- | frameshift_variant | -26 | HIGH | 16 |
| | | | | 53879244 | 53879245 | AC/GT | missense_variant | 0 | MODERATE | 1 |
| | | | | 53879245 | 53879246 | CA/GT | missense_variant | 0 | MODERATE | 5 |
| | | | | 53879245 | 53879255 | CACTAGCGGTG/- | frameshift_variant | -11 | HIGH | 20 |
| | | | | 53879246 | 53879248 | ACT/- | inframe_deletion | -3 | MODERATE | 20 |
| *neo1a* | 7 | ENSDARG00000102855 | ENSDART00000158160<br>ENSDART00000163261<br>ENSDART00000164768<br>ENSDART00000181629 | 53879247 | 53879246 | -/GCGGTGCGAGGAGT | frameshift_variant | 14 | HIGH | 1 |
| | | | | 53879247 | 53879246 | -/TCCAT | frameshift_variant | 5 | HIGH | 14 |
| | | | | 53879247 | 53879247 | C/G | missense_variant | 0 | MODERATE | 1 |
| | | | | 53879247 | 53879248 | CT/TC | missense_variant | 0 | MODERATE | 14 |
| | | | | 53879247 | 53879250 | CTAG/- | frameshift_variant | -4 | HIGH | 82 |
| | | | | 53879247 | 53879252 | CTAGCG/- | inframe_deletion | -6 | MODERATE | 10 |
| | | | | 53879247 | 53879255 | CTAGCGGTG/- | inframe_deletion | -9 | MODERATE | 69 |
| | | | | 53879248 | 53879247 | -/GGTGCG | protein_altering_variant | 6 | MODERATE | 6 |
| | | | | 53879248 | 53879248 | T/G | missense_variant | 0 | MODERATE | 6 |
| | | | | 53879248 | 53879248 | T/C | missense_variant | 0 | MODERATE | 10 |
| | | | | 53879248 | 53879258 | TAGCGGTGCGA/- | frameshift_variant | -11 | HIGH | 5 |
| | | | | 53879249 | 53879249 | A/G | synonymous_variant | 0 | LOW | 2 |
| | | | | 53879249 | 53879260 | AGCGGTGCGAGG/- | inframe_deletion | -12 | MODERATE | 5 |
| | | | | 53879250 | 53879254 | GCGGT/- | frameshift_variant | -5 | HIGH | 2 |
| | | | | 53879253 | 53879254 | GT/AA | missense_variant | 0 | MODERATE | 10 |
| | | | | 53879262 | 53879265 | GCGC/- | frameshift_variant | -4 | HIGH | 5 |
| | | | | 53879263 | 53879262 | -/CGCCAGTTCT | frameshift_variant | 10 | HIGH | 89 |
| | | | | 53879266 | 53879266 | C/T | missense_variant | 0 | MODERATE | 5 |
| *neo1b* | 25 | ENSDARG00000075100 | ENSDART00000115280 | 2899698 | 2899698 | G/A | missense_variant | 0 | MODERATE | 2 |
| | | | | 2899707 | 2899728 | GAGATGCTCGGCCTGTGGAGCT/- | frameshift_variant | -22 | HIGH | 2 |
| | | | | 2899710 | 2899728 | ATGCTCGGCCTGTGGAGCT/- | frameshift_variant | -19 | HIGH | 7 |
| | | | | 2899711 | 2899719 | TGCTCGGCC/- | inframe_deletion | -9 | MODERATE | 19 |
| | | | | 2899713 | 2899718 | CTCGGC/- | inframe_deletion | -6 | MODERATE | 120 |
| | | | | 2899715 | 2899718 | CGGC/- | frameshift_variant | -4 | HIGH | 13 |
| | | | | 2899715 | 2899731 | CGGCCTGTGGAGCTGGA/- | frameshift_variant | -17 | HIGH | 6 |
| | | | | 2899716 | 2899722 | GGCCTGT/- | frameshift_variant | -7 | HIGH | 7 |
| | | | | 2899718 | 2899718 | C/- | frameshift_variant | -1 | HIGH | 58 |
| | | | | 2899719 | 2899718 | -/AGCAGGGT | frameshift_variant | 8 | HIGH | 15 |
| | | | | 2899719 | 2899718 | -/TCGG | frameshift_variant | 4 | HIGH | 50 |
| | | | | 2899719 | 2899718 | -/AG | frameshift_variant | 2 | HIGH | 1 |
| | | | | 2899719 | 2899724 | CTGTGG/- | inframe_deletion | -6 | MODERATE | 50 |
| | | | | 2899722 | 2899721 | -/GGTC | frameshift_variant | 4 | HIGH | 15 |
| | | | | 2899734 | 2899737 | GCAG/TTCA | missense_variant | 0 | MODERATE | 7 |
| | | | | 2899740 | 2899740 | T/A | missense_variant | 0 | MODERATE | 7 |

*Continued Supplemental Table 3*

| Orthologue | Chr | ENSDARG | Affected transcripts | Start (bp) | End (bp) | Mutation | Annotation | Base pair change | VEP impact | Nr affected alleles |
|---|---|---|---|---|---|---|---|---|---|---|
| | | | | 2051654 | 2051734 | ATGACCCAACTTATCACAAGCATGGTCCAAGCAAGACAGCATCAC AAGTCATTCCTCACAGGGCAACCGGATCTCCCTCAG/- | inframe_deletion | -81 | MODERATE | 13 |
| | | | | 2051699 | 2051699 | A/T | stop_gained | 0 | HIGH | 10 |
| | | | | 2051701 | 2051715 | GTCATTCCTCACAGG/- | inframe_deletion | -15 | MODERATE | 10 |
| | | | | 2051703 | 2051716 | CATTCCTCACAGGG/- | frameshift_variant | -14 | HIGH | 61 |
| | | | | 2051706 | 2051708 | TCC/- | inframe_deletion | -3 | MODERATE | 17 |
| | | | | 2051709 | 2051715 | TCACAGG/- | frameshift_variant | -7 | HIGH | 9 |
| | | | | 2051710 | 2051716 | CACAGGG/- | frameshift_variant | -7 | HIGH | 53 |
| | | | | 2051710 | 2051719 | CACAGGGCAA/- | frameshift_variant | -10 | HIGH | 51 |
| | | | | 2051712 | 2051711 | -/CCGG | frameshift_variant | 4 | HIGH | 1 |
| | | | | 2051712 | 2051711 | -/ACCGGACT | frameshift_variant | 8 | HIGH | 7 |
| | | | | 2051712 | 2051712 | C/T | missense_variant | 0 | MODERATE | 15 |
| | | | | 2051712 | 2051714 | CAG/ACC | missense_variant | 0 | MODERATE | 9 |
| | | | | 2051712 | 2051716 | CAGGG/- | frameshift_variant | -5 | HIGH | 14 |
| | | | ENSDART00000109679 | 2051712 | 2051728 | CAGGGCAACCGGATCTC/- | frameshift_variant | -17 | HIGH | 23 |
| | | | ENSDART00000153568 | 2051713 | 2051712 | -/G | frameshift_variant | 1 | HIGH | 15 |
| *kiaa1755_1* | 6 | ENSDARG00000073684 | ENSDART00000187502 | 2051713 | 2051712 | -/A | frameshift_variant | 1 | HIGH | 19 |
| | | | ENSDART00000187544 | 2051713 | 2051712 | -/TTG | stop_gained,inframe_insertion | 3 | HIGH | 70 |
| | | | ENSDART00000191165 | 2051713 | 2051713 | A/C | synonymous_variant | 0 | LOW | 22 |
| | | | | 2051713 | 2051714 | AG/TA | missense_variant | 0 | MODERATE | 70 |
| | | | | 2051713 | 2051716 | AGGG/- | frameshift_variant | -4 | HIGH | 4 |
| | | | | 2051714 | 2051713 | -/ACC | inframe_insertion | 3 | MODERATE | 51 |
| | | | | 2051714 | 2051714 | G/- | frameshift_variant | -1 | HIGH | 22 |
| | | | | 2051714 | 2051714 | G/A | missense_variant | 0 | MODERATE | 40 |
| | | | | 2051714 | 2051714 | G/C | missense_variant | 0 | MODERATE | 15 |
| | | | | 2051715 | 2051714 | -/C | frameshift_variant | 1 | HIGH | 22 |
| | | | | 2051715 | 2051715 | G/C | missense_variant | 0 | MODERATE | 22 |
| | | | | 2051716 | 2051716 | G/T | synonymous_variant | 0 | LOW | 18 |
| | | | | 2051716 | 2051716 | G/A | synonymous_variant | 0 | LOW | 10 |
| | | | | 2051719 | 2051720 | AC/TT | missense_variant | 0 | MODERATE | 1 |
| | | | | 2051719 | 2051723 | ACCGG/- | frameshift_variant | -5 | HIGH | 17 |
| | | | | 2051724 | 2051724 | A/T | missense_variant | 0 | MODERATE | 17 |
| | | | | 2051736 | 2051736 | C/A | missense_variant | 0 | MODERATE | 13 |

*Continued Supplemental Table 3*

| Orthologue | Chr | ENSDARG | Affected transcripts | Start (bp) | End (bp) | Mutation | Annotation | Base pair change | VEP impact | Nr affected alleles |
|---|---|---|---|---|---|---|---|---|---|---|
| | | | | 43213133 | 43213153 | GGACGGTTTGGCTCCAGCAGT/- | inframe_deletion | -21 | MODERATE | 62 |
| | | | | 43213135 | 43213160 | ACGGTTTGGCTCCAGCAGTGGTCGGC/- | frameshift_variant | -26 | HIGH | 1 |
| | | | | 43213136 | 43213149 | CGGTTTGGCTCCAG/- | frameshift_variant | -14 | HIGH | 21 |
| | | | | 43213136 | 43213156 | CGGTTTGGCTCCAGCAGTGGT/- | inframe_deletion | -21 | MODERATE | 101 |
| | | | | 43213136 | 43213164 | CGGTTTGGCTCCAGCAGTGGTCGGCACAT/- | frameshift_variant | -29 | HIGH | 50 |
| | | | | 43213137 | 43213153 | GGTTTGGCTCCAGCAGT/- | frameshift_variant | -17 | HIGH | 15 |
| | | | | 43213138 | 43213138 | G/A | missense_variant | 0 | MODERATE | 4 |
| | | | | 43213138 | 43213168 | GTTTGGCTCCAGCAGTGGTCGGCACATCAGA/- | frameshift_variant | -31 | HIGH | 3 |
| | | | | 43213139 | 43213139 | T/G | synonymous_variant | 0 | LOW | 18 |
| | | | | 43213139 | 43213143 | TTTGG/CACAT | missense_variant | 0 | MODERATE | 9 |
| | | | | 43213140 | 43213140 | T/A | missense_variant | 0 | MODERATE | 3 |
| | | | | 43213140 | 43213147 | TTGGCTCC/- | frameshift_variant | -8 | HIGH | 18 |
| | | | | 43213140 | 43213151 | TTGGCTCCAGCA/- | inframe_deletion | -12 | MODERATE | 7 |
| | | | | 43213140 | 43213160 | TTGGCTCCAGCAGTGGTCGGC/- | inframe_deletion | -21 | MODERATE | 12 |
| | | | | 43213141 | 43213152 | TGGCTCCAGCAG/- | inframe_deletion | -12 | MODERATE | 32 |
| | | | ENSDART00000158832 | 43213142 | 43213141 | -/AAAAATAA | frameshift_variant | 8 | HIGH | 7 |
| | | | ENSDART00000164262 | 43213142 | 43213157 | GGCTCCAGCAGTGGTC/- | frameshift_variant | -16 | HIGH | 3 |
| *kiaa1755_2* | 23 | ENSDARG00000103586 | ENSDART00000186065 | 43213143 | 43213153 | GCTCCAGCAGT/- | frameshift_variant | -11 | HIGH | 13 |
| | | | ENSDART00000190315 | 43213143 | 43213157 | GCTCCAGCAGTGGTC/- | inframe_deletion | -15 | MODERATE | 57 |
| | | | ENSDART00000193300 | 43213144 | 43213144 | C/- | frameshift_variant | -1 | HIGH | 1 |
| | | | | 43213145 | 43213149 | TCCAG/- | frameshift_variant | -5 | HIGH | 9 |
| | | | | 43213146 | 43213146 | C/- | frameshift_variant | -1 | HIGH | 41 |
| | | | | 43213146 | 43213150 | CCAGC/- | frameshift_variant | -5 | HIGH | 7 |
| | | | | 43213146 | 43213161 | CCAGCAGTGGTCGGCA/- | frameshift_variant | -16 | HIGH | 34 |
| | | | | 43213147 | 43213147 | C/G | missense_variant | 0 | MODERATE | 1 |
| | | | | 43213147 | 43213149 | CAG/- | inframe_deletion | -3 | MODERATE | 69 |
| | | | | 43213149 | 43213149 | G/T | missense_variant | 0 | MODERATE | 41 |
| | | | | 43213149 | 43213149 | G/C | missense_variant | 0 | MODERATE | 18 |
| | | | | 43213149 | 43213149 | G/A | missense_variant | 0 | MODERATE | 1 |
| | | | | 43213152 | 43213152 | G/A | missense_variant | 0 | MODERATE | 3 |
| | | | | 43213153 | 43213153 | T/A | missense_variant | 0 | MODERATE | 41 |
| | | | | 43213155 | 43213154 | -/AAACACAGAGA | frameshift_variant | 11 | HIGH | 41 |
| | | | | 43213155 | 43213157 | GTC/AAT | missense_variant | 0 | MODERATE | 41 |
| | | | | 43213159 | 43213160 | GC/- | frameshift_variant | -2 | HIGH | 3 |

The predicted impact of unique CRISPR-Cas9 induced mutations on protein function was assessed using Ensembl's Variant Effect Predictor (VEP). An allele- and target-specific dosage score was subsequently calculated for each larva by weighting the mutation with the highest predicted impact by a factor 0.33, 0.66, or 1 for mutations with a low, moderate or high predicted impact, respectively. Modification of expression was only observed for transcripts of genes located near the targeted gene. Start and end coordinates are based on GRCz11. For simplicity, *kiaa1755_1* refers to *quo*, and *kiaa1755_2* to *si:dkey-65j6.2*.

**Supplemental Table 4: Mutant allele frequencies**

| | Nr mutated alleles | | | | | | Expected nr mutated alleles | | | |
|---|---|---|---|---|---|---|---|---|---|---|
| **Gene** | **0** | **1** | **2** | **Missing** | **Sample call rate** | **Mutant allele freq** | **0** | **1** | **2** | **$P_{HWE}$** |
| *gngt1* | 234 | 132 | 12 | 4 | 0.990 | 0.206 | 238 | 124 | 16 | 2.70E-01 |
| *syt10* | 193 | 131 | 54 | 4 | 0.990 | 0.316 | 177 | 163 | 38 | 2.10E-04 |
| *rgs6* | 346 | 34 | 1 | 1 | 0.997 | 0.047 | 346 | 34 | 1 | 5.79E-01 |
| *hcn4* | 268 | 100 | 9 | 5 | 0.987 | 0.156 | 268 | 100 | 9 | 4.69E-01 |
| *hcn4l* | 351 | 29 | 1 | 1 | 0.997 | 0.041 | 351 | 30 | 1 | - |
| *neo1a* | 20 | 113 | 241 | 8 | 0.979 | 0.795 | 16 | 122 | 237 | 1.16E-01 |
| *neo1b* | 15 | 19 | 271 | 77 | 0.798 | 0.920 | 2 | 45 | 258 | 2.12E-13 |
| *kiaa1755_1* | 55 | 42 | 283 | 2 | 0.995 | 0.800 | 15 | 122 | 243 | 3.33E-32 |
| *kiaa1755_2* | 24 | 60 | 295 | 3 | 0.992 | 0.858 | 8 | 93 | 279 | 5.65E-10 |

Number of larvae with 0, 1 and 2 mutated alleles, as well as the number of larvae with a missing call. *P*-value for a Hardy-Weinberg equilibrium (HWE) exact test, considering a ±30 bp window around the CRISPR targeted site as a single locus (*P*<2.9E-3 is significant after Bonferroni correction). Larvae with more than two missing genotypes were excluded from the statistical analysis (i.e. n_total=382). For simplicity, *kiaa1755_1* refers to *quo*, and *kiaa1755_2* to *si:dkey-65j6.2*.

**Supplemental Table 5: Transcript-specific association analysis for dichotomous cardiac outcomes**

| | Sinoatrial pause | | | | | | | |
|---|---|---|---|---|---|---|---|---|
| | 2dpf (n=323, 39 cases) | | | | 5dpf (n=318, 9 cases) | | | |
| **Gene** | **OR** | **LCI** | **UCI** | **P** | **OR** | **LCI** | **UCI** | **P** |
| *gngt1* | 1.581 | 0.711 | 3.517 | 2.61E-01 | 0.123 | 0.009 | 1.649 | 1.13E-01 |
| *syt10* | 1.734 | 1.018 | 2.953 | 4.27E-02 | 0.732 | 0.241 | 2.221 | 5.81E-01 |
| *rgs6* | 2.209 | 0.862 | 5.666 | 9.90E-02 | 3.862 | 0.637 | 23.411 | 1.42E-01 |
| *hcn4* | 3.041 | 1.656 | 5.584 | 3.34E-04 | 1.209 | 0.359 | 4.072 | 7.59E-01 |
| *hcn4l* | 1.269 | 0.327 | 4.930 | 7.31E-01 | 3.112 | 0.328 | 29.534 | 3.23E-01 |
| *neo1a* | 0.936 | 0.465 | 1.881 | 8.52E-01 | 0.747 | 0.218 | 2.558 | 6.42E-01 |
| *neo1b* | 2.014 | 0.705 | 5.749 | 1.91E-01 | 0.379 | 0.081 | 1.785 | 2.20E-01 |
| *kiaa1755_1* | 0.749 | 0.426 | 1.318 | 3.16E-01 | 0.582 | 0.219 | 1.547 | 2.78E-01 |
| *kiaa1755_2* | 1.045 | 0.479 | 2.278 | 9.12E-01 | 8.170 | 1.077 | 61.988 | 4.22E-02 |
| time of day | 0.932 | 0.704 | 1.234 | 6.25E-01 | 1.079 | 0.583 | 1.998 | 8.09E-01 |
| intercept | 0.030 | 0.003 | 0.298 | 2.81E-03 | 0.017 | 0.000 | 0.830 | 4.00E-02 |

| | Sinoatrial arrest | | | |
|---|---|---|---|---|
| | 2dpf (n=321, 36 cases) | | | |
| **Gene** | **OR** | **LCI** | **UCI** | **P** |
| *gngt1* | 1.586 | 0.707 | 3.556 | 2.63E-01 |
| *syt10* | 1.639 | 0.952 | 2.821 | 7.47E-02 |
| *rgs6* | 1.988 | 0.737 | 5.357 | 1.75E-01 |
| *hcn4* | 2.906 | 1.556 | 5.428 | 8.19E-04 |
| *hcn4l* | 1.267 | 0.331 | 4.852 | 7.30E-01 |
| *neo1a* | 1.016 | 0.491 | 2.101 | 9.67E-01 |
| *neo1b* | 1.590 | 0.549 | 4.605 | 3.93E-01 |
| *kiaa1755_1* | 0.823 | 0.458 | 1.480 | 5.16E-01 |
| *kiaa1755_2* | 1.143 | 0.507 | 2.578 | 7.47E-01 |
| time of day | 0.928 | 0.697 | 1.236 | 6.10E-01 |
| intercept | 0.030 | 0.003 | 0.303 | 3.02E-03 |

| | Cardiac edema | | | | | | | |
|---|---|---|---|---|---|---|---|---|
| | 2dpf (n=369, 15 cases) | | | | 5dpf (n=322, 14 cases) | | | |
| **Gene** | **OR** | **LCI** | **UCI** | **P** | **OR** | **LCI** | **UCI** | **P** |
| *gngt1* | 1.518 | 0.489 | 4.706 | 4.70E-01 | 7.780 | 1.755 | 34.480 | 6.92E-03 |
| *syt10* | 0.584 | 0.226 | 1.509 | 2.67E-01 | 0.901 | 0.291 | 2.787 | 8.57E-01 |
| *rgs6* | 0.702 | 0.086 | 5.739 | 7.42E-01 | 2.730 | 0.456 | 16.336 | 2.71E-01 |
| *hcn4* | 0.546 | 0.146 | 2.043 | 3.68E-01 | 0.380 | 0.065 | 2.213 | 2.82E-01 |
| *hcn4l* | 0.800 | 0.111 | 5.770 | 8.25E-01 | 0.039 | 0.000 | 63.816 | 3.90E-01 |
| *neo1a* | 0.844 | 0.309 | 2.307 | 7.41E-01 | 0.253 | 0.080 | 0.796 | 1.88E-02 |
| *neo1b* | 1.154 | 0.328 | 4.064 | 8.23E-01 | 0.217 | 0.046 | 1.028 | 5.42E-02 |
| *kiaa1755_1* | 1.137 | 0.505 | 2.563 | 7.56E-01 | 2.126 | 0.604 | 7.486 | 2.40E-01 |
| *kiaa1755_2* | 1.317 | 0.430 | 4.032 | 6.29E-01 | 2.011 | 0.414 | 9.761 | 3.86E-01 |
| time of day | 0.963 | 0.633 | 1.465 | 8.59E-01 | 1.675 | 0.930 | 3.016 | 8.57E-02 |
| intercept | 0.036 | 0.002 | 0.697 | 2.78E-02 | 0.017 | 0.001 | 0.513 | 1.90E-02 |

***Continued Supplemental Table 5***

| | Uncontrolled atrial contractions 5dpf (n=326, 9 cases) | | | |
|---|---|---|---|---|
| **Gene** | **OR** | **LCI** | **UCI** | **P** |
| *gngt1* | 2.578 | 0.502 | 13.247 | 2.57E-01 |
| *syt10* | 0.343 | 0.065 | 1.813 | 2.08E-01 |
| *rgs6* | 1.313 | 0.138 | 12.517 | 8.13E-01 |
| *hcn4* | 1.310 | 0.339 | 5.064 | 6.96E-01 |
| *hcn4l* | - | - | - | - |
| *neo1a* | 0.294 | 0.085 | 1.012 | 5.23E-02 |
| *neo1b* | 0.988 | 0.203 | 4.810 | 9.88E-01 |
| *kiaa1755_1* | 0.644 | 0.230 | 1.802 | 4.02E-01 |
| *kiaa1755_2* | 2.107 | 0.352 | 12.615 | 4.14E-01 |
| time of day | 0.648 | 0.335 | 1.251 | 1.96E-01 |
| intercept | 0.245 | 0.004 | 14.946 | 5.03E-01 |

| | Abnormal morphology and impaired contractility 5dpf (n=326, 6 cases) | | | |
|---|---|---|---|---|
| **Gene** | **OR** | **LCI** | **UCI** | **P** |
| *gngt1* | 41.908 | 3.402 | 516.185 | 3.55E-03 |
| *syt10* | 0.928 | 0.206 | 4.187 | 9.23E-01 |
| *rgs6* | - | - | - | - |
| *hcn4* | 0.348 | 0.021 | 5.885 | 4.64E-01 |
| *hcn4l* | - | - | - | - |
| *neo1a* | 0.15 | 0.026 | 0.851 | 3.21E-02 |
| *neo1b* | 0.145 | 0.015 | 1.379 | 9.29E-02 |
| *kiaa1755_1* | 1.915 | 0.371 | 9.882 | 4.38E-01 |
| *kiaa1755_2* | 0.628 | 0.099 | 3.98 | 6.21E-01 |
| time of day | 1.316 | 0.582 | 2.978 | 5.09E-01 |
| intercept | 0.076 | 0.001 | 5.739 | 2.43E-01 |

Associations of cardiac outcomes with the number of mutated alleles across the nine orthologues, weighted by their predicted effect on protein function. At 2 and 5 days post fertilization (dpf), associations were analyzed using logistic regression for outcomes that were observed in at least five larvae. Associations were adjusted for time of day and for the weighted number of mutated alleles in the other genes as fixed factors. '-' indicates that parameters could not be estimated. For simplicity, *kiaa1755_1* refers to *quo*, and *kiaa1755_2* to *si:dkey-65j6.2*.

**Supplemental Table 6: Transcript-specific association analysis for HRV and heart rate**

| | | | | Heart rate variability | | | | |
|---|---|---|---|---|---|---|---|---|
| **Age** | **n** | **Factor** | **Gene** | **Effect size** | **SE** | **LCI** | **UCI** | **P** |
| 2 | 279 | fixed effects | *gngt1* | -0.052 | 0.107 | -0.261 | 0.157 | 6.25E-01 |
| | | | *syt10* | -0.070 | 0.077 | -0.221 | 0.081 | 3.62E-01 |
| | | | *rgs6* | 0.000 | 0.175 | -0.343 | 0.344 | 9.98E-01 |
| | | | *hcn4* | -0.004 | 0.101 | -0.202 | 0.194 | 9.70E-01 |
| | | | *hcn4l* | 0.165 | 0.178 | -0.184 | 0.514 | 3.55E-01 |
| | | | *neo1a* | -0.028 | 0.095 | -0.214 | 0.158 | 7.69E-01 |
| | | | *neo1b* | -0.065 | 0.113 | -0.287 | 0.158 | 5.68E-01 |
| | | | *kiaa1755_1* | 0.152 | 0.076 | 0.003 | 0.302 | 4.61E-02 |
| | | | *kiaa1755_2* | 0.074 | 0.097 | -0.115 | 0.264 | 4.42E-01 |
| | | | time of day | 0.503 | 0.045 | 0.414 | 0.592 | 1.77E-28 |
| | | | Heart rate (in SD) | -0.459 | 0.056 | -0.570 | -0.348 | 4.59E-16 |
| | | | intercept | -1.614 | 0.300 | -2.202 | -1.026 | 7.54E-08 |
| | | random effects | variation by batch | 0.340 | 0.113 | 0.177 | 0.652 | - |
| | | | residual | 0.765 | 0.033 | 0.704 | 0.832 | - |
| 5 | 291 | fixed effects | *gngt1* | 0.278 | 0.108 | 0.067 | 0.489 | 9.81E-03 |
| | | | *syt10* | 0.047 | 0.071 | -0.093 | 0.187 | 5.12E-01 |
| | | | *rgs6* | -0.009 | 0.157 | -0.317 | 0.299 | 9.56E-01 |
| | | | *hcn4* | -0.032 | 0.095 | -0.219 | 0.154 | 7.35E-01 |
| | | | *hcn4l* | 0.142 | 0.177 | -0.205 | 0.489 | 4.22E-01 |
| | | | *neo1a* | 0.017 | 0.096 | -0.171 | 0.204 | 8.62E-01 |
| | | | *neo1b* | 0.077 | 0.121 | -0.160 | 0.313 | 5.25E-01 |
| | | | *kiaa1755_1* | 0.000 | 0.077 | -0.150 | 0.150 | 1.00E+00 |
| | | | *kiaa1755_2* | 0.008 | 0.100 | -0.189 | 0.204 | 9.40E-01 |
| | | | time of day | 0.524 | 0.052 | 0.422 | 0.626 | 7.54E-24 |
| | | | Heart rate (in SD) | -0.645 | 0.054 | -0.751 | -0.540 | 2.86E-33 |
| | | | intercept | -1.893 | 0.383 | -2.643 | -1.142 | 7.67E-07 |
| | | random effects | variation by batch | 0.540 | 0.185 | 0.276 | 1.056 | - |
| | | | residual | 0.769 | 0.032 | 0.708 | 0.834 | - |

| | | | | Heart rate | | | | |
|---|---|---|---|---|---|---|---|---|
| **Age** | **n** | **Factor** | **Gene** | **Effect size** | **SE** | **LCI** | **UCI** | **P** |
| 2 | 279 | fixed effects | *gngt1* | -0.061 | 0.102 | -0.261 | 0.139 | 5.48E-01 |
| | | | *syt10* | -0.026 | 0.074 | -0.170 | 0.118 | 7.22E-01 |
| | | | *rgs6* | -0.045 | 0.168 | -0.374 | 0.284 | 7.88E-01 |
| | | | *hcn4* | 0.047 | 0.096 | -0.142 | 0.236 | 6.27E-01 |
| | | | *hcn4l* | 0.105 | 0.169 | -0.226 | 0.436 | 5.35E-01 |
| | | | *neo1a* | 0.055 | 0.090 | -0.122 | 0.233 | 5.39E-01 |
| | | | *neo1b* | -0.121 | 0.108 | -0.333 | 0.091 | 2.62E-01 |
| | | | *kiaa1755_1* | 0.120 | 0.073 | -0.022 | 0.263 | 9.83E-02 |
| | | | *kiaa1755_2* | 0.078 | 0.092 | -0.104 | 0.259 | 4.01E-01 |
| | | | time of day | 0.550 | 0.040 | 0.472 | 0.627 | 9.14E-44 |
| | | | HRV (in SD) | -0.408 | 0.051 | -0.508 | -0.308 | 1.23E-15 |
| | | | intercept | -1.770 | 0.258 | -2.276 | -1.264 | 7.14E-12 |
| | | random effects | variation by batch | 0.185 | 0.077 | 0.082 | 0.420 | - |
| | | | residual | 0.734 | 0.031 | 0.675 | 0.798 | - |
| 5 | 291 | fixed effects | *gngt1* | 0.094 | 0.097 | -0.095 | 0.283 | 3.31E-01 |
| | | | *syt10* | -0.033 | 0.063 | -0.157 | 0.091 | 6.02E-01 |
| | | | *rgs6* | -0.087 | 0.139 | -0.360 | 0.186 | 5.32E-01 |
| | | | *hcn4* | 0.150 | 0.084 | -0.014 | 0.315 | 7.37E-02 |
| | | | *hcn4l* | 0.204 | 0.157 | -0.104 | 0.512 | 1.94E-01 |
| | | | *neo1a* | 0.002 | 0.085 | -0.165 | 0.168 | 9.82E-01 |
| | | | *neo1b* | 0.006 | 0.107 | -0.204 | 0.216 | 9.57E-01 |
| | | | *kiaa1755_1* | 0.031 | 0.068 | -0.102 | 0.164 | 6.50E-01 |
| | | | *kiaa1755_2* | 0.197 | 0.088 | 0.024 | 0.369 | 2.59E-02 |
| | | | time of day | 0.564 | 0.043 | 0.480 | 0.648 | 1.97E-39 |
| | | | HRV (in SD) | -0.516 | 0.043 | -0.599 | -0.432 | 7.79E-34 |
| | | | intercept | -2.137 | 0.375 | -2.872 | -1.402 | 1.20E-08 |
| | | random effects | variation by batch | 0.619 | 0.204 | 0.324 | 1.181 | - |
| | | | residual | 0.682 | 0.029 | 0.629 | 0.740 | - |

Associations of heart rate variability (HRV) and heart rate (mutually adjusted) with the number of mutated alleles across the nine orthologues, weighted by their predicted effect on protein function. Associations were examined for the main transcript of each targeted zebrafish orthologue using hierarchical linear models (xtmixed in Stata), using inverse-normally transformed outcomes, so effect sizes and SEs can be interpreted as z-score units. Associations were adjusted for time of day and the weighted number of mutated alleles in the other genes as fixed factors, with larvae nested in batches (random factor). For simplicity, *kiaa1755_1* refers to *quo*, and *kiaa1755_2* to *si:dkey-65j6.2*.

**Supplemental Table 7: Transcript-specific association analysis for heart rate variability and heart rate in larvae without a sinoatrial pause before or after the recording**

| | | | | Heart rate variability | | | | |
|---|---|---|---|---|---|---|---|---|
| **Age** | **n** | **Factor** | **Gene** | **Effect size** | **SE** | **LCI** | **UCI** | **P** |
| 2 | 234 | fixed effects | *gngt1* | -0.066 | 0.122 | -0.306 | 0.173 | 5.88E-01 |
| | | | *syt10* | -0.058 | 0.084 | -0.223 | 0.107 | 4.91E-01 |
| | | | *rgs6* | 0.036 | 0.201 | -0.358 | 0.429 | 8.60E-01 |
| | | | *hcn4* | 0.029 | 0.111 | -0.189 | 0.247 | 7.95E-01 |
| | | | *hcn4l* | 0.171 | 0.206 | -0.232 | 0.575 | 4.05E-01 |
| | | | *neo1a* | -0.056 | 0.105 | -0.263 | 0.151 | 5.95E-01 |
| | | | *neo1b* | -0.094 | 0.125 | -0.338 | 0.150 | 4.50E-01 |
| | | | *kiaa1755_1* | 0.180 | 0.082 | 0.019 | 0.340 | 2.81E-02 |
| | | | *kiaa1755_2* | 0.093 | 0.102 | -0.107 | 0.292 | 3.64E-01 |
| | | | time of day | 0.555 | 0.050 | 0.456 | 0.654 | 4.10E-28 |
| | | | Heart rate (in SD) | -0.534 | 0.063 | -0.658 | -0.411 | 1.81E-17 |
| | | | intercept | -1.770 | 0.316 | -2.388 | -1.151 | 2.05E-08 |
| | | random effects | variation by batch | 0.344 | 0.118 | 0.176 | 0.674 | - |
| | | | residual | 0.769 | 0.036 | 0.702 | 0.843 | - |
| 5 | 283 | fixed effects | *gngt1* | 0.264 | 0.106 | 0.056 | 0.472 | 1.27E-02 |
| | | | *syt10* | -0.005 | 0.071 | -0.144 | 0.134 | 9.42E-01 |
| | | | *rgs6* | -0.025 | 0.157 | -0.333 | 0.282 | 8.72E-01 |
| | | | *hcn4* | -0.042 | 0.094 | -0.226 | 0.142 | 6.56E-01 |
| | | | *hcn4l* | 0.135 | 0.173 | -0.203 | 0.474 | 4.33E-01 |
| | | | *neo1a* | -0.002 | 0.094 | -0.185 | 0.182 | 9.86E-01 |
| | | | *neo1b* | 0.055 | 0.118 | -0.176 | 0.286 | 6.41E-01 |
| | | | *kiaa1755_1* | 0.020 | 0.077 | -0.131 | 0.170 | 7.99E-01 |
| | | | *kiaa1755_2* | 0.081 | 0.102 | -0.119 | 0.281 | 4.28E-01 |
| | | | time of day | 0.534 | 0.051 | 0.434 | 0.633 | 8.87E-26 |
| | | | Heart rate (in SD) | -0.623 | 0.053 | -0.727 | -0.519 | 5.00E-32 |
| | | | intercept | -1.978 | 0.372 | -2.707 | -1.250 | 1.01E-07 |
| | | random effects | variation by batch | 0.516 | 0.178 | 0.263 | 1.013 | - |
| | | | residual | 0.747 | 0.032 | 0.687 | 0.812 | - |

| | | | | Heart rate | | | | |
|---|---|---|---|---|---|---|---|---|
| **Age** | **N** | **Factor** | **Gene** | **Effect size** | **SE** | **LCI** | **UCI** | **P** |
| 2 | 234 | fixed effects | *gngt1* | -0.008 | 0.112 | -0.228 | 0.212 | 9.43E-01 |
| | | | *syt10* | -0.012 | 0.077 | -0.162 | 0.139 | 8.78E-01 |
| | | | *rgs6* | -0.114 | 0.184 | -0.474 | 0.245 | 5.33E-01 |
| | | | *hcn4* | 0.041 | 0.101 | -0.157 | 0.240 | 6.82E-01 |
| | | | *hcn4l* | 0.048 | 0.187 | -0.317 | 0.414 | 7.95E-01 |
| | | | *neo1a* | 0.050 | 0.095 | -0.137 | 0.236 | 6.01E-01 |
| | | | *neo1b* | -0.165 | 0.113 | -0.386 | 0.057 | 1.45E-01 |
| | | | *kiaa1755_1* | 0.153 | 0.075 | 0.007 | 0.300 | 4.00E-02 |
| | | | *kiaa1755_2* | 0.113 | 0.093 | -0.069 | 0.295 | 2.24E-01 |
| | | | time of day | 0.586 | 0.041 | 0.505 | 0.666 | 5.48E-46 |
| | | | HRV (in SD) | -0.434 | 0.051 | -0.535 | -0.333 | 3.28E-17 |
| | | | intercept | -1.890 | 0.256 | -2.392 | -1.388 | 1.60E-13 |
| | | random effects | variation by batch | 0.171 | 0.077 | 0.071 | 0.414 | - |
| | | | residual | 0.705 | 0.033 | 0.643 | 0.773 | - |
| 5 | 283 | fixed effects | *gngt1* | 0.099 | 0.098 | -0.093 | 0.291 | 3.11E-01 |
| | | | *syt10* | -0.056 | 0.065 | -0.183 | 0.072 | 3.92E-01 |
| | | | *rgs6* | -0.085 | 0.144 | -0.366 | 0.197 | 5.55E-01 |
| | | | *hcn4* | 0.157 | 0.085 | -0.010 | 0.325 | 6.54E-02 |
| | | | *hcn4l* | 0.198 | 0.158 | -0.111 | 0.508 | 2.09E-01 |
| | | | *neo1a* | 0.007 | 0.086 | -0.161 | 0.176 | 9.31E-01 |
| | | | *neo1b* | -0.002 | 0.108 | -0.213 | 0.210 | 9.86E-01 |
| | | | *kiaa1755_1* | 0.037 | 0.070 | -0.100 | 0.175 | 5.94E-01 |
| | | | *kiaa1755_2* | 0.208 | 0.093 | 0.027 | 0.390 | 2.47E-02 |
| | | | time of day | 0.574 | 0.044 | 0.488 | 0.659 | 2.21E-39 |
| | | | HRV (in SD) | -0.530 | 0.045 | -0.617 | -0.443 | 1.35E-32 |
| | | | intercept | -2.187 | 0.377 | -2.927 | -1.448 | 6.58E-09 |
| | | random effects | variation by batch | 0.617 | 0.204 | 0.323 | 1.178 | - |
| | | | residual | 0.684 | 0.029 | 0.629 | 0.743 | - |

Associations of heart rate variability (HRV) and heart rate (mutually adjusted) with the number of mutated alleles across the nine orthologues, weighted by their predicted effect on protein function. Associations were examined for the main transcript of each targeted zebrafish orthologue using hierarchical linear models (xtmixed in Stata), using inverse-normally transformed outcomes, so effect sizes and SEs can be interpreted as z-score units. Larvae with a sinoatrial pause before or after the recording were excluded from the analysis in this sensitivity analysis. Analyses were adjusted for time of day and the weighted number of mutated alleles in the other genes as fixed factors, with larvae nested in batches (random factor). For simplicity, *kiaa1755_1* refers to *quo*, and *kiaa1755_2* to *si:dkey-65j6.2*.

**Supplemental Table 8: Transcript-specific association analyses for body size**

| | | Body length | | | | | | | | | |
|---|---|---|---|---|---|---|---|---|---|---|---|
| | | 2dpf (n=332) | | | | | 5dpf (n=240) | | | | |
| **Factor** | **Gene** | **Effect size** | **SE** | **LCI** | **UCI** | **P** | **Effect size** | **SE** | **LCI** | **UCI** | **P** |
| fixed effects | *gngt1* | -0.053 | 0.114 | -0.278 | 0.171 | 6.41E-01 | 0.027 | 0.112 | -0.193 | 0.246 | 8.12E-01 |
| | *syt10* | 0.086 | 0.080 | -0.070 | 0.242 | 2.79E-01 | 0.040 | 0.073 | -0.103 | 0.183 | 5.85E-01 |
| | *rgs6* | 0.015 | 0.171 | -0.321 | 0.350 | 9.31E-01 | -0.271 | 0.157 | -0.577 | 0.036 | 8.38E-02 |
| | *hcn4* | -0.092 | 0.103 | -0.294 | 0.109 | 3.69E-01 | 0.050 | 0.096 | -0.138 | 0.238 | 6.02E-01 |
| | *hcn4l* | 0.159 | 0.204 | -0.241 | 0.559 | 4.37E-01 | -0.003 | 0.208 | -0.411 | 0.406 | 9.90E-01 |
| | *neo1a* | -0.201 | 0.103 | -0.403 | 0.001 | 5.08E-02 | 0.061 | 0.094 | -0.123 | 0.246 | 5.16E-01 |
| | *neo1b* | -0.117 | 0.119 | -0.350 | 0.116 | 3.26E-01 | -0.079 | 0.118 | -0.311 | 0.152 | 5.02E-01 |
| | *kiaa1755_1* | 0.107 | 0.078 | -0.046 | 0.260 | 1.70E-01 | -0.005 | 0.075 | -0.152 | 0.143 | 9.50E-01 |
| | *kiaa1755_2* | -0.208 | 0.107 | -0.417 | 0.001 | 5.12E-02 | -0.071 | 0.107 | -0.281 | 0.139 | 5.07E-01 |
| | Time of day | 0.113 | 0.042 | 0.030 | 0.195 | 7.49E-03 | 0.081 | 0.048 | -0.013 | 0.175 | 9.26E-02 |
| | Intercept | 0.166 | 0.330 | -0.480 | 0.812 | 6.15E-01 | -0.235 | 0.429 | -1.077 | 0.607 | 5.84E-01 |
| random effects | Variation by batch | 0.407 | 0.131 | 0.217 | 0.764 | - | 0.711 | 0.231 | 0.376 | 1.345 | - |
| | Residual | 0.897 | 0.035 | 0.831 | 0.969 | - | 0.719 | 0.033 | 0.657 | 0.787 | - |

| | | Dorsal body surface area | | | | | | | | | |
|---|---|---|---|---|---|---|---|---|---|---|---|
| | | 2dpf (n=322) | | | | | 5dpf (n=233) | | | | |
| **Factor** | **Gene** | **Effect size** | **SE** | **LCI** | **UCI** | **P** | **Effect size** | **SE** | **LCI** | **UCI** | **P** |
| fixed effects | *gngt1* | 0.112 | 0.109 | -0.101 | 0.324 | 3.04E-01 | -0.328 | 0.136 | -0.595 | -0.060 | 1.63E-02 |
| | *syt10* | -0.057 | 0.076 | -0.206 | 0.091 | 4.48E-01 | -0.040 | 0.087 | -0.211 | 0.132 | 6.48E-01 |
| | *rgs6* | 0.038 | 0.163 | -0.282 | 0.358 | 8.16E-01 | -0.135 | 0.191 | -0.508 | 0.239 | 4.80E-01 |
| | *hcn4* | -0.106 | 0.098 | -0.298 | 0.086 | 2.80E-01 | -0.016 | 0.113 | -0.238 | 0.205 | 8.84E-01 |
| | *hcn4l* | -0.151 | 0.196 | -0.535 | 0.233 | 4.41E-01 | 0.359 | 0.243 | -0.118 | 0.835 | 1.41E-01 |
| | *neo1a* | 0.218 | 0.099 | 0.025 | 0.412 | 2.66E-02 | 0.025 | 0.113 | -0.195 | 0.246 | 8.23E-01 |
| | *neo1b* | -0.100 | 0.115 | -0.325 | 0.126 | 3.86E-01 | -0.075 | 0.147 | -0.363 | 0.213 | 6.12E-01 |
| | *kiaa1755_1* | 0.016 | 0.075 | -0.131 | 0.163 | 8.32E-01 | 0.006 | 0.090 | -0.170 | 0.183 | 9.43E-01 |
| | *kiaa1755_2* | 0.060 | 0.102 | -0.139 | 0.259 | 5.55E-01 | -0.015 | 0.127 | -0.264 | 0.233 | 9.03E-01 |
| | Time of day | -0.046 | 0.040 | -0.125 | 0.032 | 2.49E-01 | -0.084 | 0.055 | -0.192 | 0.024 | 1.26E-01 |
| | Intercept | -0.152 | 0.338 | -0.815 | 0.510 | 6.52E-01 | 0.386 | 0.383 | -0.365 | 1.137 | 3.13E-01 |
| random effects | Variation by batch | 0.492 | 0.154 | 0.267 | 0.910 | - | 0.325 | 0.127 | 0.151 | 0.697 | - |
| | Residual | 0.842 | 0.034 | 0.779 | 0.911 | - | 0.852 | 0.040 | 0.777 | 0.934 | - |

| | | Lateral body surface area | | | | | | | | | |
|---|---|---|---|---|---|---|---|---|---|---|---|
| | | 2dpf (n=300) | | | | | 5dpf (n=256) | | | | |
| **Factor** | **Gene** | **Effect size** | **SE** | **LCI** | **UCI** | **P** | **Effect size** | **SE** | **LCI** | **UCI** | **P** |
| fixed effects | *gngt1* | -0.056 | 0.121 | -0.293 | 0.181 | 6.41E-01 | -0.063 | 0.124 | -0.306 | 0.179 | 6.09E-01 |
| | *syt10* | 0.042 | 0.085 | -0.124 | 0.208 | 6.21E-01 | 0.027 | 0.083 | -0.135 | 0.189 | 7.45E-01 |
| | *rgs6* | -0.128 | 0.183 | -0.487 | 0.231 | 4.84E-01 | -0.022 | 0.175 | -0.365 | 0.322 | 9.01E-01 |
| | *hcn4* | 0.151 | 0.108 | -0.061 | 0.363 | 1.64E-01 | -0.087 | 0.107 | -0.297 | 0.122 | 4.14E-01 |
| | *hcn4l* | -0.047 | 0.221 | -0.479 | 0.385 | 8.32E-01 | 0.442 | 0.216 | 0.019 | 0.864 | 4.04E-02 |
| | *neo1a* | -0.036 | 0.110 | -0.252 | 0.180 | 7.42E-01 | -0.024 | 0.107 | -0.234 | 0.186 | 8.23E-01 |
| | *neo1b* | 0.257 | 0.130 | 0.002 | 0.512 | 4.80E-02 | -0.096 | 0.141 | -0.373 | 0.180 | 4.96E-01 |
| | *kiaa1755_1* | 0.027 | 0.085 | -0.140 | 0.194 | 7.52E-01 | 0.099 | 0.088 | -0.073 | 0.271 | 2.61E-01 |
| | *kiaa1755_2* | -0.224 | 0.117 | -0.454 | 0.005 | 5.53E-02 | 0.018 | 0.120 | -0.216 | 0.252 | 8.79E-01 |
| | Time of day | -0.049 | 0.045 | -0.138 | 0.039 | 2.72E-01 | -0.070 | 0.052 | -0.173 | 0.032 | 1.79E-01 |
| | Intercept | 0.061 | 0.335 | -0.595 | 0.718 | 8.55E-01 | 0.073 | 0.391 | -0.694 | 0.839 | 8.53E-01 |
| random effects | Variation by batch | 0.340 | 0.117 | 0.173 | 0.669 | - | 0.471 | 0.162 | 0.240 | 0.924 | - |
| | Residual | 0.914 | 0.038 | 0.843 | 0.991 | - | 0.829 | 0.037 | 0.760 | 0.905 | - |

| | | Body volume | | | | | | | | | |
|---|---|---|---|---|---|---|---|---|---|---|---|
| | | 2dpf (n=299) | | | | | 5dpf (n=198) | | | | |
| **Factor** | **Gene** | **Effect size** | **SE** | **LCI** | **UCI** | **P** | **Effect size** | **SE** | **LCI** | **UCI** | **P** |
| fixed effects | *gngt1* | -0.051 | 0.111 | -0.270 | 0.167 | 6.45E-01 | -0.071 | 0.132 | -0.330 | 0.187 | 5.88E-01 |
| | *syt10* | 0.008 | 0.079 | -0.147 | 0.163 | 9.20E-01 | 0.046 | 0.082 | -0.114 | 0.207 | 5.73E-01 |
| | *rgs6* | -0.250 | 0.181 | -0.606 | 0.106 | 1.68E-01 | -0.202 | 0.173 | -0.542 | 0.137 | 2.43E-01 |
| | *hcn4* | 0.123 | 0.099 | -0.070 | 0.317 | 2.12E-01 | -0.044 | 0.104 | -0.249 | 0.160 | 6.71E-01 |
| | *hcn4l* | -0.066 | 0.194 | -0.446 | 0.314 | 7.35E-01 | 0.319 | 0.246 | -0.163 | 0.800 | 1.94E-01 |
| | *neo1a* | 0.105 | 0.103 | -0.097 | 0.307 | 3.07E-01 | 0.043 | 0.105 | -0.162 | 0.248 | 6.82E-01 |
| | *neo1b* | 0.175 | 0.121 | -0.063 | 0.413 | 1.49E-01 | -0.061 | 0.146 | -0.347 | 0.225 | 6.78E-01 |
| | *kiaa1755_1* | -0.035 | 0.079 | -0.190 | 0.120 | 6.57E-01 | 0.192 | 0.083 | 0.028 | 0.355 | 2.14E-02 |
| | *kiaa1755_2* | -0.019 | 0.106 | -0.226 | 0.188 | 8.58E-01 | -0.036 | 0.124 | -0.279 | 0.207 | 7.72E-01 |
| | Time of day | -0.056 | 0.042 | -0.139 | 0.027 | 1.85E-01 | -0.053 | 0.053 | -0.158 | 0.051 | 3.18E-01 |
| | Intercept | -0.184 | 0.345 | -0.860 | 0.492 | 5.94E-01 | -0.296 | 0.441 | -1.160 | 0.569 | 5.03E-01 |
| random effects | Variation by batch | 0.496 | 0.155 | 0.268 | 0.916 | - | 0.598 | 0.199 | 0.311 | 1.149 | - |
| | Residual | 0.841 | 0.035 | 0.776 | 0.912 | - | 0.733 | 0.037 | 0.663 | 0.809 | - |

Associations were analyzed for the main transcript of each targeted zebrafish orthologue using hierarchical linear models (xtmixed in Stata) using inverse-normally transformed outcomes, so effect sizes and SEs can be interpreted as z-score units. Associations were adjusted for time of day and for the weighted number of mutated alleles in the other genes as fixed factors, with larvae nested in batches (random factor). For simplicity, *kiaa1755_1* refers to *quo*, and *kiaa1755_2* to *si:dkey-65j6.2*.

**Supplemental Table 9: Druggability of interacting partners**

| Candidate | Interaction partner | DGIdb categories | Drug available? (y/n) | Drug name (FDA approved) | Drug category |
|---|---|---|---|---|---|
| | *GNAI1* | Tumor supressor | yes | | |
| | *GNAI3* | | | | |
| | *GNAL* | | | | |
| | *GNAS* | Druggable genome, Drug resistance, Clinically actionable | yes | Fluorouracil | Anti-neoplastic agents |
| | *GNAT1* | | | | |
| | *GNB1* | | | | |
| | *GNB2* | Transporter, Ion channel | | | |
| | *GNB3* | | | | |
| | *GNB4* | | | | |
| | *GNB5* | Transporter, Ion channel | | | |
| *GNGT1* | *OR10W1* | Druggable genome, G-protein coupled receptor | | | |
| | *OR1L6* | Druggable genome, G-protein coupled receptor | | | |
| | *OR2AJ1* | Druggable genome, G-protein coupled receptor | | | |
| | *OR4C5* | Druggable genome, G-protein coupled receptor | | | |
| | *OR4F21* | Druggable genome, G-protein coupled receptor | | | |
| | *OR4K15* | Druggable genome, G-protein coupled receptor | | | |
| | *OR51H1* | Druggable genome, G-protein coupled receptor | | | |
| | *PDC* | Phospolipase | | | |
| | *PDCL* | | | | |
| | *PLEKHB1* | | | | |
| | *RHO* | Druggable genome, G-protein coupled receptor | yes | Halothane | Anestethics |
| | | | | Telmisartan, Irbesartan, Valsartan, Eprosartan, Losartan | Anti-hypertensive agents |
| | | | | Atorvastatin | Anti-cholesterimic agents |
| | *AGTR1* | Druggable genome, G-protein coupled receptor, Phospolipase | yes | Cyclosporine | Immunosuppresive agents |
| | | | | Indomethacin, Dexamethasone | Anti-inflammatory agents |
| | | | | Levodopa | Anti-parkinson agents |
| | *GNAI1* | Tumor supressor | yes | | |
| | *GNAI3* | | | | |
| | *GNAT1* | | | | |
| | *GNAT2* | G-protein coupled receptor | | | |
| *GNG11* | *GNAT3* | | | | |
| | *GNB1* | | | | |
| | *GNB2* | Transporter, Ion channel | | | |
| | *GNB3* | | | | |
| | *GNB4* | | | | |
| | *NMB* | Druggable genome, Hormone activity | | | |
| | *PDC* | Phospolipase | | | |
| | *PTGIR* | Druggable genome, G-protein coupled receptor | yes | Iloprost, Treprostinil, Selexipag, Epoprostenol | Anti-hypertensive agents |
| | | | | Dinoprost thromethamine, Misoprostol | Abortifacient agents |
| | *SMURF1* | | | | |
| | *BOP1* | Tumor supressor | | | |
| | *SNAP23* | Druggable genome | | | |
| | *SNAP25* | Druggable genome | yes | Diazoxide | Anti-hypertensive agents |
| *SYT10* | | | | Botulinum toxin type A | Neuromuscular blocking agents |
| | *SNAP29* | Druggable genome | | | |
| | *SNAP47* | | | | |
| | *SYT6* | | | | |
| | *HCN1* | Druggable genome, Transporter, Ion channel | yes | Ivabradine | Channel blocker |
| *HCN4* | *HCN2* | Druggable genome, Transporter, Ion channel | yes | | |
| | *HCN3* | Druggable genome, Transporter, Ion channel | yes | Ivabradine | Channel blocker |
| | *PEX5L* | | | | |
| | *CDH15* | | | | |
| | *CDON* | | | | |
| | *HFE2* | Kinase, Serine-threonine kinase, Cell surface | | | |
| | *NTN1* | Druggable genome | | | |
| | *NTN3* | Druggable genome | | | |
| *NEO1* | *NTN4* | Druggable genome | | | |
| | *PITPNA* | Transporter | | | |
| | *PTK2* | Druggable genome, Kinase, Tyrosine kinase, Lipid kinase | yes | | |
| | *RGMA* | | | | |
| | *RGMB* | | | | |
| | *TTN* | Druggable genome, Kinase, Serine-threonine kinase, Tyrosine kinase | | | |
| | *UNC5B* | | | | |
| *KIAA1755* | - | | | | |

Human candidate genes were examined for their interaction partners using STRING and Genemania, and their classification according to the Drug gene interaction database (DGIdb). Proteins that are already targeted by a drug are indicated by a "y". A selection of FDA-approved drugs was distilled from DGIdb, including their categorization.